NASA CR-54788
BPAD 863-16719R

FINAL REPORT
PNEUMATIC NUTATOR ACTUATOR MOTOR

By
G. R. Howland

Prepared For
NATIONAL AERONAUTICS AND SPACE ADMINISTRATION
October 17, 1965
CONTRACT NAS3-5214

TECHNICAL MANAGEMENT
NASA LEWIS RESEARCH CENTER
CLEVELAND, OHIO
ADVANCED DEVELOPMENT AND EVALUATION DIVISION
VERNON D. GEBBEN

THE BENDIX CORPORATION
BENDIX PRODUCTS AEROSPACE DIVISION
SOUTH BEND, INDIANA

NOTICE

This report was prepared as an account of Government sponsored work. Neither the United States, nor the National Aeronautics and Space Administration (NASA), nor any person acting on behalf of NASA:

A.) Makes any warranty or representation, expressed or implied, with respect to the accuracy, completeness, or usefulness of the information contained in this report, or that the use of any information, apparatus, method, or process disclosed in this report may not infringe privately owned rights; or

B.) Assumes any liabilities with respect to the use of, or for damages resulting from the use of any information, apparatus, method or process disclosed in this report.

As used above, "person acting on behalf of NASA" includes any employee or contractor of NASA, or employee of such contractor, to the extent that such employee or contractor of NASA, or employee of such contractor prepares, disseminates, or provides access to, any information persuant to his employment or contract with NASA, or his employment with such contractor.

Requests for copies of this report should be referred to

National Aeronautics and Space Administration
Office of Scientific and Technical Information
Attention: AFSS-A
Washington, D. C. 20546

NASA CR-54788
BPAD 863-16719R

NASA

FINAL REPORT
PNEUMATIC NUTATOR ACTUATOR MOTOR

By
G. R. Howland

Prepared For
NATIONAL AERONAUTICS AND SPACE ADMINISTRATION
October 17, 1965
Contract NAS3-5214

Technical Management
NASA Lewis Research Center
Cleveland, Ohio
Advanced Development and Evaluation Division
Vernon D. Gebben

THE BENDIX CORPORATION
BENDIX PRODUCTS AEROSPACE DIVISION
SOUTH BEND, INDIANA

ABSTRACT

12149

The report describes the design, development, and test of a new type of low speed, high torque motor designed for manipulating the control drums of nuclear rocket engines similar to NERVA. The motor consists of a pair of bevel gears with an unequal number of teeth. Rotational output is obtained from nutational motion of the input gear driven by pressurized bellows located around its periphery. Flow to the bellows is commutated by vortex amplifiers operating in a closed loop logic sequence. The pneumatic logic circuit operates without moving mechanical parts.

Author

TABLE OF CONTENTS

TABLE OF CONTENTS (Continued)

LIST OF ILLUSTRATIONS

LIST OF ILLUSTRATIONS (Continued)

SUMMARY

The pneumatic nutator actuator provides a low speed high output torque device with a minimum number of moving parts. The lack of high speed rotary components and minimum volume under compression gives the concept design an inherently high reliability and wide closed-loop frequency response. Since the basic actuator can be used as either an analog or digital stepping motor, depending on the commutation circuit employed, the concept provides a versatility which is unusual in pneumatic actuator design.

The development program performed under this contract successfully demonstrated the feasibility of the pneumatic nutator actuator concept. The operation of the commutation circuit demonstrates the ability of vortex type fluid amplifier to operate in a complex combination of series and parallel logic sequence.

During the course of the program, unforeseen development problems were encountered which could not be solved under the scope of the contract. The results obtained, however indicated the actuator's potential and gave an indication of the direction of effort required to obtain the design performance.

SECTION I

INTRODUCTION

1.1 PROGRAM OBJECTIVE

The Pneumatic Nutator Actuator Motor was developed by Bendix Products Aerospace Division under Contract NAS3-5214 for NASA-Lewis Research Center. The purpose of the contract is to build and evaluate a pneumatic actuator motor for control of a nuclear reactor. The required performance specifications are listed in Para. 1.2. The motor is of a different concept from the conventional gear, vane or piston type actuators. The logic circuits required to operate the motor have no moving parts and are composed of fluid interaction (vortex type) devices.

1.2 SPECIFICATIONS

The actuator motor was designed to meet the following performance specifications.

a.	Working Fluid	Hydrogen gas
b.	Gas Temperature	-350 to +300°F
c.	Output shaft rotation	0 to 180° ±2°
d.	Supply pressure	215 psia
e.	Return pressure	50 psia
f.	Minimum static output torque	300 inch lbs.
g.	Minimum output torque during 10° per second output motion	200 inch lbs.
h.	Minimum Output torque during 40° per second output motion	75 inch lbs.
i.	Linearity of static output torque versus position for constant differential input pressure for analog actuator motor	±20% of full scale

j.	Saturated output velocity	Between 50 and 300 degrees/sec. for plus and minus directions of rotation
k.	Load inertia	95 lbm-in^2
l.	Load friction	0 to 32 inch-lbs.
m.	Size (excluding output shaft)	Fit within a cylindrical envelope of 10" diameter by 18" length. Center line of output shaft must be parallel to, and within 3" of envelope-length center line.
n.	Ambient temperature	-400 to +300°F
o.	Ambient pressure	0 to 15 psia
p.	Gas pressure on actuator motor output shaft	0 to 650 psia
q.	Vibration	4 G amplitude from 0 to 100 cps; 20 G amplitude from 100 to 20,000 cps.
u.	Neutron flux	3×10^{11} fast neutrons/cm^2 sec. 1×10^{10} slow neutrons/cm^2 sec.
s.	Gamma heating	350 watts/lb aluminum

The actuator motor design shall respond to scram mode operation. In the scram mode, the output shaft shall return to the zero position within 0.5 second from the time of initiation of either a scram command signal or loss of pneumatic supply pressure. A soft stop device shall be designed to prevent decelerations greater than 2000 radians/sec.^{2}. The soft stop rebound after scram shall be less than one-fourth of the initial shaft angle.

For purposes of acceptance testing operation shall be demonstrated on nitrogen and helium gases at room temperature conditions. Vibration, neutron flux and gamma heating tests need not be performed.

1.3 ACTUATOR CONCEPT

In order to provide a low speed, high torque output, the actuator motor makes use of the nutating gear concept to obtain a high gear reduction. The nutator transmission consists of a pair of bevel gears. One gear is attached to the output shaft, and the other is attached to the case through a pair of gimbal rings. The gimbal rings allow the input gear to wobble or nutate, but not rotate.

If a force is applied at a point on the circumference of the input gear, the gears will mesh along the pitch line of a single tooth. By moving the point of application of the force around the circumference, the input gear will mesh consecutively with each of the teeth in the output gear. If the output gear has one less tooth than the input gear,

the output will be displaced by one tooth for each complete nutation of the input gear. Gear reductions between 50:1 to 200:1 can be accomplished in this manner by a single pair of gears.

The force can be applied to the input gear by a number of electromagnetic solenoids (for an electrical input) or by pressure force elements (bellows or pistons) for a hydraulic or pneumatic input.

The pneumatic nutator actuator motor developed under this contract employs eight bellows assemblies. Four of the bellows are pressurized at any given time. Nutation is caused by increasing the pressure to the fifth bellows and simultaneously decreasing the pressure in the first bellows. The actuator is shown schematically in Figure 1-1.

The actuator motor can be operated as a digital stepping motor if the appropriate commutation circuit is employed. For the actuator motor designed a pulse input would cause an output step of 0.25 degree.

The commutation circuit developed is a proportional closed loop analog design. The input is a pressure differential which results in an output torque proportional in magnitude and direction to the input differential.

The position of the input nutating gear is indicated by a leaf spring attached to the gear which covers a bleed hole in the actuator motor case (see schematic). Four bleed holes are used, equally spaced around one-half of the circumference. Each bleed hole is a downstream variable restrictor of two restrictors in series. The intermediate pressures obtained are therefore an indication of the input gear position.

Four of the eight bellows are pressurized at any given time. The four bellows pressurized will cause the nutating gear to assume a given position. The resultant change in pickoff pressures will cause the fifth bellows to become pressurized and the first bellows to reduce in pressure. As the gear moves under the pressure forces, the pickoff pressures will again change, resulting in a further change in bellows pressure. The commutation is therefore similar to a conventional electric motor, except that the action is proportional.

The nutator actuator has a number of desirable features which make it superior to a conventional actuator, particularly where extreme environmental conditions exist. These advantages may be outlined as follows:

(a) Minimum number of moving parts. The only rotary motion is in the slow moving output gear and shaft. Only two bearings are employed in the entire actuator. The input motion is a nutation motion with a small axial movement.

(b) High speed of response. Since there are no high speed rotating components, the input inertia is low. This allows a rapid reversal of direction to a step command.

(c) Automatic declutch. If the pressure to the bellows is nulled, the spring rate of the bellows will cause the nutating gear to disengage and lie in a plane parallel to the output gear. The output shaft is then free of the input. A spiral preloaded spring will then drive the output shaft to the zero angle position. A small brake drum and torque tube

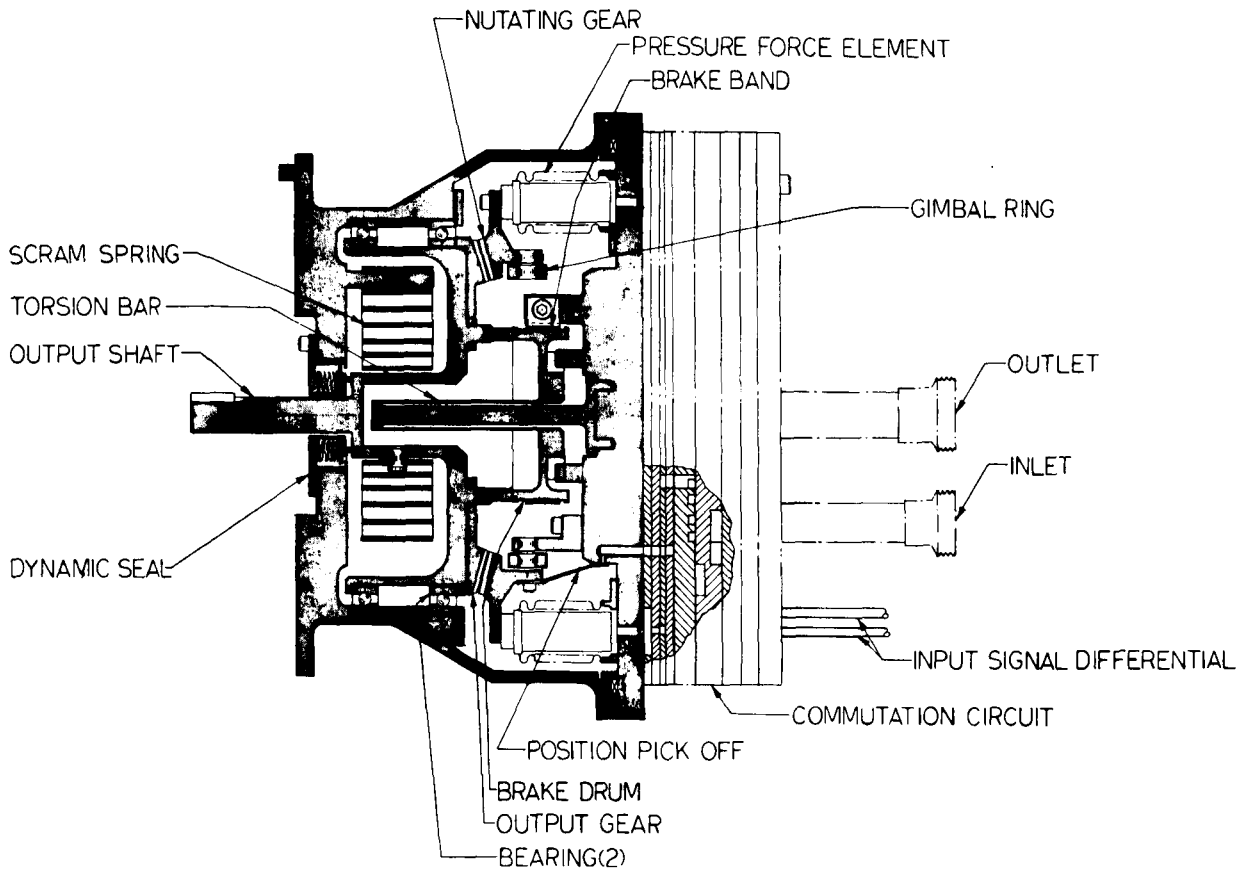

Figure 1-1. Pneumatic Nutating Actuator Motor

absorb the energy of impact. This scram feature, which is mandatory in nuclear reactor control, is inherent in the nutator actuator design.

(d) Fail safe features. The most critical component in the actuator is the pressure force elements. A bellows failure will not cause a seizure but only a reduction in output torque. Multiple bellows failure will result in disengagement of the gears, and a scram to zero will occur.

The design and testing performed on the mechanical components of the actuator are described in Section II. The development of the fluid control commutation circuit is given in Section III. The performance obtained from the complete actuator motor is discussed in Section IV. Section V discusses a comparison of the nutator actuator and conventional vane, piston and gear motor actuators. The actuator performance is summarized in Section VI with recommendations for improving and optimizing the actuator configuration. Component design calculations are given in Appendix A.

SECTION II

DESIGN AND TEST OF MECHANICAL COMPONENTS

2.1 DESIGN APPROACH

The design and material requirements of the critical components of the actuator motor are described below.

2.1.1 Gears

The gears designed for this application are based on principles used to design gears for nutator transmissions manufactured by Bendix over the past four years. They are a straight-flank bevel design and, in this case, have a cone angle of 140 degrees. The input gear has 181 teeth and the output gear 180 teeth, resulting in a reduction ratio of 180:1. Both gears are made of AMS 5643 heat treated to Rockwell C 35-42. The teeth are treated with 76 x 10^{-4} to 178 x 10^{-4} mm (0.0003-0.0007 in) thick coating of Hi-T-Lube, which is a dry lubrication process applied by the General Magnaplate Corporation. Of the many nutator transmissions built to date, all gears and bearings have used this lubrication. No gear or bearing failure has occurred during normal operational testing and some customer units have accumulated over 200 hours of operation.

To permit its nutation, the input gear is supported by a gimbal mounting incorporating four Bendix "Free-Flex" frictionless pivots. This arrangement provides axial rigidity while allowing the input gear to nutate freely with no "play" or waste motion at the pivot points. The input gear and gimbal ring assembly are shown in Figures 2-1 and 2-2.

2.1.2 Bearings

For the past six years, Bendix has supported an intensive test program to develop bearing materials which have a long operating life in extreme environments. Tests conducted by the Research Laboratories and Products Aerospace Divisions have utilized a Bendix' designed, rolling contact bearing test machine which has an ambient temperature capability of 56°K to 1470°K (-360°F to 2180°F) and a pressure range from 10^{-9} mm Hg to 800 mm Hg with a variety of ambient gases. In addition, various dry-film lubricants for use in bearings have been tested in cryogenic environments resulting in the selection of two similar lubrication methods which produce excellent results.

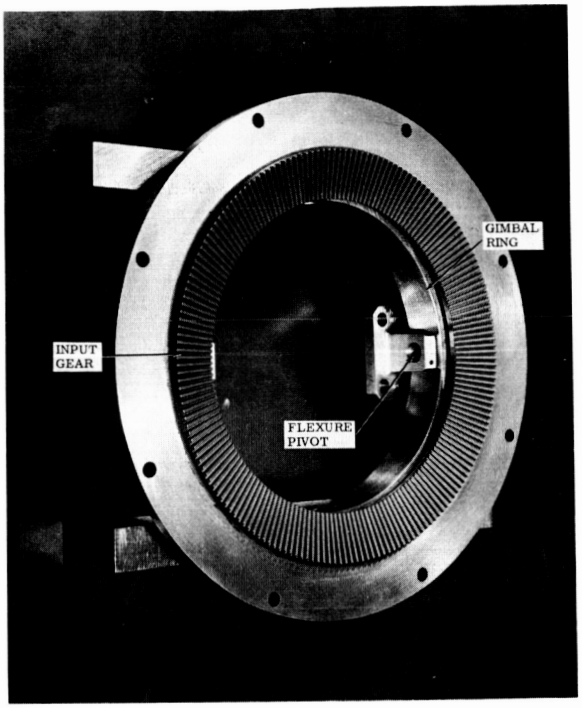

Figure 2-1. Input Gear and Gimbal Ring - Front View

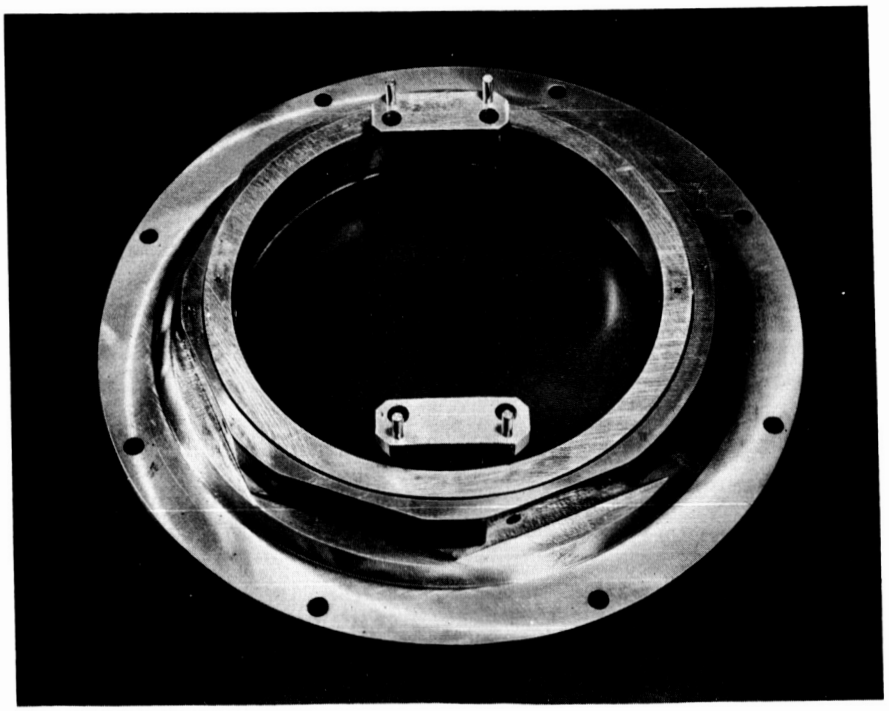

Figure 2-2. Input Gear and Gimbal Ring - Rear View

With the first method, the bearing balls and races are made of Type 440C stainless steel. The ribbon-type ball separators are made of Type 300 series stainless steel and coated with Hi-T-Lube. In operation, the balls transfer the dry film material from the separators to the races to provide a lubricating film.

The second method again uses bearings containing Type 440C stainless steel balls and races with ball separators made of DuPont's SP-1 Polymer. Bearing action transfers the SP-1 material to the metal parts of the bearing to provide a lubricating film. Comparative tests indicate that in a hydrogen atmosphere this method is slightly superior to the Hi-T-Lube method with respect to bearing life. However, either lubricating method will be satisfactory and result in a device which can meet specification requirements. Choice of material depends to some extent upon bearing size and ease of manufacture of the ball separators.

Pertaining to the bearings for the actuator motor, only two ball bearings are used. Angular contact type bearings have been selected. These bearings axially locate the output shaft, absorb the thrust load caused by the gear separating force and absorb the pressure force created by the dynamic shaft seal. The selection of bearing size was based on the maximum bearing load, the mean effective speed, and a B-10 catalog life based on at least ten times the desired life of the actuator. Experience has shown that this method of derating provides satisfactory results.

2.1.3 Scram Mechanism

The pneumatic pressure to the actuator may be interrupted due to a failure or by a scram command signal. This interruption automatically disengages the transmission and the load inertia becomes free-wheeling. A spiral spring preloaded to the output shaft ensures the required scram action. A schematic drawing of the scram system is shown in Figure 2-3 and a summary of scram characteristics based on a constant dynamic load friction of -37 m kg (32 inch-pounds) is shown in the table below. This scram concept has been used by Bendix on previous projects with environments of nitrogen and hydrogen gas and a temperature range from 110°K to 650°K (-260°F to +650°F). The spring material and operating stress level are based upon this past experience. Bendix Engineering Specification CNPD-188, which covers the scram spring, is included in Appendix C.

SCRAM CHARACTERISTICS

Maximum Scram Time	0.21 second
Maximum Impact Velocity	21.7 radian/second
Spring Size (Approximately)	1.32 x 31.8 mm (0.052 x 1.25 in.) cross section (11 turns)
Spiral Spring Rate	.046m kg/rad (4 in. lbs./radian)
Preload	.58m kg (50 in. lbs.) (at zero)

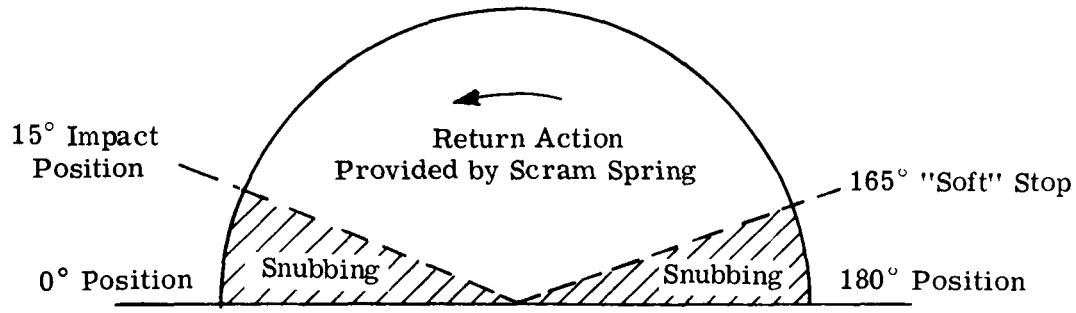

Figure 2-3. Scram System - Schematic

2.1.4 Snubbing Mechanism

A snubbing device is required to ensure that the deceleration on completion of scram action is less than 2000 radians/second. The snubbing action is designed to take place during the 15-degree to zero-degree portion of output shaft travel.

A lever, keyed to the output shaft, engages a small brake drum, which is attached to the actuator housing through a torsion bar. The mechanism is designed so that the torsion bar will store a portion of the kinetic energy, allowing the output shaft to return to the 15-degree position under all conditions. The brake will dissipate the remaining kinetic energy to prevent excessive rebound.

SNUBBER DESIGN DATA

Impact Velocity	2.17 radians/second
Kinetic Energy at Impact (Maximum)*	1.05m kg (91 inch-pounds)
Kinetic Energy Absorbed by Brake (Maximum)*	.43m kg (37 inch-pounds)
Kinetic Energy Absorbed by Torsion Bar (Maximum)*	.62m kg (54 inch-pounds)

* Based on a release position at 150° from impact with brake.

In addition to the stop at the 15-degree position, the brake is also designed to engage at the 165-degree position to prevent actuator damage due to an inadvertent overtravel command. The mounting plate containing the pressure elements and snubber mechanism is shown in Figure 2-4.

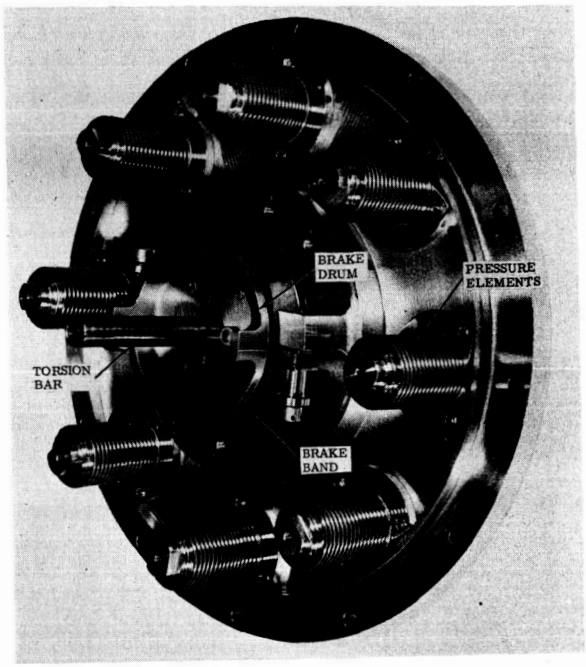

Figure 2-4. Mounting Plate Containing Pressure Elements And Snubber Mechanism

2.1.5 Dynamic Shaft Seal

The dynamic shaft seal selected for this application is a face-type seal utilizing a welded metal bellows to maintain contact between the face of the seal and a specially prepared surface on the output shaft.

In the design and construction of this type of seal, two goals are desired; a low leakage rate and a low operating torque. If sufficient bellows spring force is utilized to obtain near zero leakage, the torque required to overcome the friction will rise to an unacceptable level. In similar programs, a design goal of .00045 kg/sec. (0.001 lb./sec.) of gaseous H_2 leakage and .173m kg(15 inch-pounds) of torque was established as the maximum acceptable limit for all specified gas temperatures and pressures.

The seal is installed into the actuator, so that the pressure load is supported by the flanged portion of the housing. Leakage around the seal case is prevented by using a static seal. The seal can be installed or removed from the actuator without disturbing other components. This arrangement greatly facilitates initial installation adjustments, test inspections, and seal replacement.

A typical bellows-type face seal is shown in Figure 2-5. This seal consists of a welded Inconel X bellows assembly, attached to a back bellows plate, and a front plate or cup containing a carbon seal ring.

A seal material evaluation study was conducted at Bendix to determine the optimum dynamic sealing materials combinations for use in actuators exposed to nuclear-

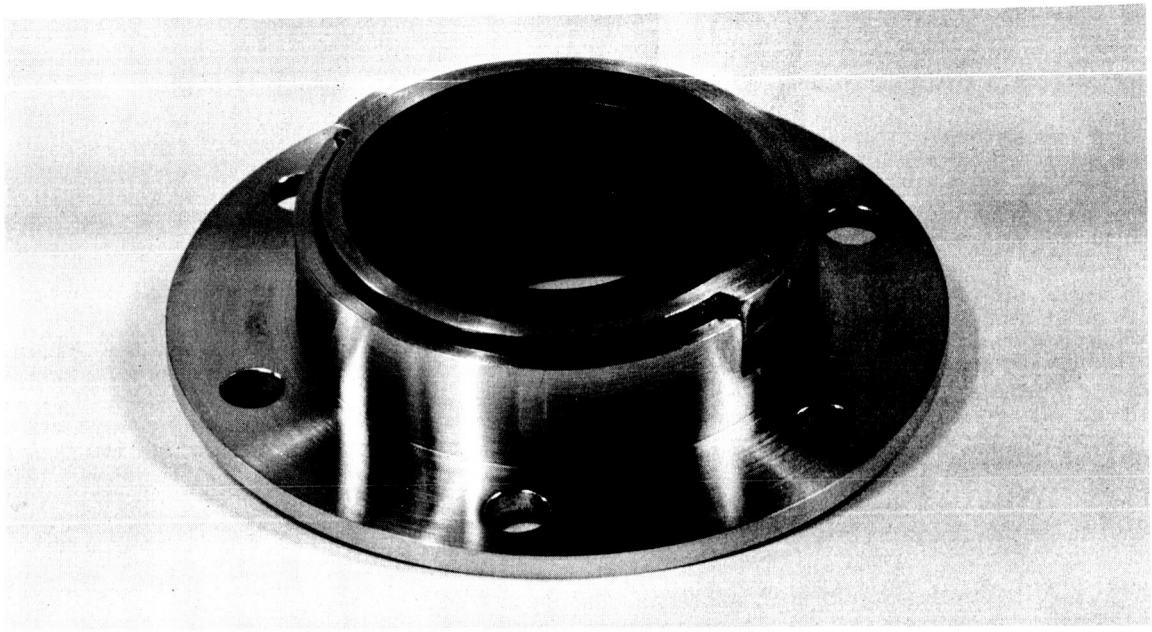

Figure 2-5. Bellows Type Face Seal

cryogenic environments. Forty-seven various seal materials were tested. The results of this test program are reflected in our present dynamic seal designs. The dynamic seal used in the latest model turbine power control valve (TPCV) actuator for the NERVA program performed successfully over a pressure range of -44.7 to 447 n/cm^2 (-65 to +650 psid) and through a temperature range of 100°K to 980°K (-280 to +1300°F) for a total accumulated operating time in excess of 100 hours.

Bendix Engineering Specification CNPD-189, which covers the dynamic shaft seal, is included in Appendix C.

2.1.6 Pressure-Force Elements

One of the critical components of the nutator motor is the pressure-force element. This device must convert the pneumatic pressure into a force efficiently and rapidly. Hence, it must be a device having minimum leakage, minimum friction, low inertia, minimum displacement volume, and a very high cycle life.

The bellows unit, Figure 2-6, is composed of a metal bellows, two end fittings, and a thin-walled cylinder placed in the center of the unit to reduce its internal volume. The unit is an interchangeable subassembly.

The face mounting flange is designed to allow incorporation of a metal sealing ring of a standard size, if pressure tests indicated a high leakage.

The metal bellows is an electrodeposited type manufactured by the Servometer Corporation of New Jersey. It is made of material composed of 99.5% nickel, 0.4% cobalt, and traces of oxygen and carbon. Based on tests conducted by the manufacturer, it has an average life cycle of 50 x 10^6 cycles at 110°K (-260°F) for a stroke of 2.54 mm (0.10 inch) and a maximum pressure drop of 58.5 N/cm^2 (85 psi). Using a

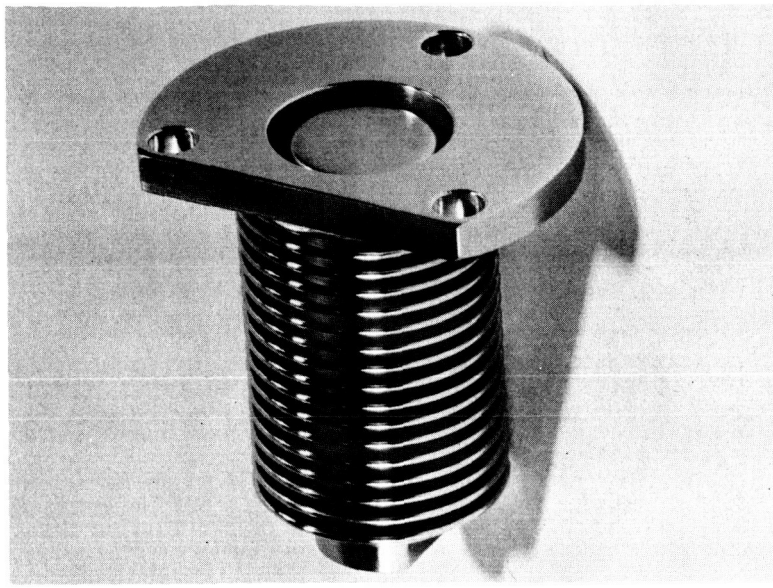

Figure 2-6. Bellows Unit

value of 40 degrees/second as a rated output velocity, a transmission ratio of 180:1 and considering eight pressure-force units, it is determined that each bellows must cycle at a rate of twenty cycles per second. Based on the cycle life given and the values assumed the pressure-force elements would have an expected life of almost 700 hours. There are several advantages associated with the bellows unit such as dirt insensitivity, the elimination of all sliding or rubbing that is normally associated with a piston element, the no-leakage characteristic, the ability to accept some slight misalignment of the two end connections during operation, and the low mass of this thin-wall member.

Specification CNPD-187, covering the bellows assembly, is included in Appendix C.

2.1.7 Housing

The outer housing for the mechanical components of the actuator was designed in accordance with the ASME Code for Unfired Pressure Vessels to withstand a maximum internal pressure of 138 N/cm^2 (200 psig). The end plate with the dynamic seal was thickened to prevent changing of the seal preload under pressure. The housing is shown in Figure 2-7. The output shaft and shaft assembly are shown in Figures 2-8 and 2-9.

2.1.8 Mechanical Commutator

The purpose of the mechanical commutator is to permit testing the motor actuator independent of the pure fluid commutator. Functionally the mechanical commutator is a series of three-way valves which sequence the pressurizing and exhausting of the eight bellows units of the actuator.

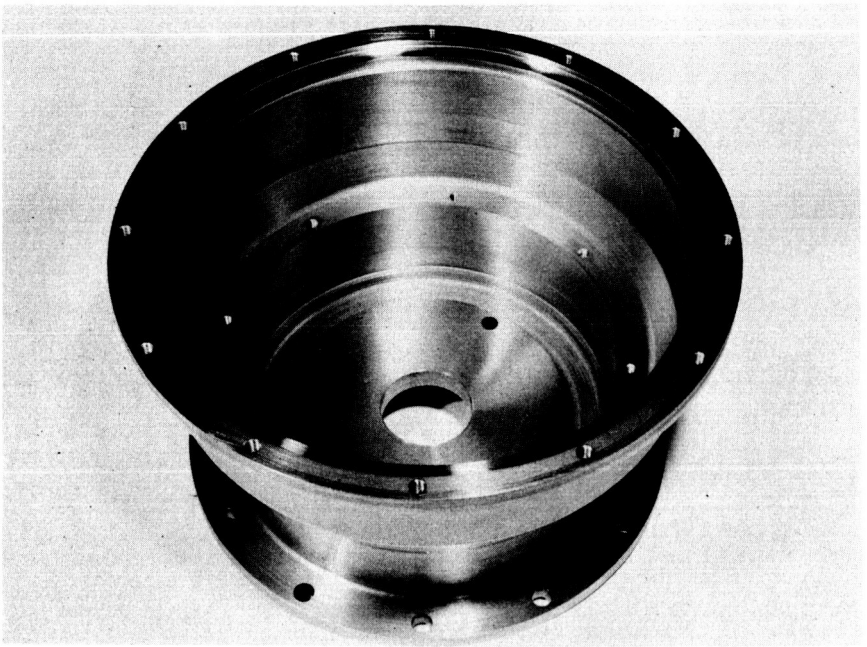

Figure 2-7. Main Housing

The device is composed of a shaft driven, combination spool and plate valve and a manifolded mounting plate which attaches to the rear of the motor. Provisions have been made for the insertion of pressure pickups in the channels supplying the bellows units.

2.2 ASSEMBLY AND TEST

2.2.1 Mechanical Assembly

Upon receipt of the two bearings from the manufacturer it was found that the bearings supplied were radial instead of angular contact. The bearings were returned to the manufacturer where they were modified by a reduction in the inner ring diameter. It is felt that the validity of this modification is questionable. However, due to the short term of the contract these bearings were accepted to prevent further assembly delay.

The components were initially assembled to verify the assembly procedure. The only problem encountered (except for a minor bearing relief requirement) was the torsional clock type scram spring. It was found that excess friction was developed by the coils rubbing together. After discussion with the vendor, the specification was rewritten and new springs ordered. Evaluation of the scram performance was carried out later in the program.

For initial evaluation of the motor performance, the unit was assembled with the mechanical commutator and without the scram spring, torsion shaft, drum brake and dynamic seal.

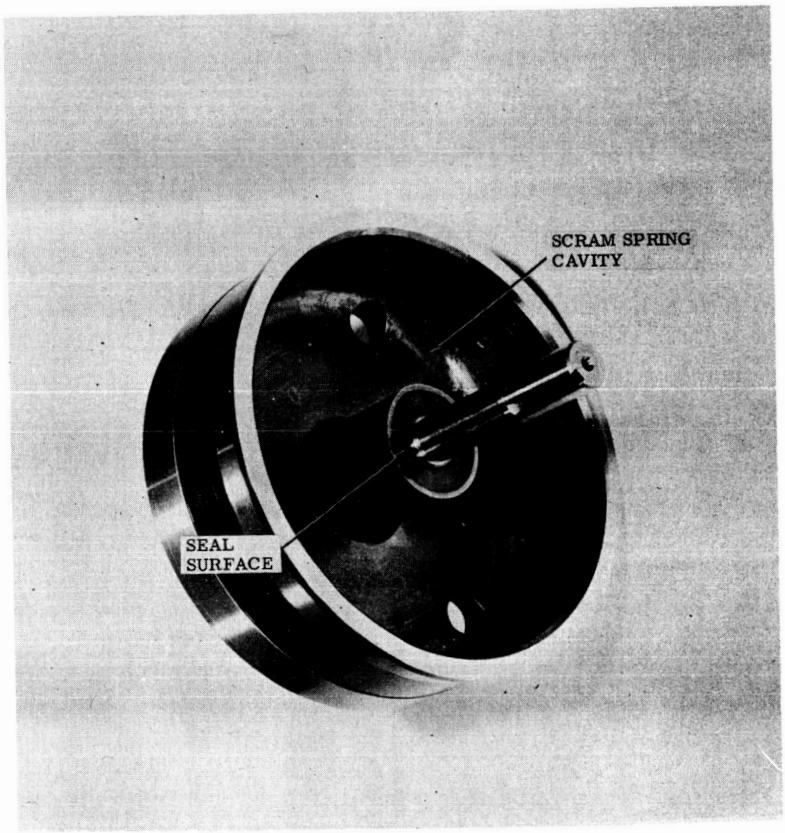

Figure 2-8. Output Shaft

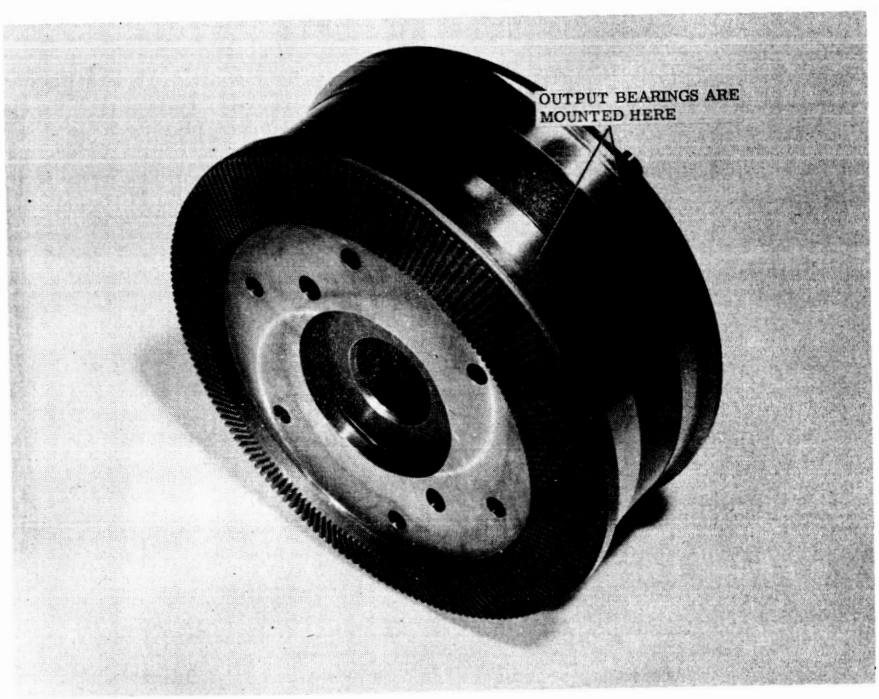

Figure 2-9. Output Shaft Assembly Containing Output Gear

2.2.2 Mechanical Commutation Test Results

After initial assembly and adjustment, the motor was run continuously at an input commutation speed of 1000 rpm (5.6 rpm output speed) for fifteen minutes in each direction. No output load was applied. On disassembly some flaking of the molybdenum disulphide lubricant on the gear teeth was noted. After approximately ten hours of running, mostly under high load condition, no further flaking of the lubricant was evident and the gear teeth appear in excellent condition.

After run-in, the pressure supplied to the bellows were monitored by gages on the mechanical commutator. It was found that the commutator was "breaking before making", causing the number of pressurized bellows to vary between three and four, depending on the angular position on the commutator. The distribution slot in the commutator was modified to provide a more even pressure distribution. Figure 2-10 shows the pressure variation in bellows number 1 and number 5. It can be seen that the reduction in one bellows pressure is accompanied by a corresponding increase in the other bellows pressure. In order to obtain this symmetry, the supply and vent ports of the commutator are "short circuited" during portions of the commutation cycle. This short circuit causes an increase in the supply flow and a consequent reduction in the bellows pressure. This reduction can be seen in Figure 2-10 each time a bellows is pressurized. Unsuccessful attempts were made to add capacitance to the inlet and bellows supply lines to minimize this pressure variation.

Maximum output torque for a given commutator speed was determined by loading the output shaft until the gear teeth disengaged. A plot of maximum output torque against input commutator speed is shown in Figure 2-11. Output shaft speed can be obtained by dividing the input speed by 180.

This method of shaft loading will indicate the torque obtained when the pressurized bellows pressure is at a minimum. By monitoring the transient bellows pressure and measuring the minimum obtained, the output torque can be corrected to determine the actuator performance assuming a uniform bellows pressure. This corrected torque versus speed curve is shown in Figure 2-12. The corrected curve indicates the maximum torque which could be obtained with the self-commutation circuit.

The torque required to back drive the motor was found by holding the mechanical commutator stationary and applying sufficient torque to the output shaft to cause tooth disengagement. This torque is shown in Figure 2-13 for various combinations of pressurized bellows.

Previous experience with nutator gear concepts has shown that the mechanical efficiency (n) is independent of the direction of drive. The efficiency can be calculated from the output torque (T_O) and the back driving torque (T_r) as follows:

$$n = \sqrt{\frac{T_o}{T_r}}$$

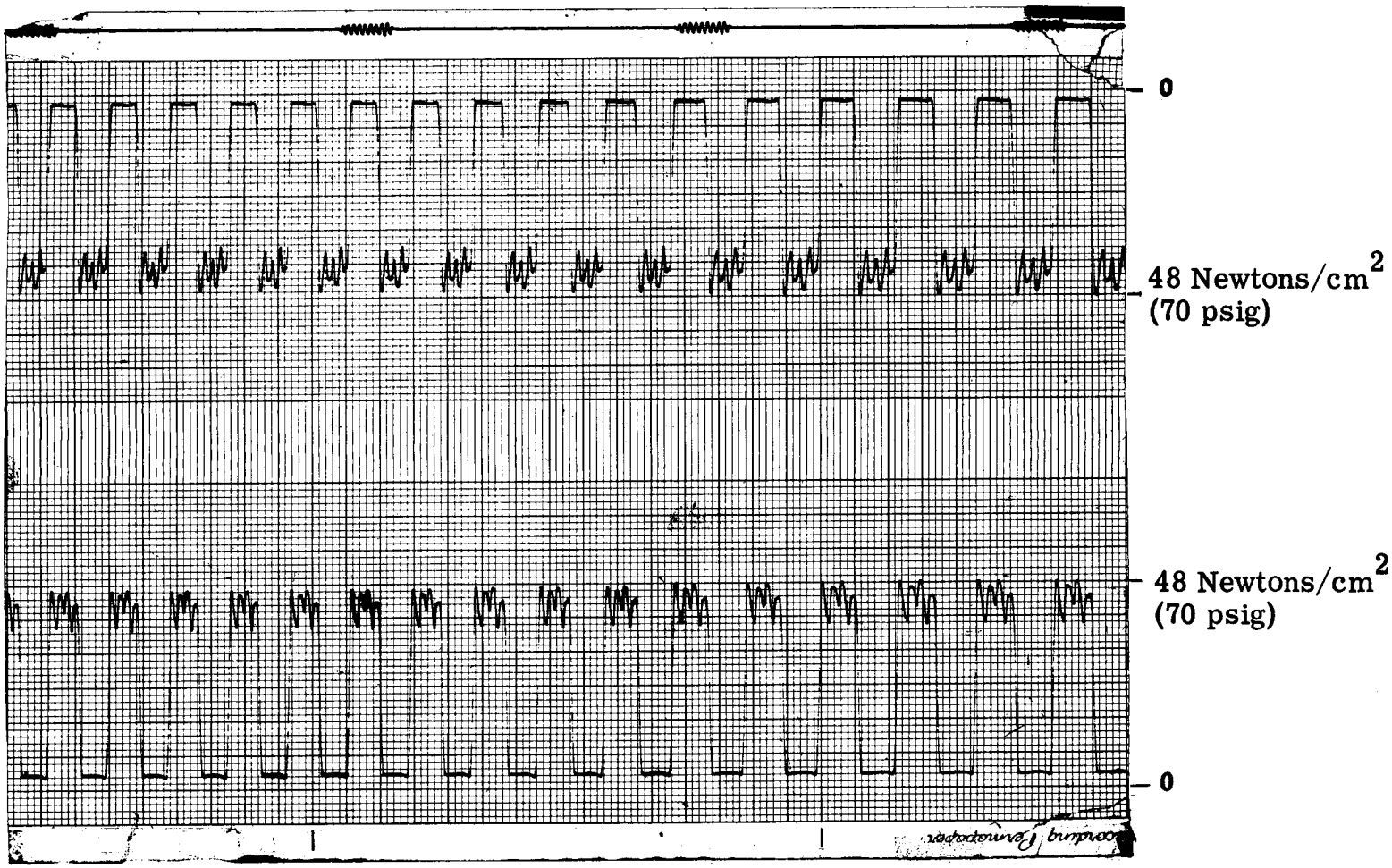

Figure 2-10. Pressure Profile - Bellows #1 and #5 Mechanical Commutator

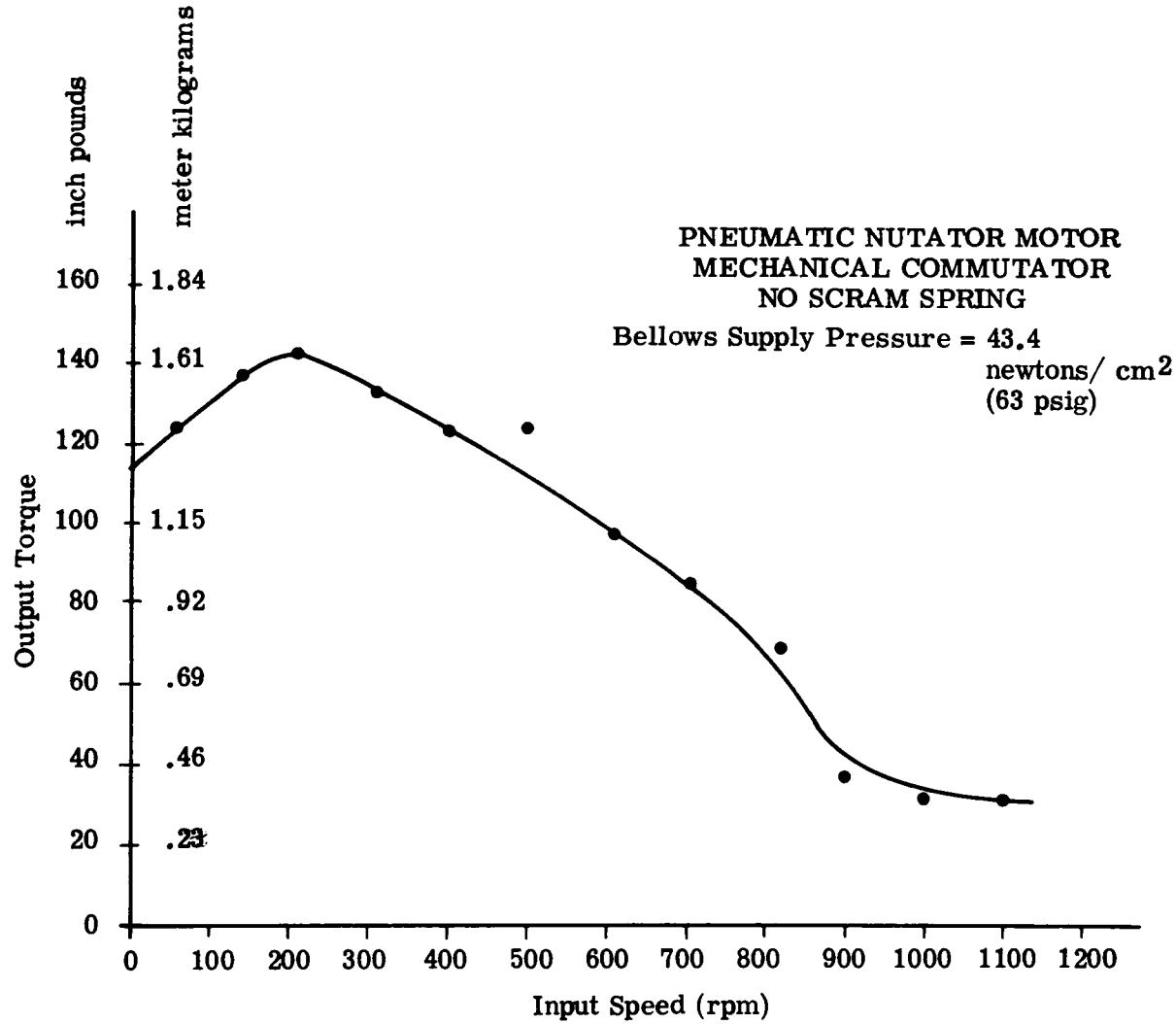

Figure 2-11. Output Torque Versus Input Speed

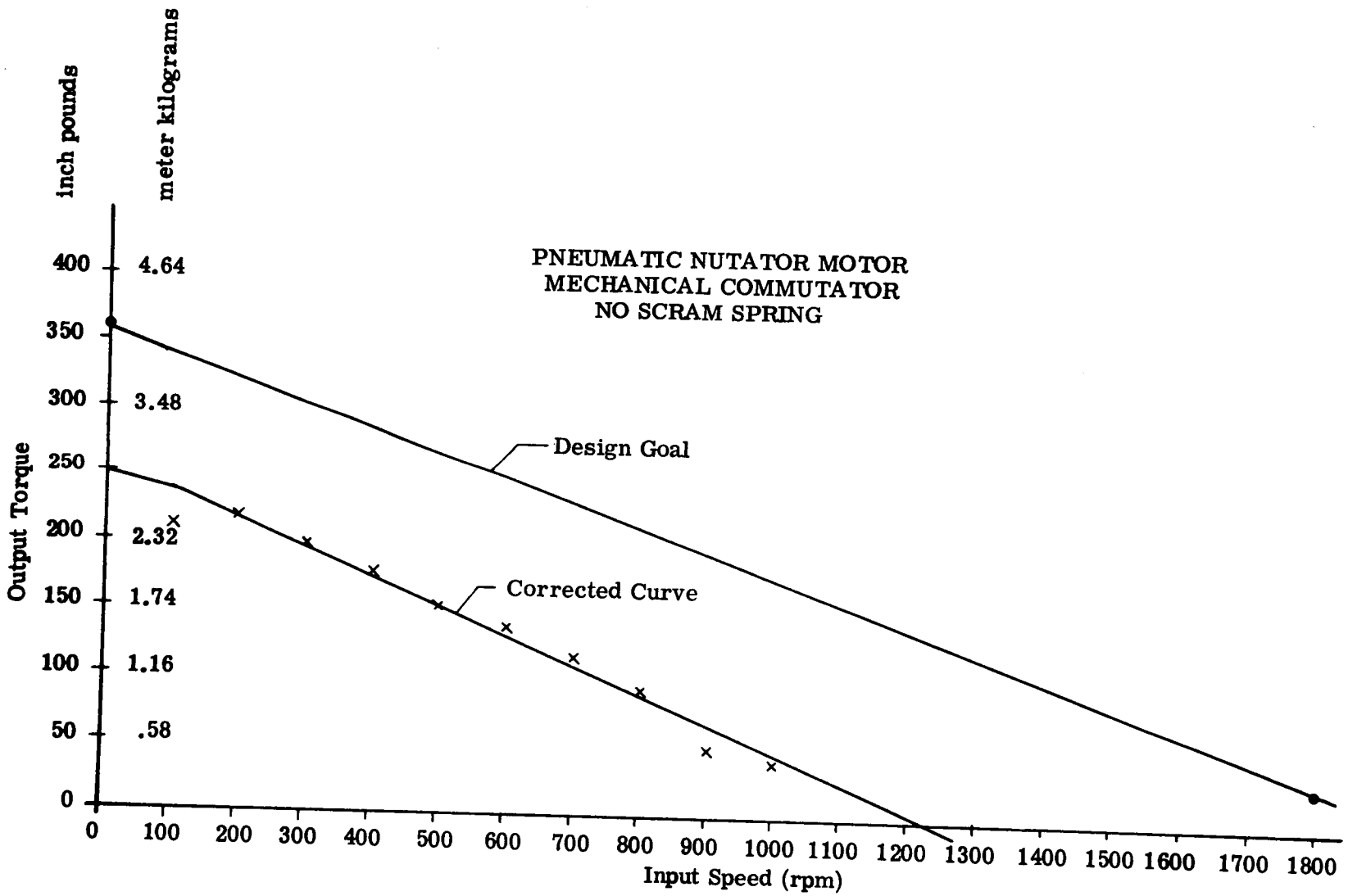

Figure 2-12. Corrected Output Torque Versus Input Speed

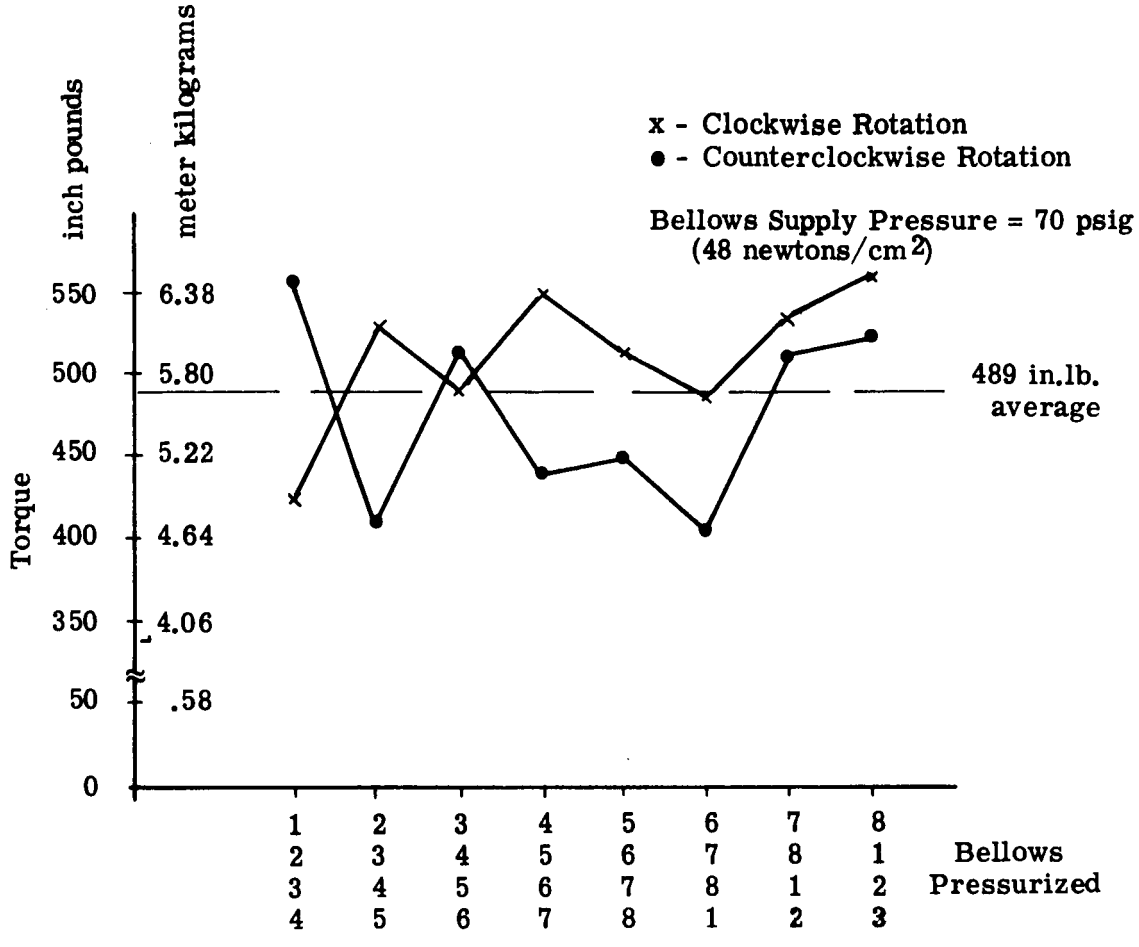

Figure 2-13. Reversed Stall Torque

or, from Figures 2-12 and 2-13,

$$n = \sqrt{\frac{2.89}{5.65}} = 71.5\%$$

This efficiency agrees closely with the original design estimate (68%).

Further testing of the motor was started to determine the torque versus supply pressure characteristics, but was terminated when a rapid deterioration in output torque was noted. Disassembly of the unit showed that all four flexure pivots were either broken or badly distorted. It is felt that a failure of the pivots resulted from the shock loading employed by the method of test and is not indicative of the performance under normal operation. The pivot holes were rebored to take larger (3/8 inch diameter) flexure pivots, which increased the torque capacity by 50%.

The maximum corrected output torque obtained was 2.89 meter-kilograms (250 inch pounds) (See Figure 2-12). With a measured efficiency of 71.5% meter-kilograms internal torque developed is 4.05 meter-kilograms (350 inch pounds). The design internal torque is 7.05 meter-kilograms (610 inch pounds). It appears that the motor is producing only 57% of the design value. This torque reduction can be caused by one or more of the following factors.

(a) Bellows pressure is measured upstream of a 1.015 mm (.040 inch) diameter orifice. Any appreciable bellows leakage would reduce the actual bellows pressure below the measured value.

(b) Bellows effective area is less than the design requirements.

(c) The nutation angle is incorrectly set.

(d) Inaccuracies in gear profiling has resulted in a reduced angle of force centroid.

To investigate these possible causes, the following action was taken:

(a) A bellows test fixture was fabricated to allow pressurization of an individual bellows assembly. A check of all the bellows showed that only two of the sixteen on hand (eight spare) had appreciable leakage. The eight bellows taken from the motor had negligible leakage.

(b) Two bellows were selected at random and the force for a given applied pressure was measured. The force measurement gave an effective bellows area of 2.67 cm^2 (.414 $in.^2$) and 2.65 cm^2 (.411 $in.^2$). These areas are within the allowable limit of 2.80 cm^2 ±5% (.435 $in.^2$ ±5%).

(c) and (d) The nutation angle and the gear profile cannot be measured directly, and any indirect measurement is open to question. After repair of the flexural pivots, the motor was run with the fluid commutator circuit. Further investigations were made at this time, the results of which are described in Section IV.

The operation of the mechanical components with the mechanical commutator demonstrated the operational capability of the pneumatic nutator motor concept and provided some indication of the overall performance.

2.2.3 Dynamic Seal Tests

The motor was partially disassembled at the intermediate flange point, and the input commutation, bellows and input gear assembly were removed, leaving the output gear, bearings and output shaft. The shaft dynamic seal was then installed and the output assembly was mounted on the drum test fixture. The test fixture (and output shaft) was then pressurized to 448 N/cm^2 (650 psig) and the output torque was measured by a torque wrench applied to the output gear. A graph of torque versus shaft angle is shown in Figure 2-14. The maximum seal torque is well below the design specification of 1.73m kg (15 inch-pounds).

A plastic bag was then placed over the output gear assembly, with an outlet tube. The tube was submersed just below a surface of water. At 448 N/cm^2 (650 psig) shaft pressure, with gaseous nitrogen no leakage (in the form of bubbles from the tube) occurred in a period of 20 minutes.

From these tests the following conclusions can be made.

1. The shaft seal friction is extremely low.

2. The output bearing friction does not increase appreciably when axially loaded to approximately 236 kg (520 pounds).

3. The seal room temperature nitrogen leakage is essentially zero.

2.2.4 Scram Characteristics

The spiral clock spring was inserted in the output shaft assembly and the dynamic seal was removed. Tests were then conducted to measure the scram spring rate. The torque versus angle for the scram spring is shown in Figure 2-15. Operation of the spring will occur between 2.0 and 2.5 revolutions, at a spring rate of .033 m kg/rad. (2.9 in. lb./rad.). This rate is within the specification of .0455 m kg (4.0 in.lb./rad.) maximum.

The torsion tube and brake bands were then assembled. With the brake bands loose, the torque from the torsion tube was recorded throughout its ±15° travel (see Figure 2-16). The brake bands were tightened until they added about 1.61 m kg (140 in.lbs.) to the system.

The scram spring was preloaded to .58 m kg (50 inch pounds) and scram tests were attempted. With .54 m kg (47 inch pounds) load friction on the output shaft the scram spring did not have enough force to return the shaft to the zero position. The scram spring was then preloaded to .69 m kg (60 inch pounds) which is the maximum allowable preload with present design scram spring. The maximum load friction against which the spring would effect a scram from full travel in 0.5 seconds was determined to be .35 m kg (30 inch pounds). A Sanborn trace of this test is shown in Figure 2-17.

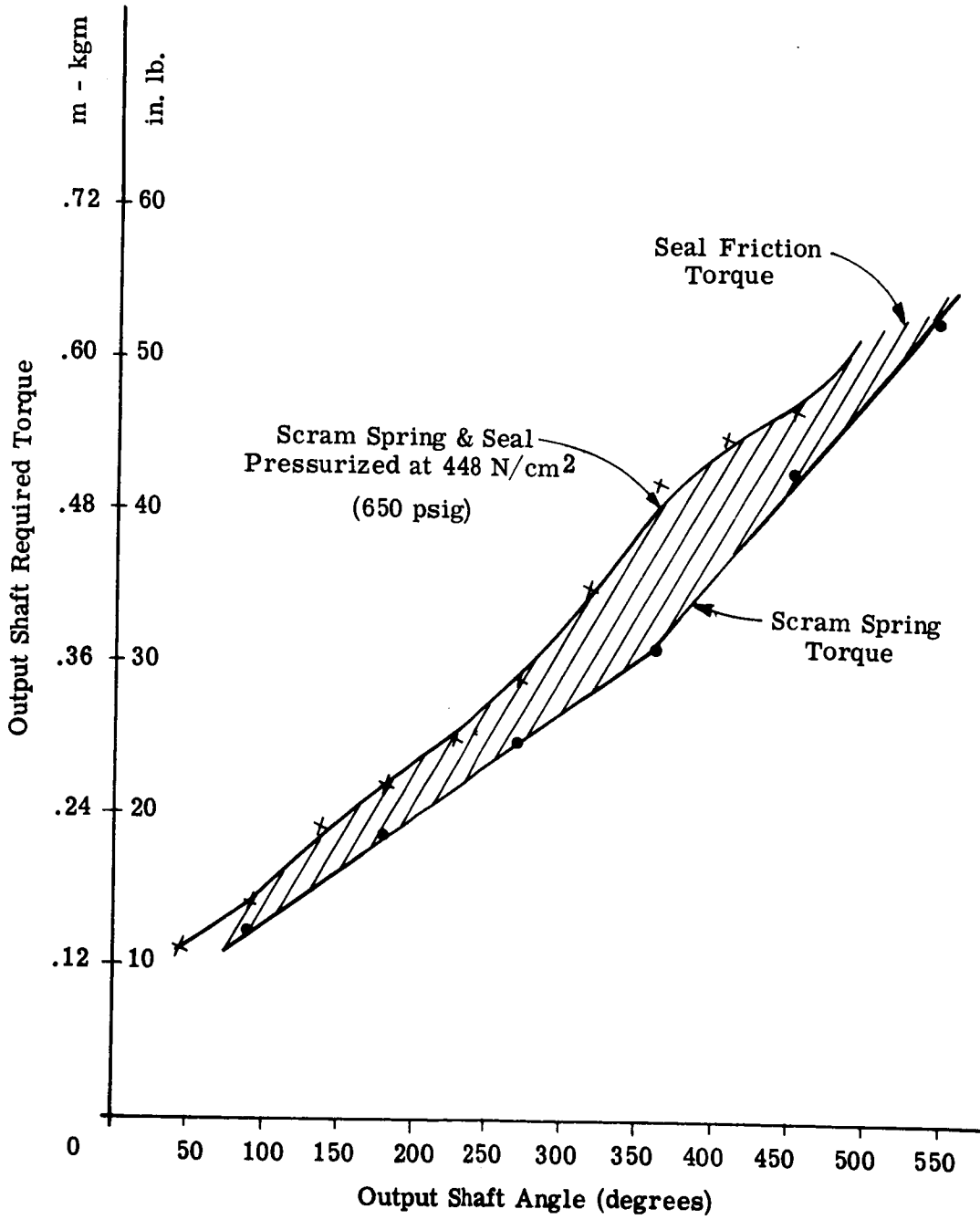

Figure 2-14. Shaft Dynamic Seal Friction Torque

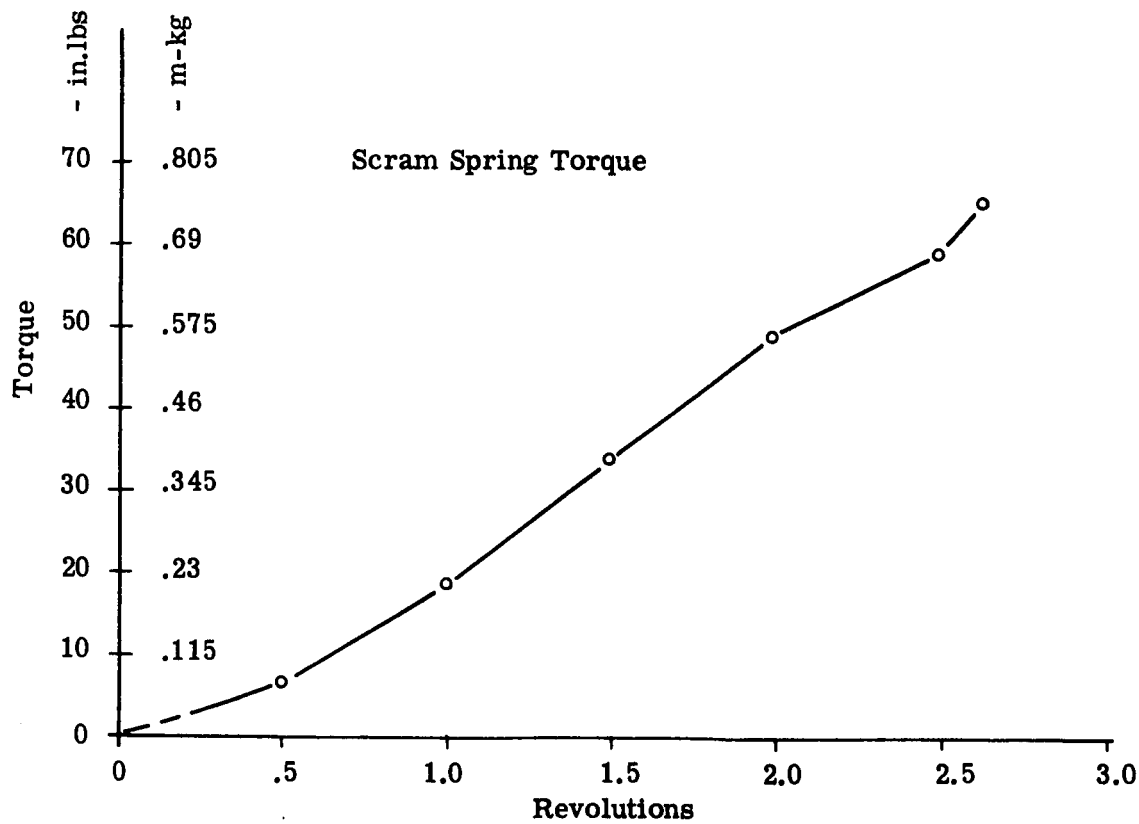

Figure 2-15. Scram Spring - Torque Versus Angle

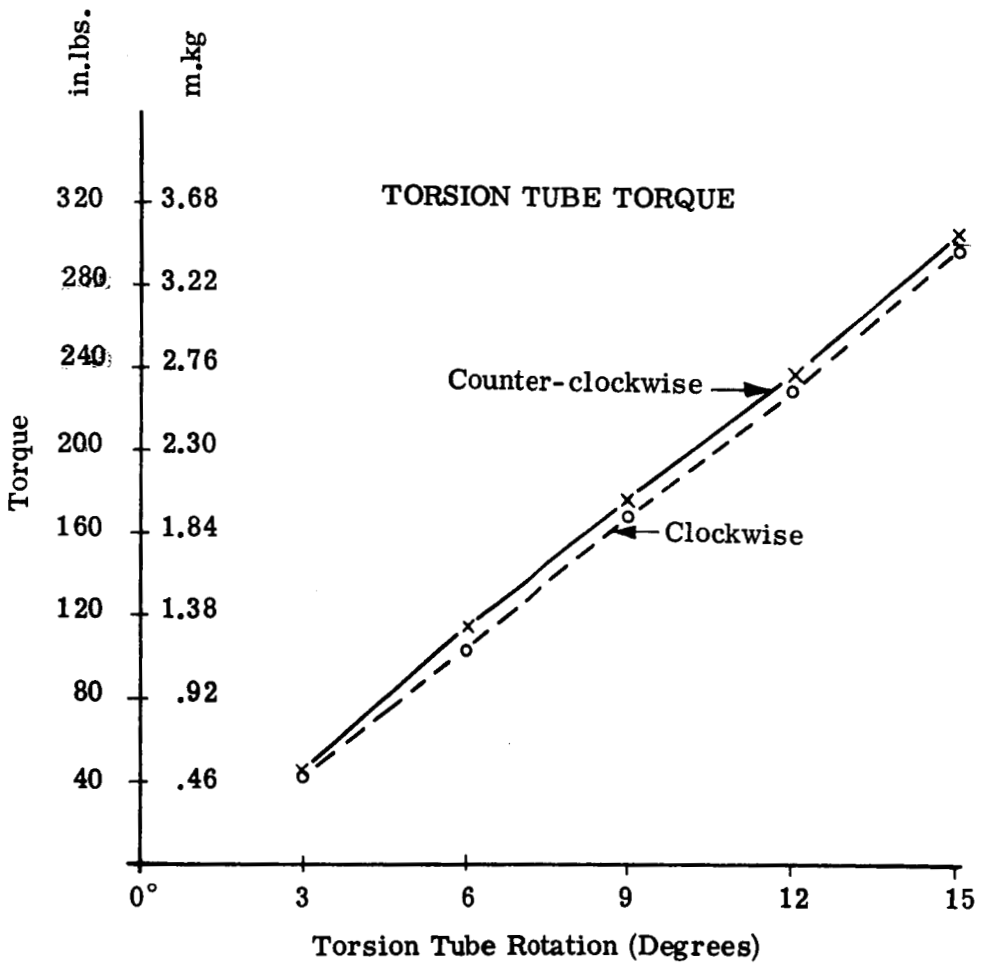

Figure 2-16. Torque Tube - Torque Versus Angle

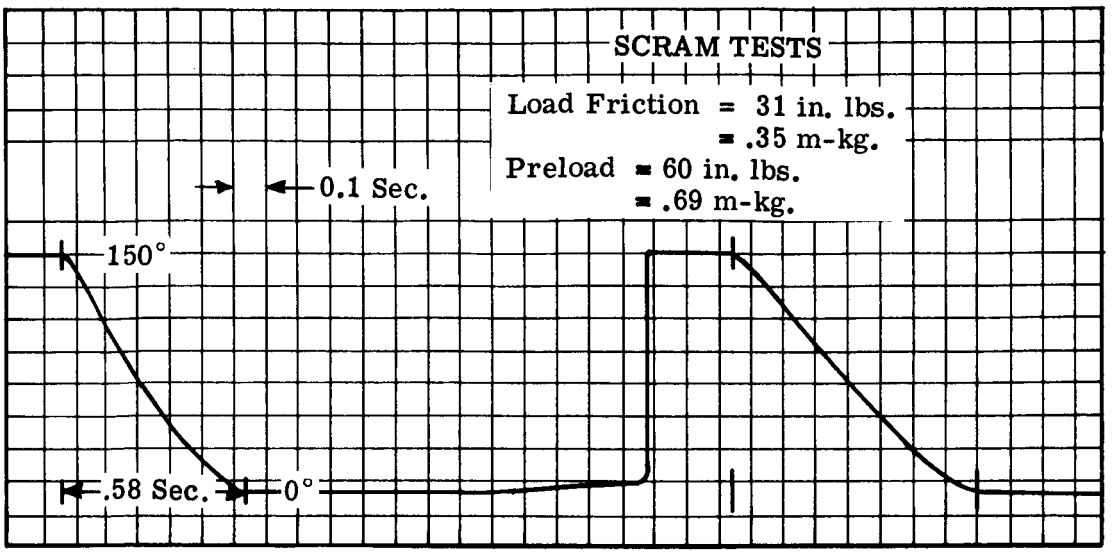

Figure 2-17. Initial Scram Characteristic

This figure shows no overshoot at the 15° position, indicating that the total energy is being absorbed by the brake band and the deceleration rate is greater than the required 2000 rad./sec.^{2}. These initial tests were performed on the Magneclutch brake test rig, which has an inertia of .224 N-m^2 (.56 lb. ft.^{2}) as opposed to the design load inertia of .264 N-m^2 (.66 lb. ft.^{2}).

Taking into consideration the inertia variation, it can be assumed from the above test results that the maximum load plus dynamic seal friction allowable is .30 m kg (26 inch pounds). Subtracting the seal friction of .081 m kg (7 inch pounds) as obtained from the tests described in Para. 2.2.3, the maximum load friction which will allow a 0.5 second scram time is .22 m kg (19 inch pounds).

This figure shows no overshoot at the 15° position, indicating that the total energy is being absorbed by the brake band and the deceleration rate is greater than the required maximum value. These initial tests were performed on the Magneclutch brake test rig, which has an inertia of .224 N-m^2 (.56 lb. $ft.^2$) as opposed to the design load inertia of .264 N-m^2 (.66 lb. $ft.^2$).

Taking into consideration the inertia variation, it can be assumed from the above test results that the maximum load plus dynamic seal friction allowable is .30 m kg (26 inch-pounds). Subtracting the seal friction of .081 m kg (7 inch-pounds) as obtained from the tests described in Paragraph 2.2.3, the maximum load friction which will allow a 0.5 second scram time is .22 m kg (19 inch-pounds).

SECTION III

DEVELOPMENT AND TEST OF THE COMMUTATION CIRCUIT

3.1 CIRCUIT CONCEPT

The requirement of the commutation circuit is to accept as an input a pressure differential signal and regulate the output torque by controlling the bellows pressure differential as a direct function of the input signal. The circuit must also sequence the pressurized bellows to provide a uniform output shaft rotation and maintain a constant output torque independent of shaft position. The direction of rotation is dictated by the sign of the input pressure differential. In order to minimize the number of moving parts in the actuator, the complete logic sequencing is performed by fluid interaction devices of the vortex amplifier concept.

The logic circuit is shown symbolically and described briefly (Figure 3-1). The circuit consists of:

a. A pressure error valve

b. A bi-stable directional amplifier

c. Eight vortex power amplifiers (one for each bellows)

d. Sixteen vortex selector valves

e. Four gimbal ring position pickoffs.

The power amplifier valves are conventional vortex valves with two outlet ports. One outlet port vents the power flow and the second outlet is connected directly to the bellows chamber. This second outlet is referred to as the "P_O tap." When no control flow is applied to the power amplifier valve, the greatest impedance to the supply flow is the outlet hole. The vortex chamber pressure and the P_O tap pressure are then essentially equal to the supply pressure. When a control flow is applied and a swirl is generated in the vortex chamber, the P_O pressure will reduce to a value equal to or lower than the outlet vent pressure. This reduction in P_O pressure allows the bellows flow (due to the bellows stroke) to cross the vortex chamber and vent through the outlet. The sequence of filling and emptying the bellows is shown in Figure 3-2.

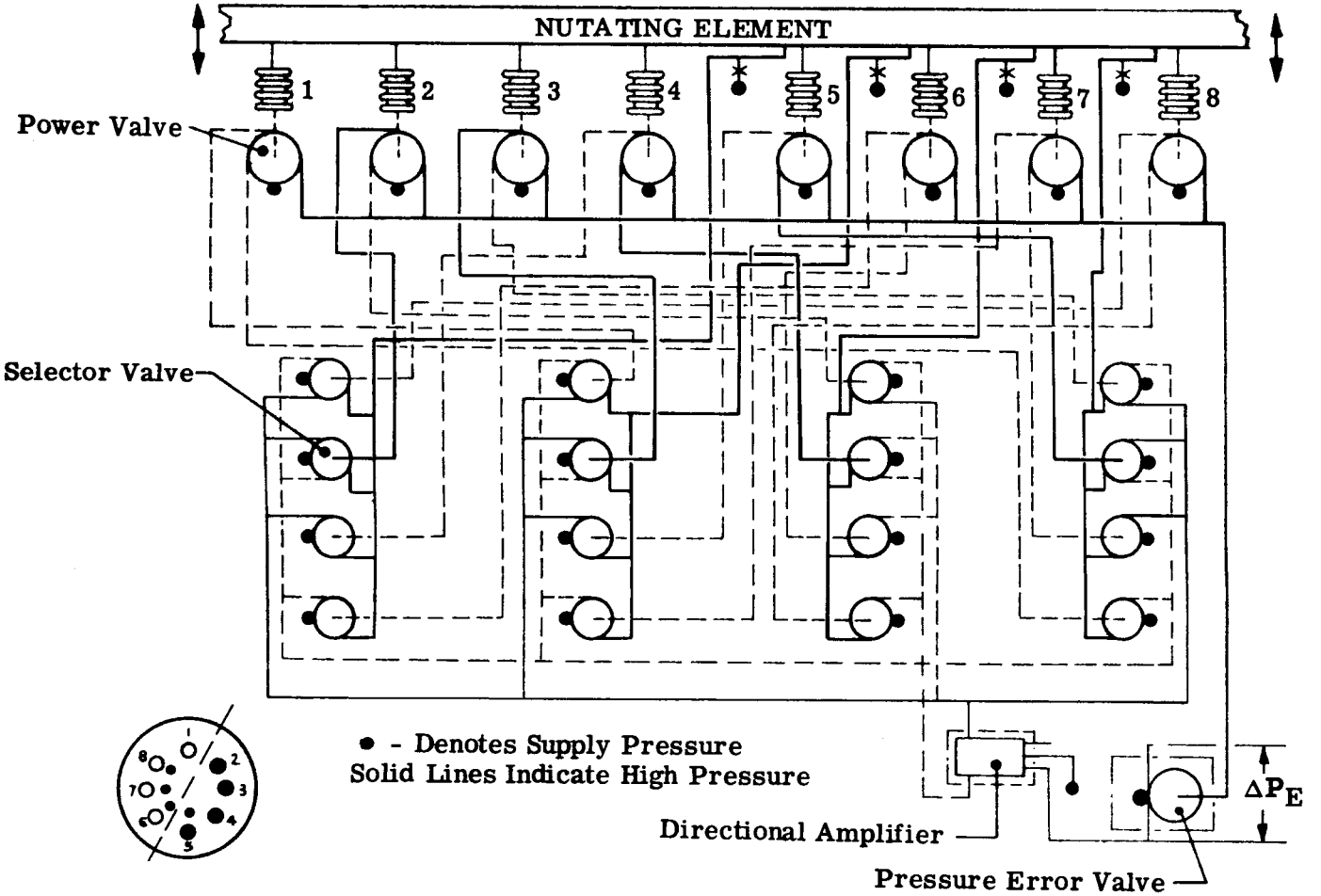

DESCRIPTION OF OPERATION

At the initiation of operation, the nutating elements are parallel and the position pickoffs' intermediate pressures are all above the threshold pressure. Signals are sent back from all pickoffs to the selector valves and bellows 2 through 5 are all pressurized.

Figure 3-1(a). Nutating Element, First Sequence

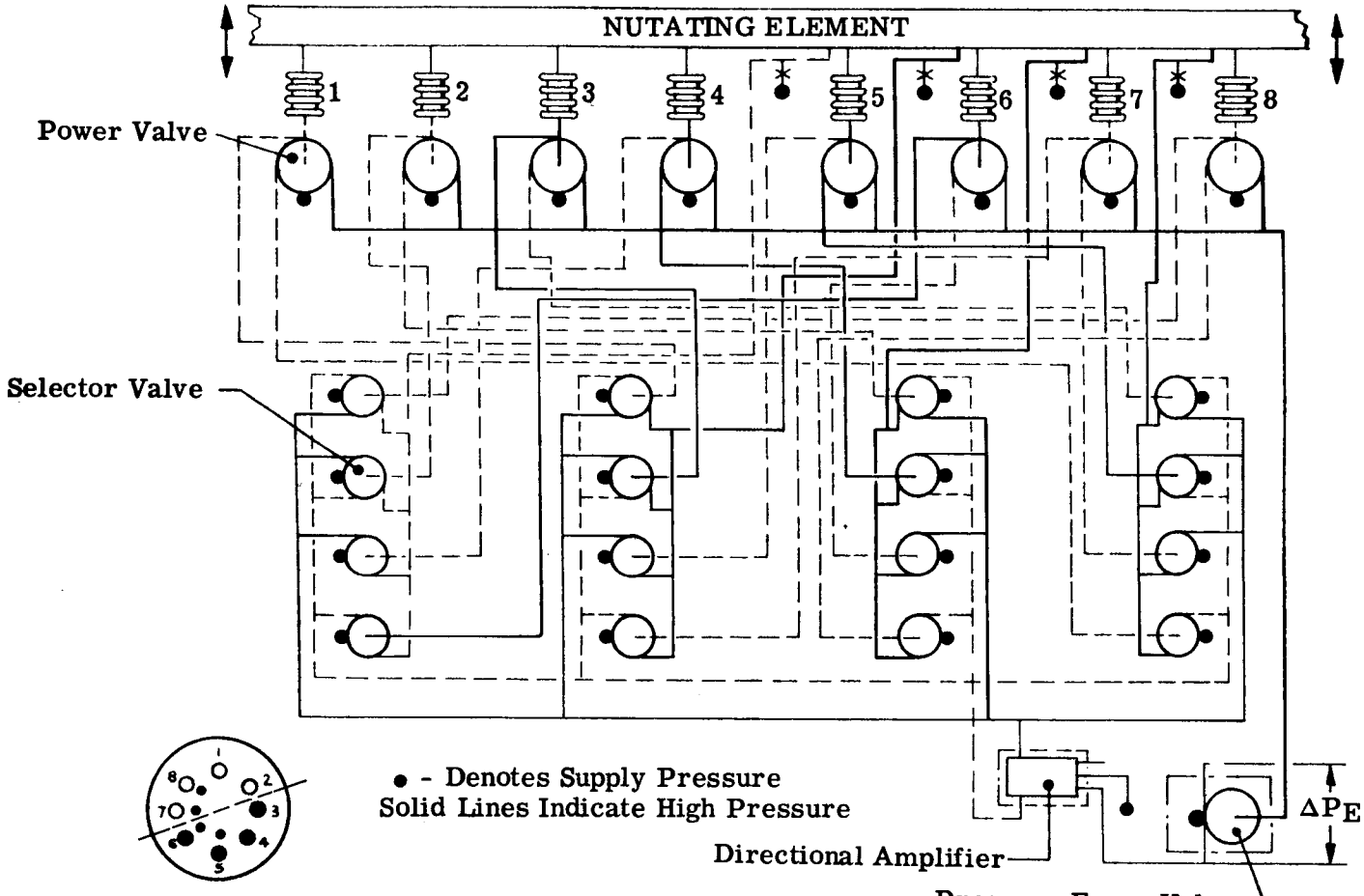

DESCRIPTION OF OPERATION

As soon as the nutating element begins to lift, the intermediate pressure of pickoff S_1 decreases. When its value is below that of the signal threshold, the second bellows loses pressure and the sixth bellows begins to fill. This moves the neutral axis of the nutating element 45° clockwise.

Figure 3-1(b). Nutating Element, Second Sequence

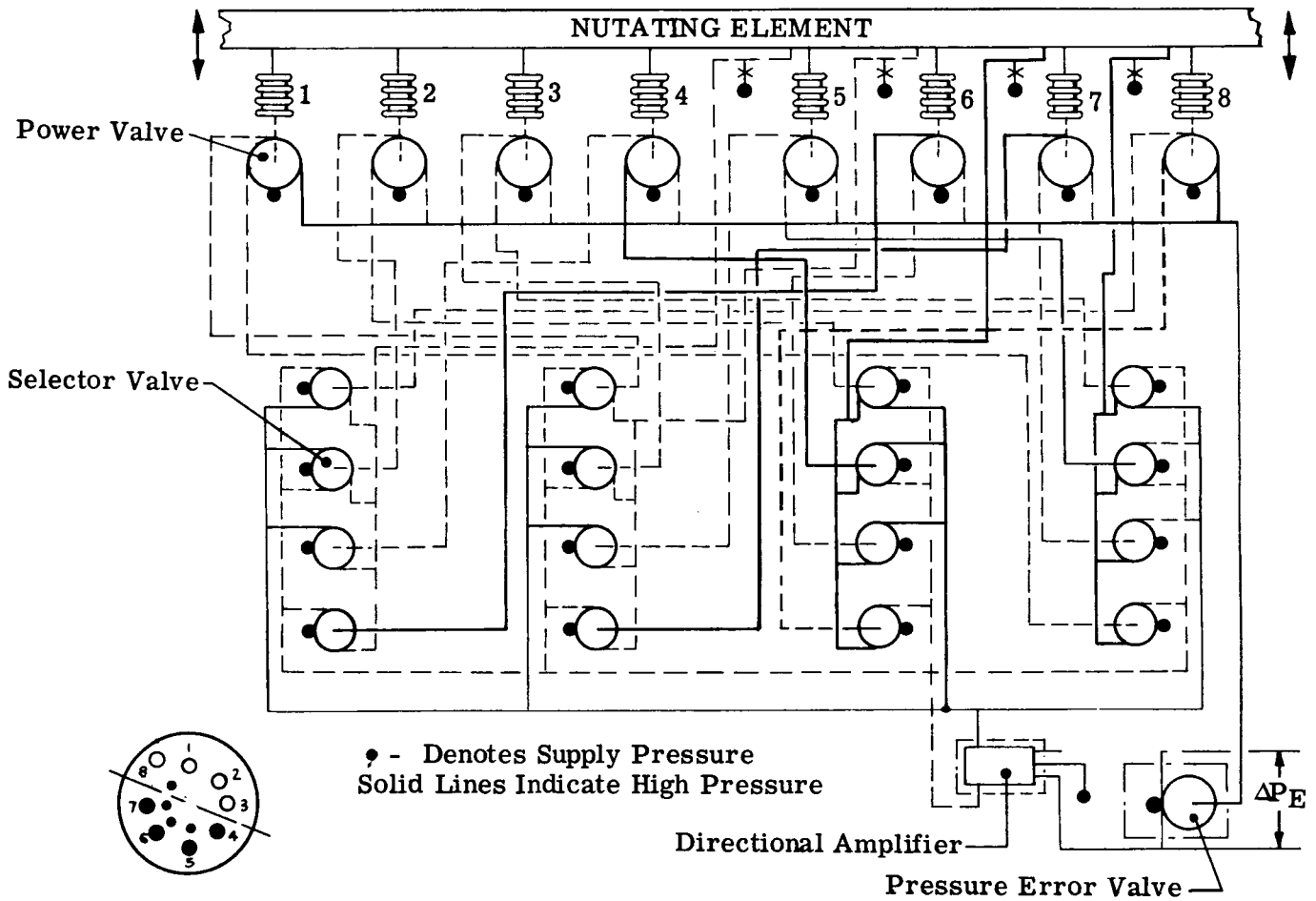

DESCRIPTION OF OPERATION

When the nuetral axis of the nutating element moves 45°, the element moves away from the pressure pickoff S_2 and its intermediate pressure begins to fall. When this pressure is below the signal threshold, bellows 3 loses pressure and 7 begins to fill. This moves the neutral axis of the nutating element another 45° clockwise.

Figure 3-1(c). Nutating Element, Third Sequence

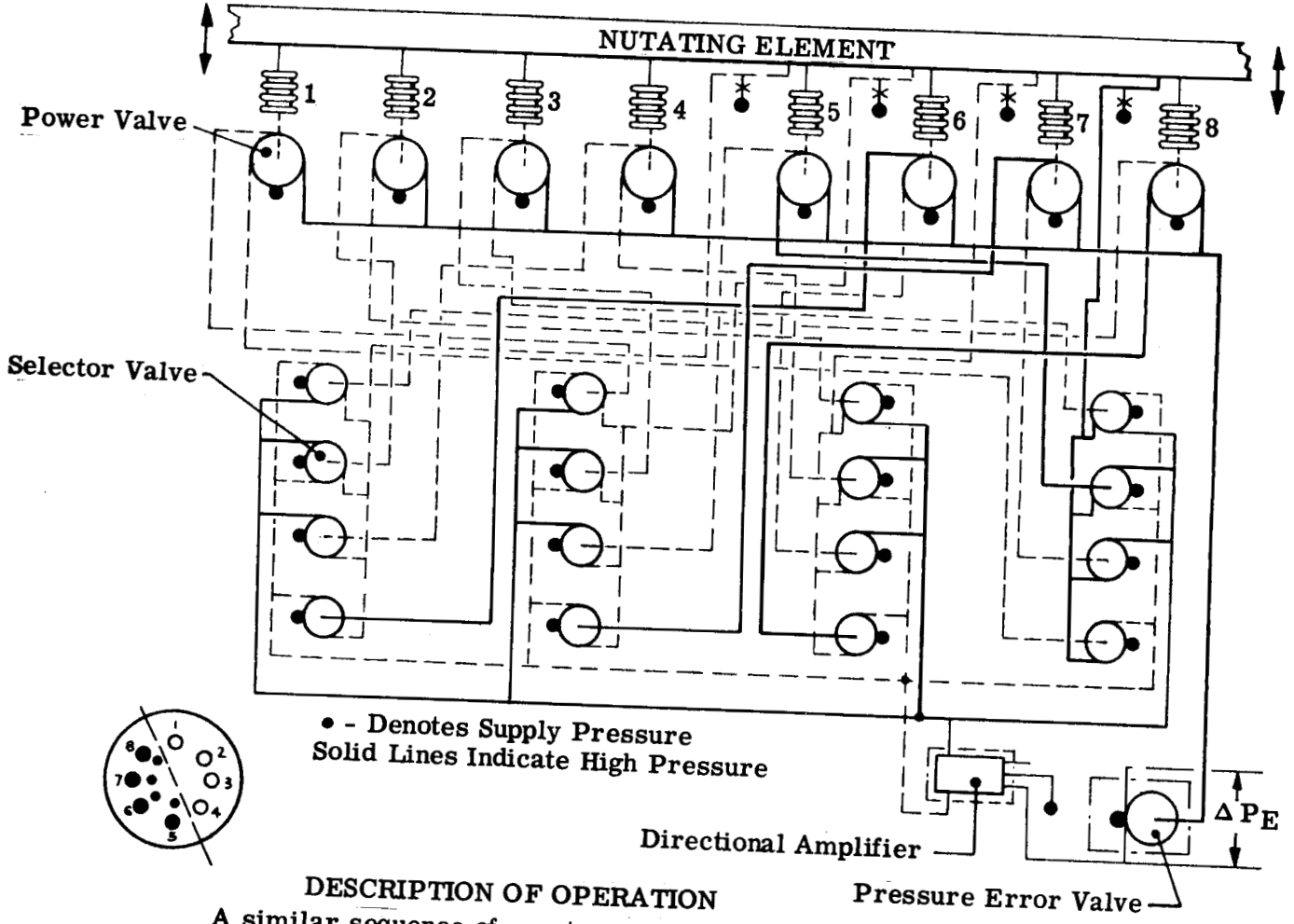

DESCRIPTION OF OPERATION

A similar sequence of events occurs as in Figure 3-1(c). The pressure pickoff S_3 loses pressure and bellows 8 fills while bellows 4 empties.

Figure 3-1(d). Nutating Element, Fourth Sequence

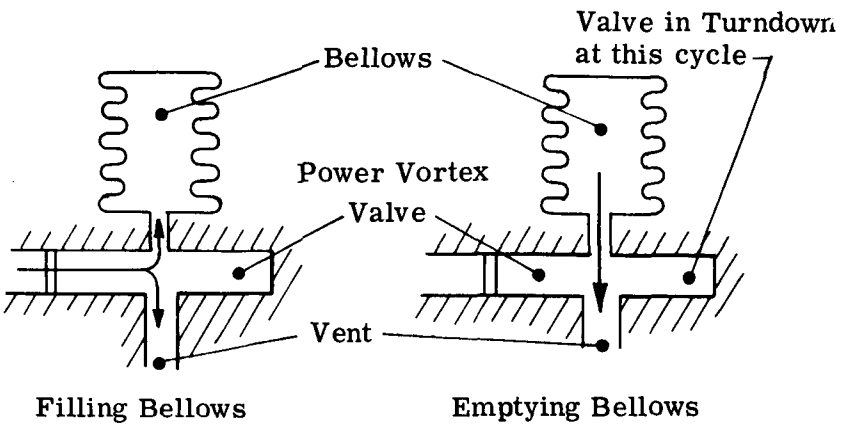

Figure 3-2. Vortex Valve-Bellows Interaction - Schematic

Referring to Figure 3-1, each power valve is controlled by a bias flow from the pressure error valve and a flow from one of two selector valves.

In order to understand the logic sequence of the circuit it is important to remember that the power valve bias flow is always greater than the signal from the selector valves. In the absence of a selector valve output, the bias flow would cause complete turndown of the eight power valves, resulting in a minimum P_O or bellows pressure. Flow from a selector valve will tend to reduce the effectiveness of the bias flow and result in an increase in the bellows pressure. The maximum pressure obtainable in the bellows will then depend on the magnitude of the bias flow relative to the selector valve output. Therefore a high bias flow will result in a low bellows pressure and vice versa. The bias flow is determined by the pressure error valve which in turn is controlled by the input pressure differential.

Since the control ports in the pressure error valve are opposing, an input pressure differential in either direction will generate a swirl and reduce the output or bias flow. The maximum obtainable bellows pressure is therefore directly proportional to the magnitude of the input error signal.

The directional amplifier is a bi-stable flip-flop. This unit provides a constant flow to one of two outputs depending on the sign of the input error signal. This flow determines the direction of rotation of the actuator.

The sixteen selector valves can be considered in groups of four. Each group has as inputs the directional signals from the bi-stable amplifier and one of the four pickoff pressures. The pickoff pressure is the intermediate pressure obtained between an upstream fixed orifice and a downstream variable bleed. The variable bleed is controlled by a leaf spring attached to the outer gimbal ring (see actuator schematic Figure 1-1). The level of the pickoff pressures is then an indication of the mesh point between the input and output gears.

An examination of the control port configuration for each group of selector valves indicates that the valves consist of two pairs, each operating in push-pull fashion. The direction signal pressure determines which pair are functioning and which pair remain in full turndown, when the pickoff pressure varies. The outputs of each pair of selector valves are connected through the corresponding power valves to bellows which are 180° apart, and each pair of the group of four connect to bellows which are displaced by 90°.

The selector valve outputs will then control the power valves to maintain four of the eight bellows at a high pressure level and the opposed four at a low pressure level. The force centroid of the pressurized bellows is designed to lead the gear mesh point by 45°, and a torque moment on the gears is produced. As the mesh point tends to move toward the force centroid, the change in pickoff pressures causes the next consecutive bellows to pressurize and the last bellows (180° opposed) to lose pressure. In this manner, the force centroid is maintained at a constant angle relative to the mesh point. When the directional signal is reversed, the bellows pressures change to shift the force centroid by 90° across the mesh point, resulting in a torque moment in the opposite direction.

Due to the closed loop nature of the commutation circuit, the application of a stall torque load, or back driving of the actuator, will not cause the gear teeth to disengage. The torque speed characteristics of the actuator are then identical to a conventional gear or vane motor and transmission.

3.2 INVESTIGATION OF VORTEX CHARACTERISTICS

Before a design was made of the commutation circuit, a detailed investigation was conducted of the basic vortex amplifier characteristics. The objective of this investigation was to determine experimentally the effects of varying the critical vortex parameters.

The results of varying control to outlet area ratio are shown in Figures 3-3 and 3-4.

The results of varying the porting aspect ratio are shown in Figures 3-5 and 3-6, and the chamber to outlet diameter ratio is shown in Figures 3-7 and 3-8.

The vortex chamber dimensions used in this study are given in the table of Figure 3-9.

From these tests the following dimensions were derived.

	Pressure Error Valve (2)		Power Valve (8)		Selector Valve (16)	
	mm.	in.	mm.	in.	mm.	in.
Chamber diameter	25.4	1.	16.5	.650	9.53	.375
Chamber depth	3.18	.125	3.18	.125	1.58	.062
Control port width	.79	.031	.79	.031	.38	.015
Supply port width	6.35	.250	6.35	.250	3.18	.125
Outlet hole diameter	3.2	.128	2.03	.080	1.02	.040
P_O tap diameter	2.1	.080	1.02	.040	0	0

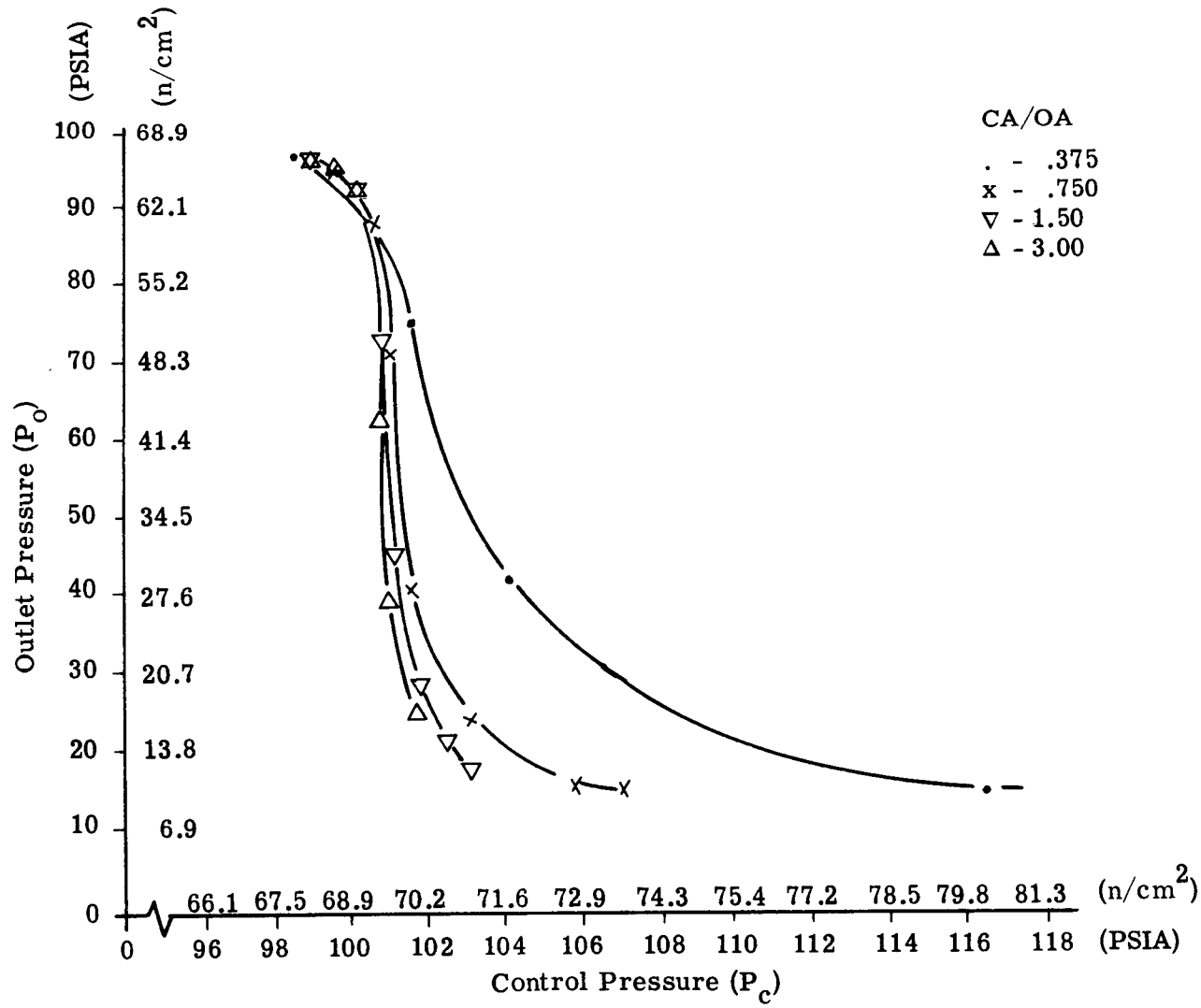

Figure 3-3. Pressure Characteristics for Various Control to Outlet Area Ratios

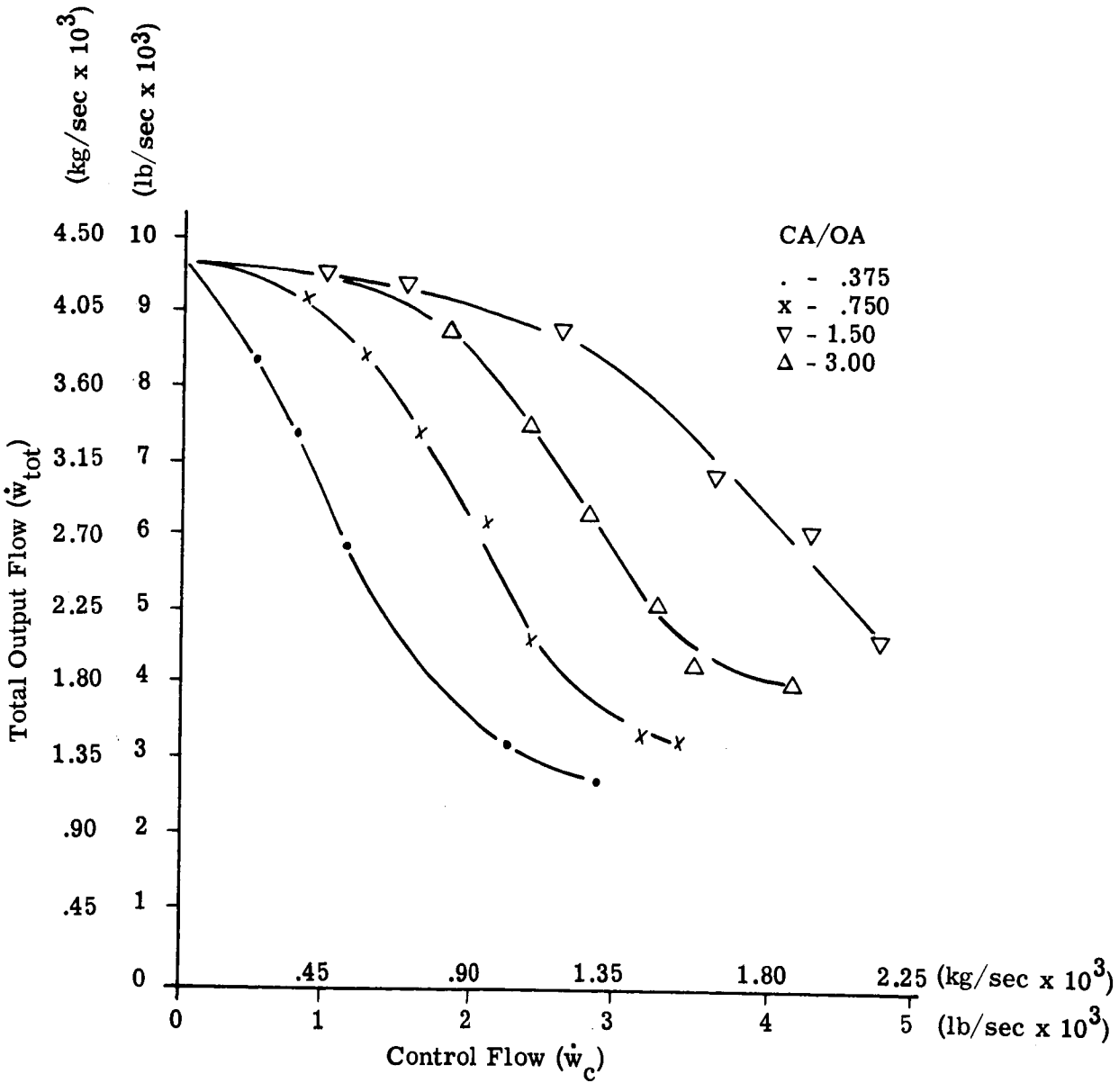

Figure 3-4. Flow Characteristics for Various Control to Outlet Area Ratios

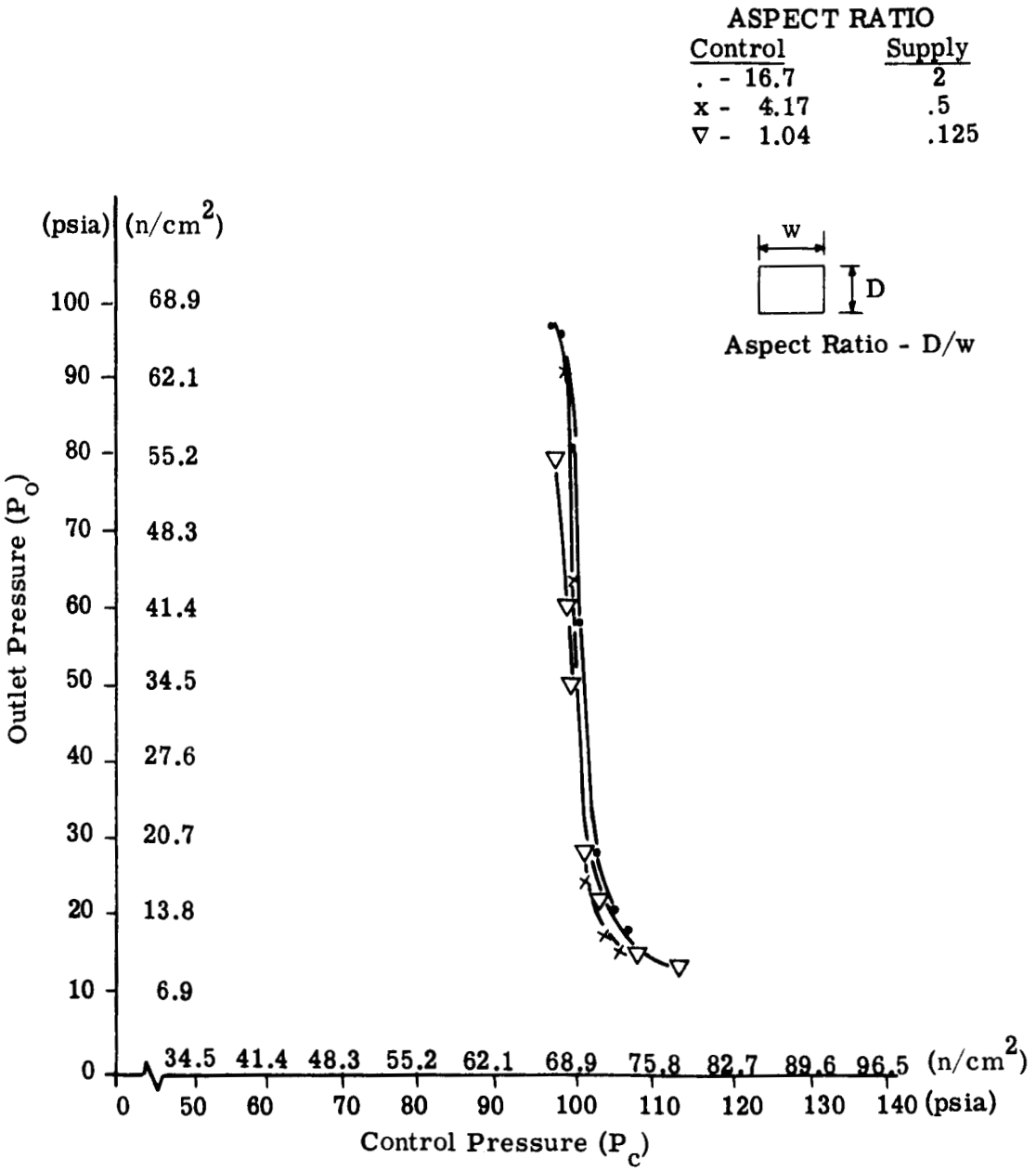

Figure 3-5. Pressure Characteristics for Various Port Aspect Ratios

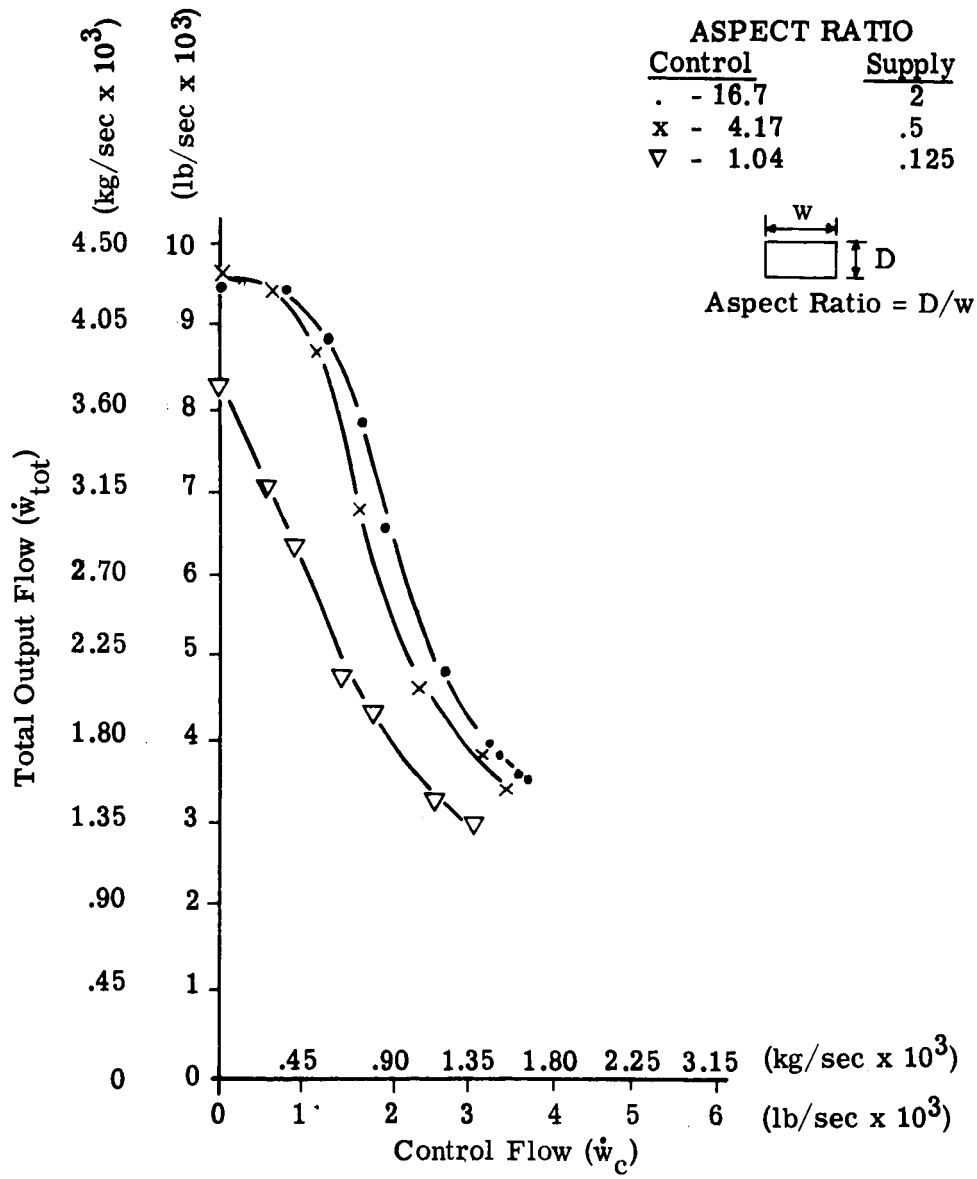

Figure 3-6. Flow Characteristics for Various Port Aspect Ratios

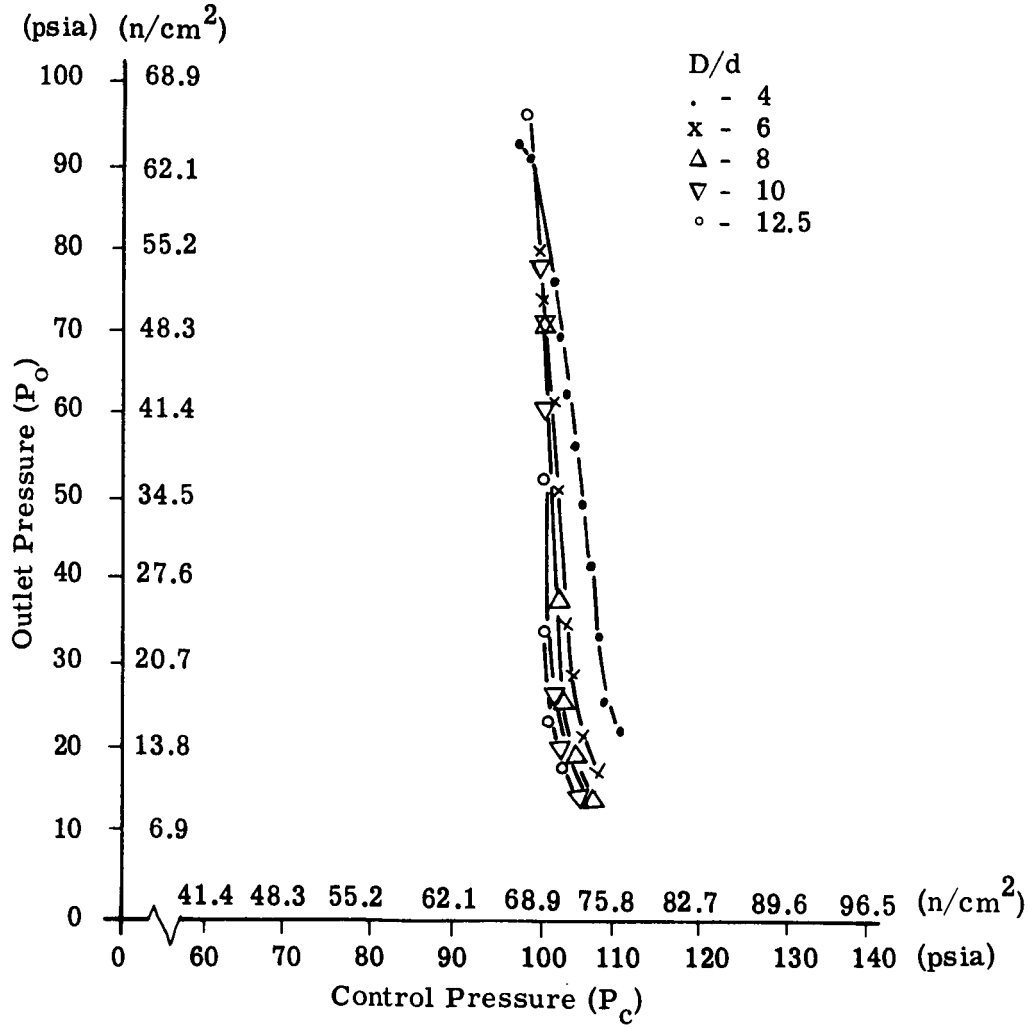

Figure 3-7. Pressure Characteristics for Various Chamber Diameter Ratios

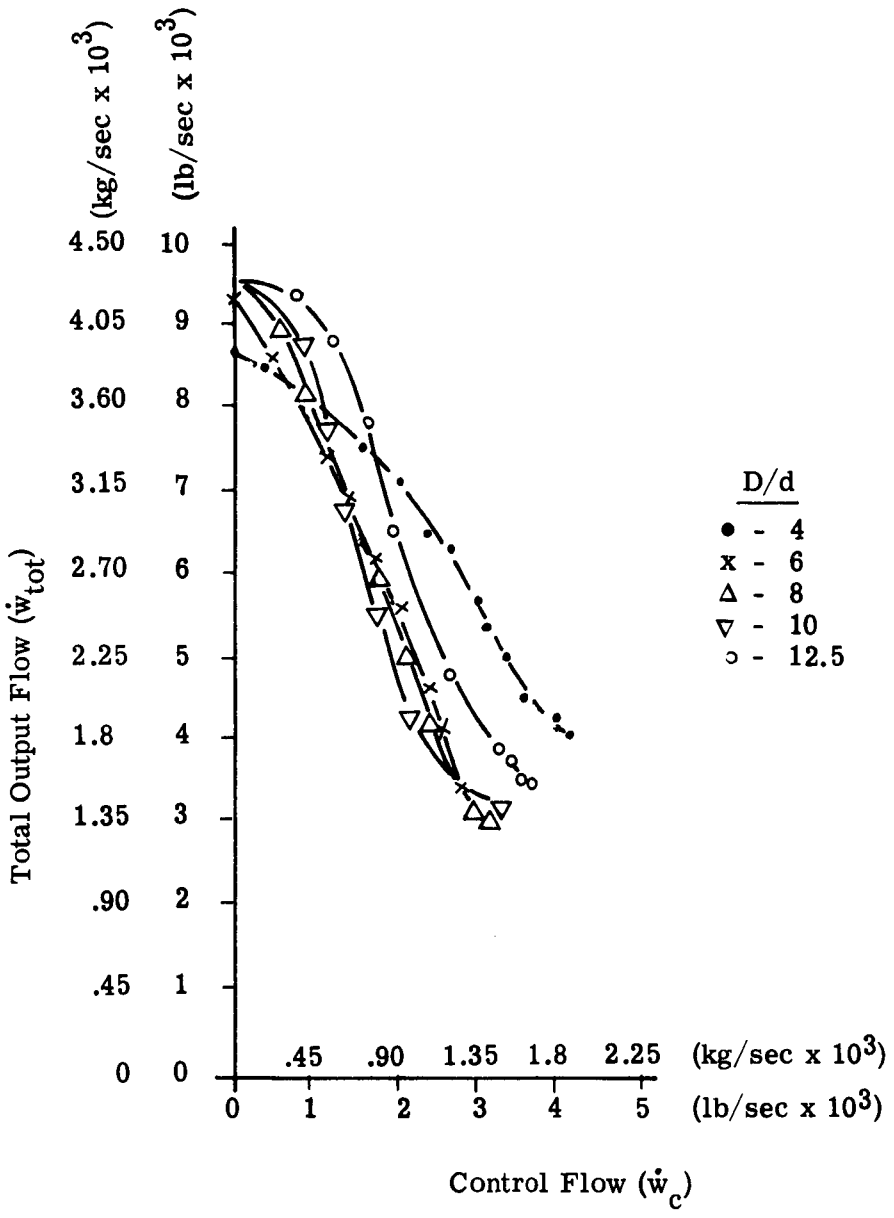

Figure 3-8. Flow Characteristics for Various Chamber Diameter Ratios

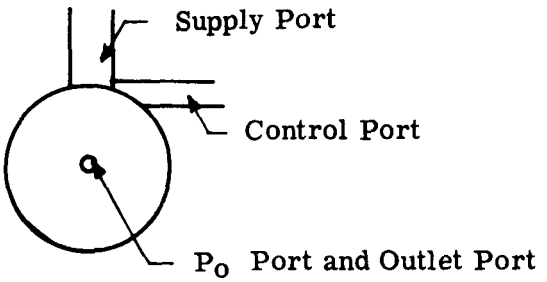

FIGURES 3-3 and 3-4

Chamber Dia.		Chamber Depth		Supply Port Width		Control Port Width		P_o Dia.		Outlet Dia.	
(mm)	(In)	(mm)	(In)	(mm)	(In)	(mm)	(In)	(mm)	(In)	(mm)	(In)
25.4	1.00	3.17	.125	6.35	.25	.381	.015	1.02	.040	2.04	.080
25.4	1.00	3.17	.125	6.35	.25	.762	.030	1.02	.040	2.04	.080
25.4	1.00	3.17	.125	6.35	.25	1.524	.060	1.02	.040	2.04	.080
25.4	1.00	3.17	.125	6.35	.25	3.048	.120	1.02	.040	2.04	.080
FIGURES 3-5 and 3-6											
25.4	1.00	6.35	.25	3.17	.125	.381	.015	1.02	.040	2.04	.080
25.4	1.00	3.17	.125	6.35	.25	.762	.030	1.02	.040	2.04	.080
25.4	1.00	1.585	.0625	12.70	.50	1.524	.060	1.02	.040	2.04	.080
FIGURES 3-7 and 3-8											
8.13	.320	3.17	.125	6.35	.25	.762	.030	1.02	.040	2.04	.080
12.19	.480	3.17	.125	6.35	.25	.762	.030	1.02	.040	2.04	.080
16.26	.640	3.17	.125	6.35	.25	.762	.030	1.02	.040	2.04	.080
20.3	.800	3.17	.125	6.35	.25	.762	.030	1.02	.040	2.04	.080
25.4	1.000	3.17	.125	6.35	.25	.762	.030	1.02	.040	2.04	.080

All Vortex Valve Dimensions: ±.001 inch
Surface Finish: 16 RMS or better
All Pressure Readings: ±0.5% full scale (250 psig)
All Weight Flow Readings: ±5%
Supply Pressure 68.9 n/cm^2 (100 psia)
Vent Pressure 10.3 n/cm^2 (15 psia)
Fluid - N_2 gas at 70°F

Figure 3-9. Vortex Valve Dimensions and Tolerances

A further series of tests was performed to ascertain the effect of certain deviations from the basic vortex configuration.

Figure 3-10 shows the effect of varying the angle at which the control flow enters the vortex chamber. The curve showing the zero degree angle indicates questionable data, since similar valves will produce a much lower P_O pressure in turndown. The general conclusion drawn was that increasing the control port angle to at least 30° did not materially affect the valve performance.

Figure 3-11 indicates the effect of reducing the control port tangent point to a smaller effective radius.

Figure 3-12 shows the negligible improvement obtained by the introduction of a second supply port.

Figure 3-13 shows the variation in turndown which can be obtained by introducing a spoiler in the chamber.

3.3 BREADBOARD COMMUTATION CIRCUIT

3.3.1 Logic Circuit

A breadboard model of one half the commutation logic circuit was fabricated in sheets of plastic. The sheets were then bolted together to form three blocks - two selector valve blocks each containing four selector valves, and one power valve block containing four power valves. One selector valve block is shown in Figure 3-14. The purpose of the breadboard tests was to demonstrate the feasibility of employing vortex amplifiers to perform the required logic, and to determine the circuit pressure and flow levels. Figure 3-15 shows the logic circuit as connected on the test bench.

The circuit was first connected as shown schematically in Figure 3-16(a). The supply pressures were controlled by external regulators. The P_O (or bellows) pressures obtained are shown in Figure 3-16(b) for each combination of pickoff pressure (P_{S2} and P_{S4}) and each directional signal (P_{DL} and P_{DR}). It can be seen from Figure 3-16(b) that the circuit does perform the required sequencing of pressure (two outputs are pressurized at any given time), and the pressure differentials obtained are equal or greater than the design goal of 48 n/cm^2 (70 psi).

Since pressure regulators cannot be used in a practical system to set the supply pressures, the regulators were replaced by fixed orifices from the common plenum, as shown in Figure 3-17(a). The results obtained with this configuration are shown in Figure 3-17(b). The use of fixed orifices to set the supply pressure levels results in variations in the supply pressures through the logic sequence. This is due to the varying flow requirements of the selector and power valves. Variations in these supply pressures (P_{SS} and P_{SP}) affect the impedance match of the selector valve outputs to the power valve control, and therefore affect the ability of the selector valve to control the power valve. The result in P_O pressures is the "Staircase" effect shown in Figure 3-17(b).

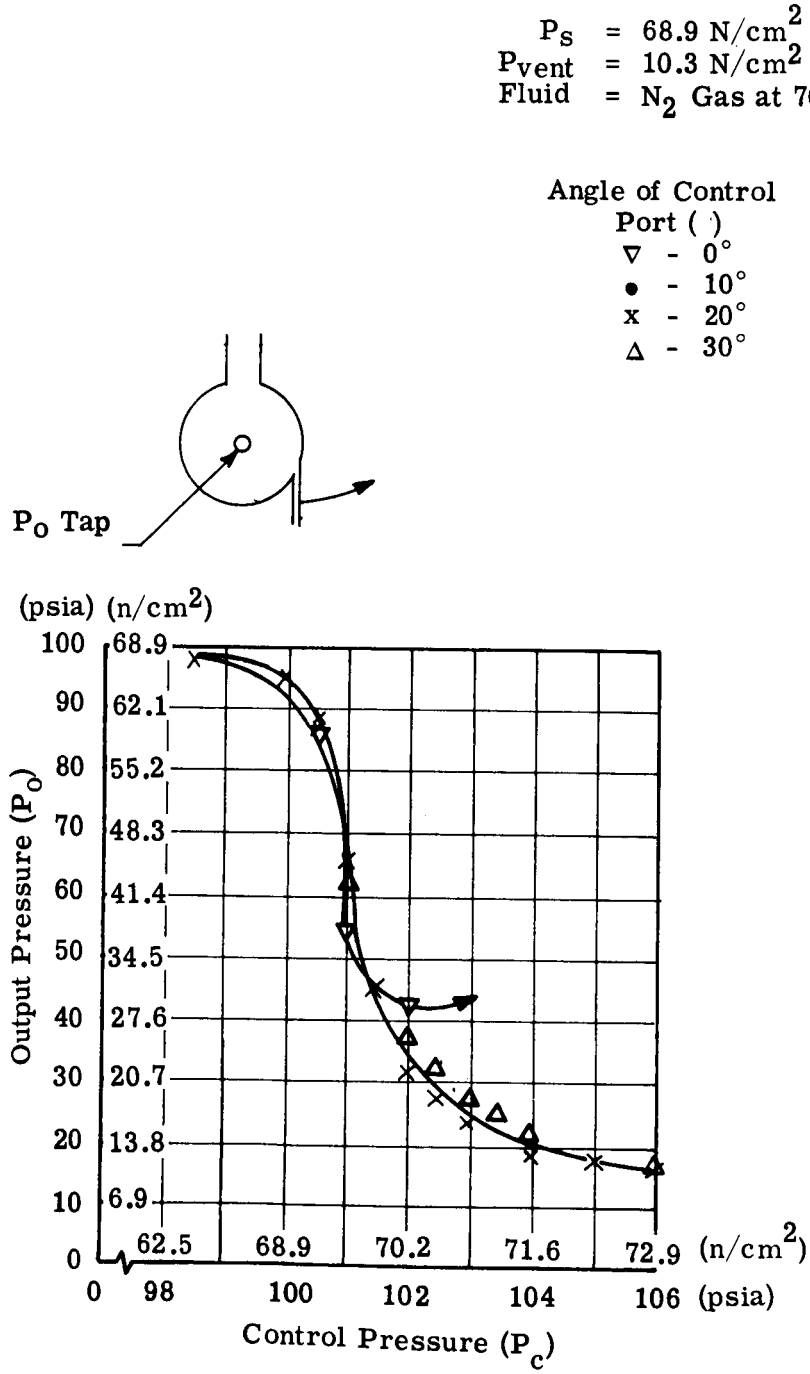

Figure 3-10. Pressure Curves for Vortex Valves with Different Control Port Angles

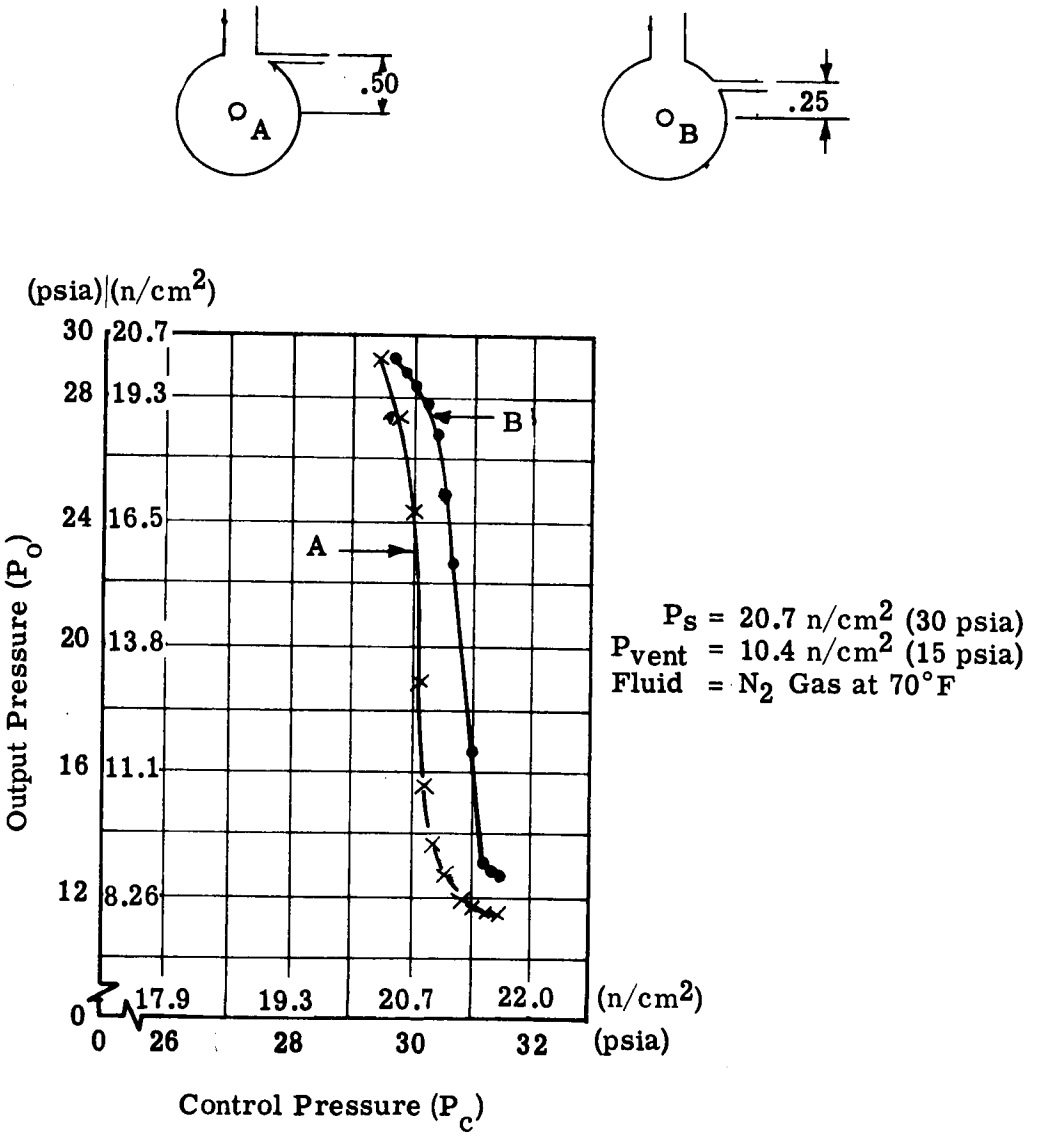

Figure 3-11. Pressure Curves for Vortex Valves with Control Ports Entering the Chambers at Different Radii

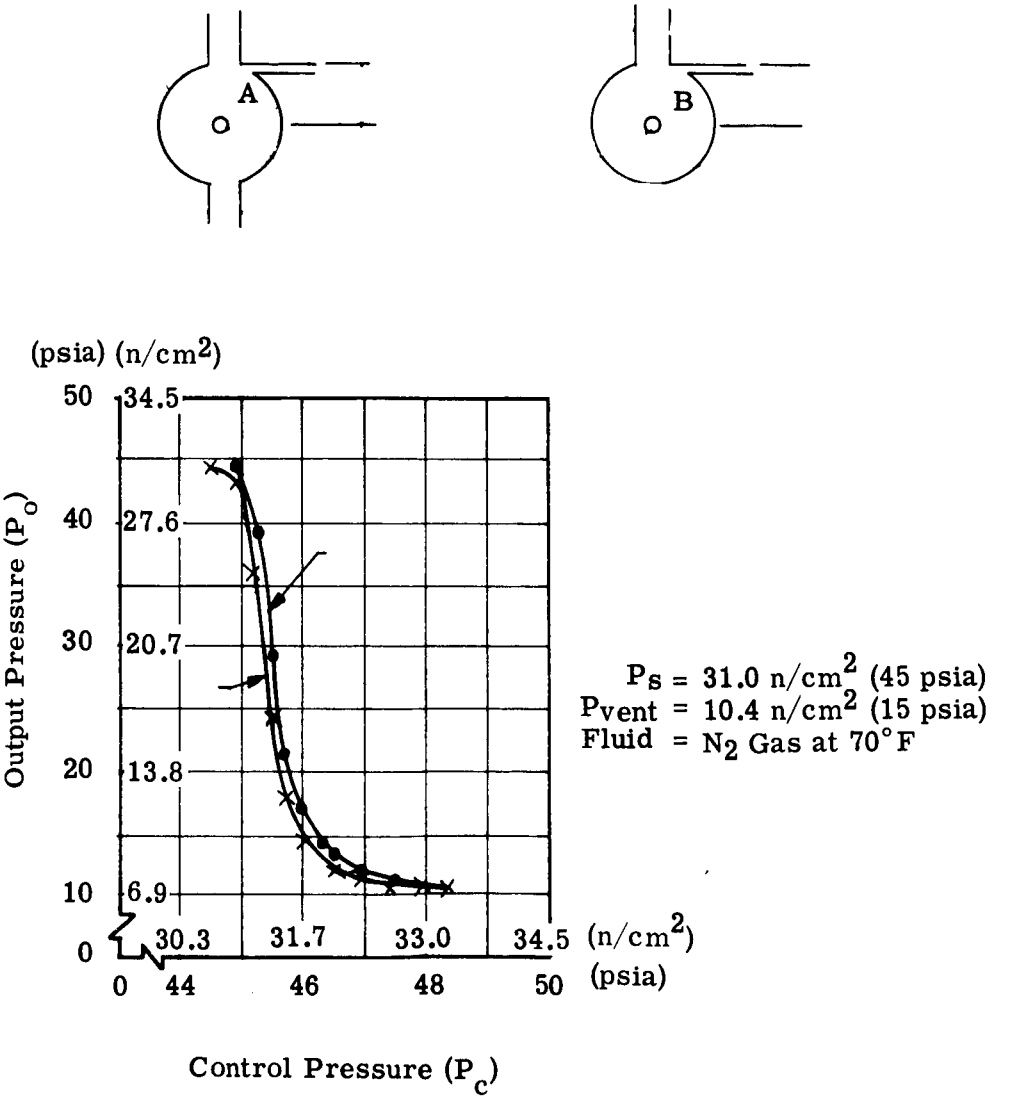

Figure 3-12. Pressure Curves for Vortex Valves with a Different Number of Supply Ports

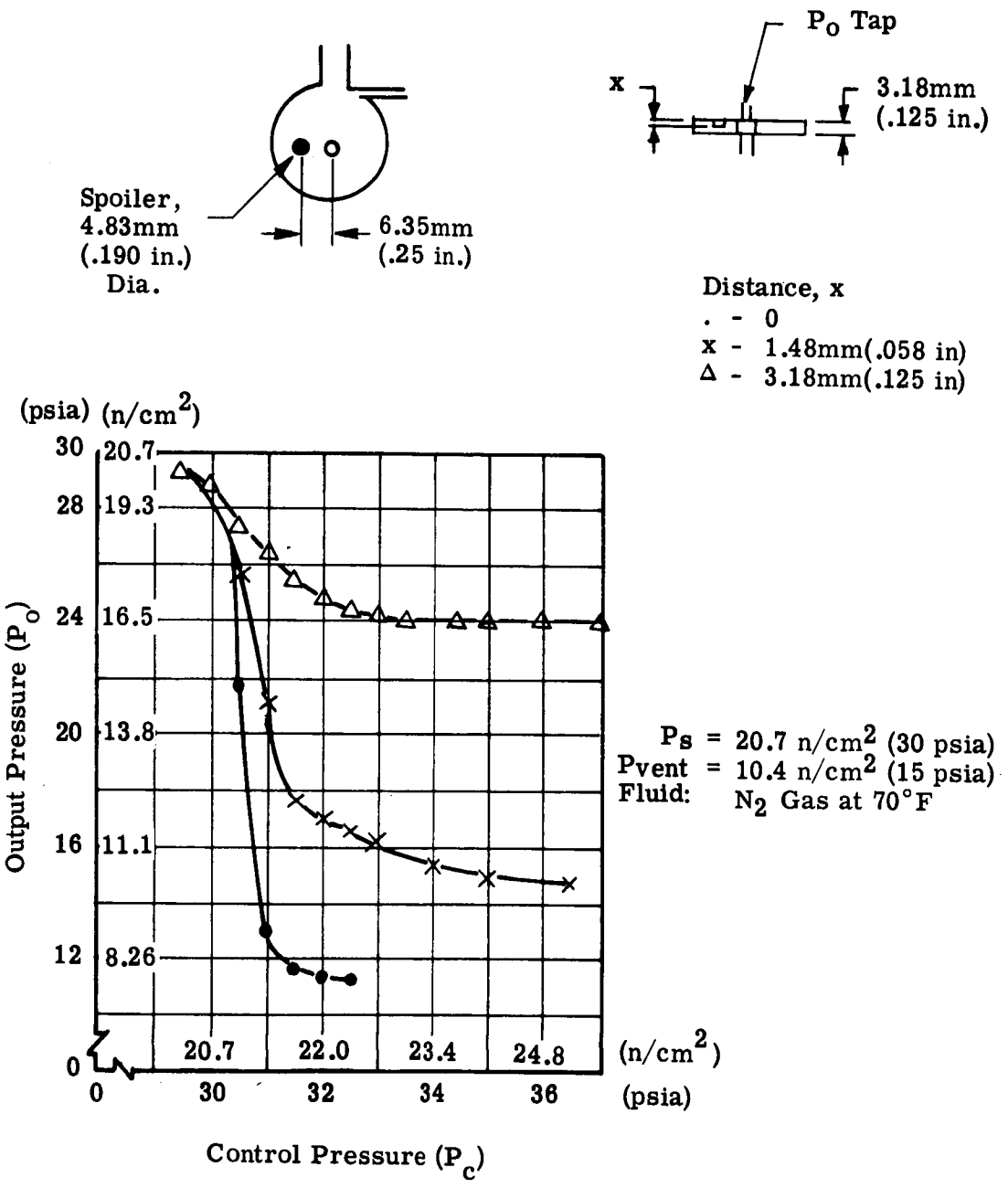

Figure 3-13. Pressure Curves for Vortex Valve using "Spoiler" Set at Varying Depths

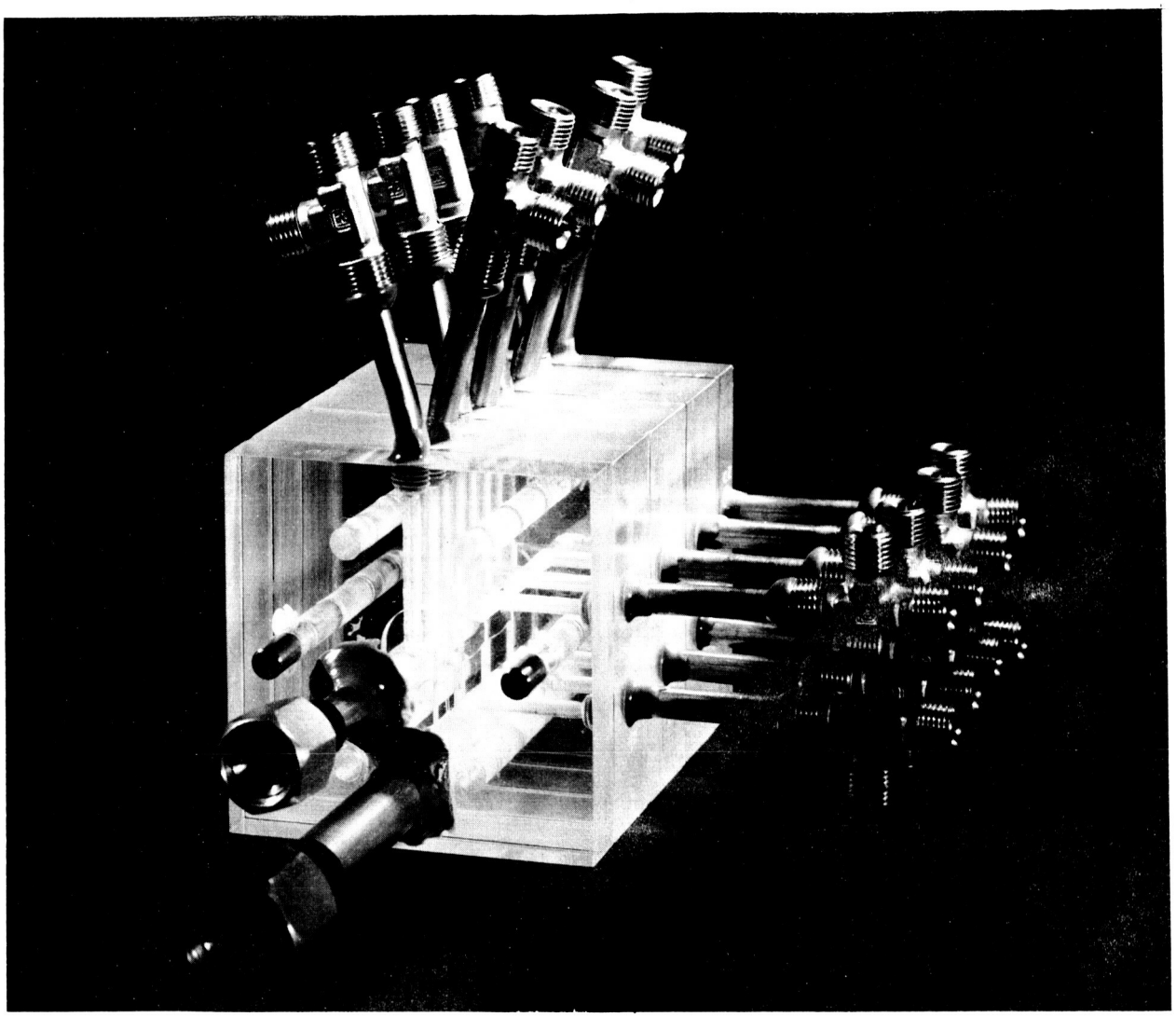

Figure 3-14. Selector Valve Block

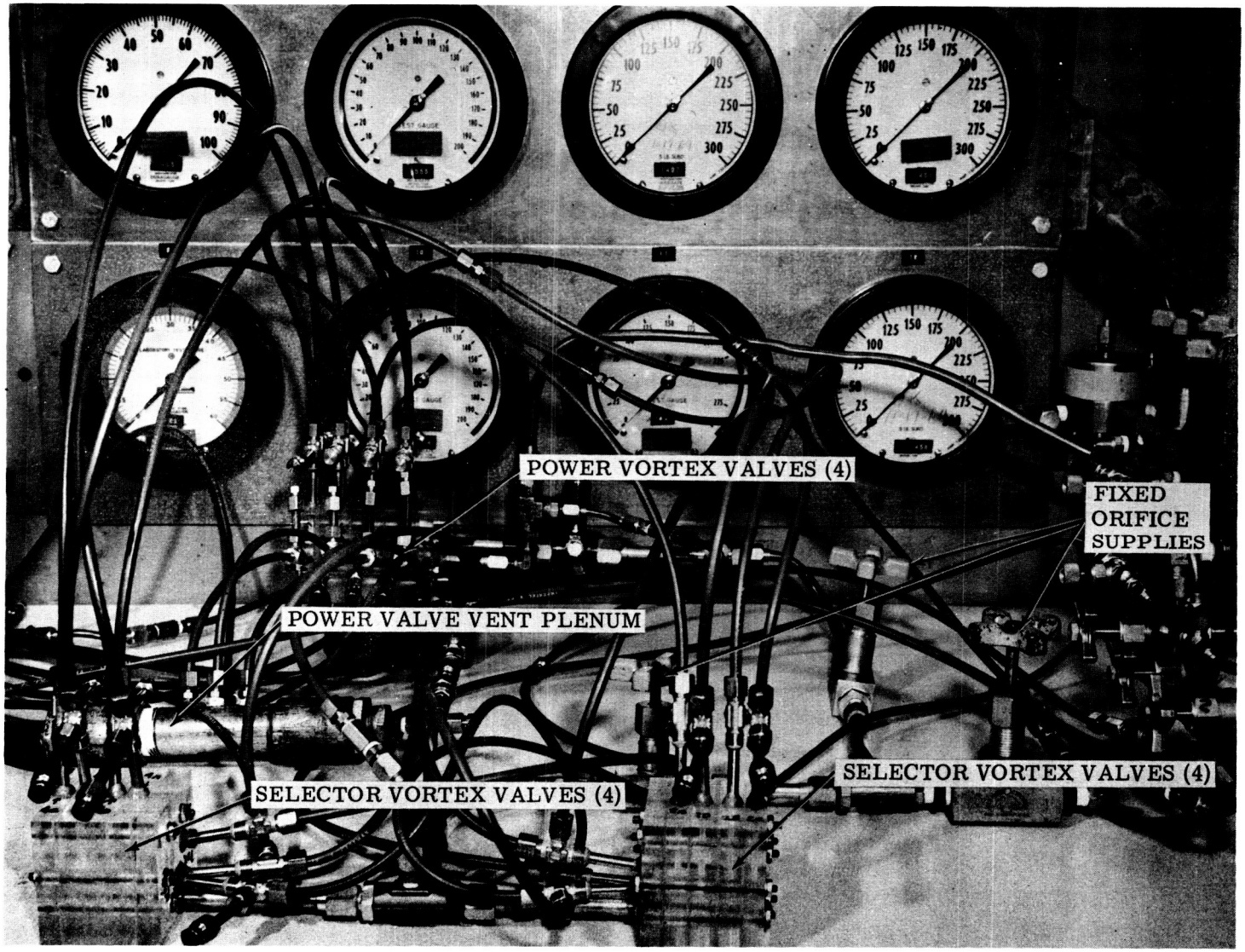

Figure 3-15. Model Commutation Circuit

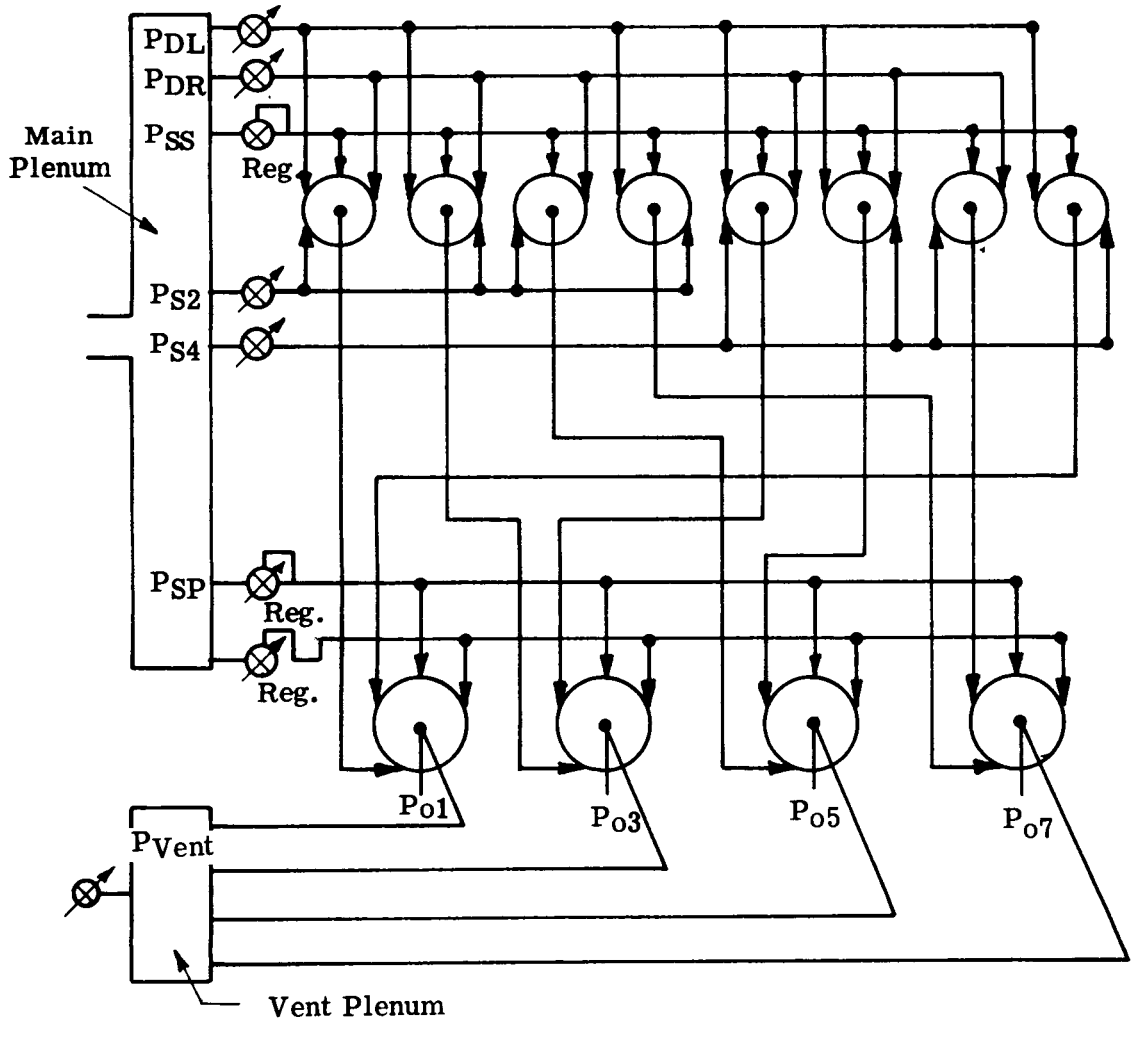

P_{DL} - Left Directional Pressure

P_{DR} - Right Directional Pressure

P_{S2} - Position Pick-Off Signal Pressure 2

P_{S4} - Position Pick-Off Signal Pressure 4

P_{Bias} - Power Valve Bias Pressure

P_{SS} - Selector Valve Supply Pressure

P_{SP} - Power Valve Supply Pressure

P_o - Power Valve Output Pressure (To Bellows)

Figure 3-16(a). Model Commutation Circuit - External Regulation

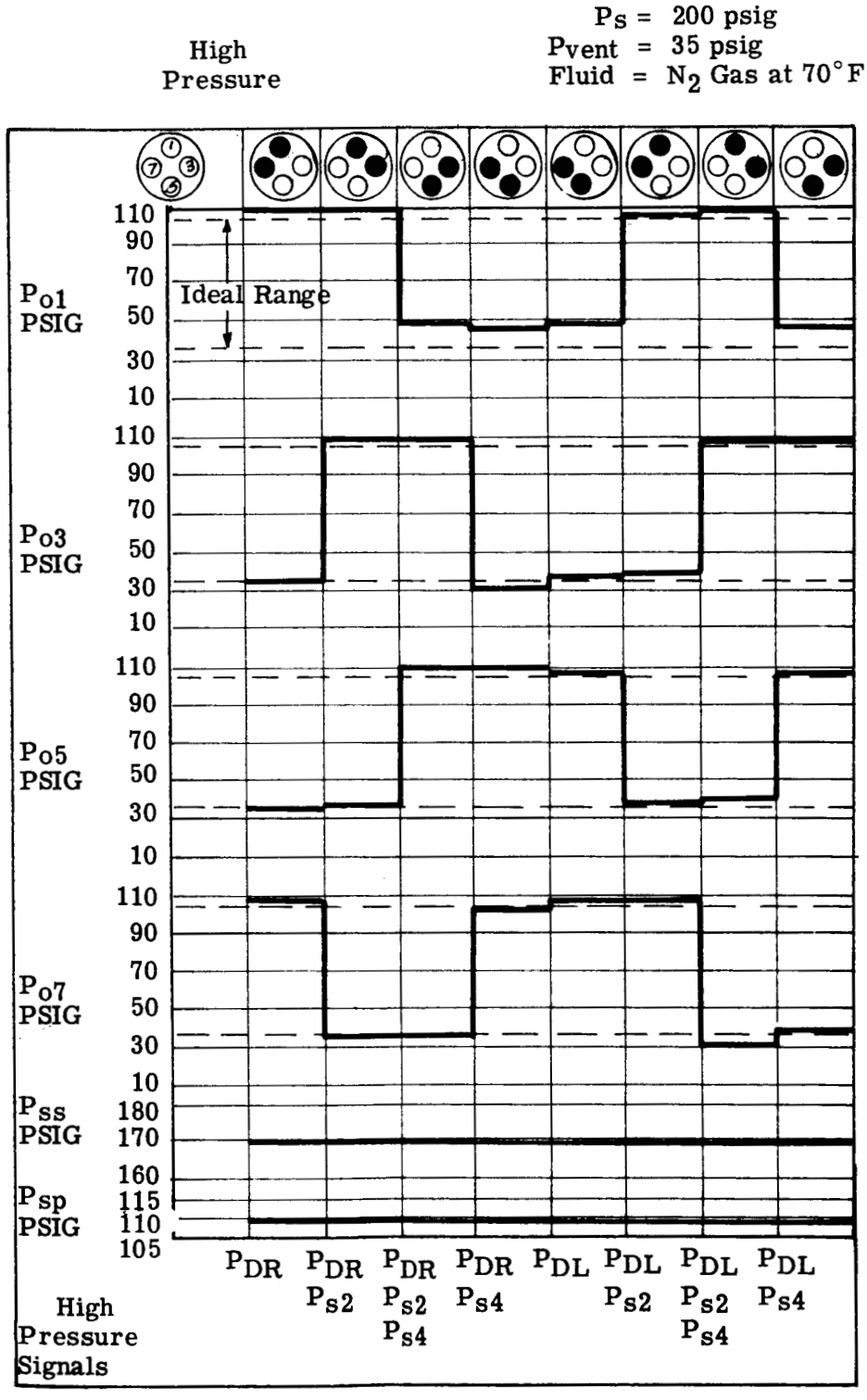

Figure 3-16(b). Model Commutation Circuit - External Regulation

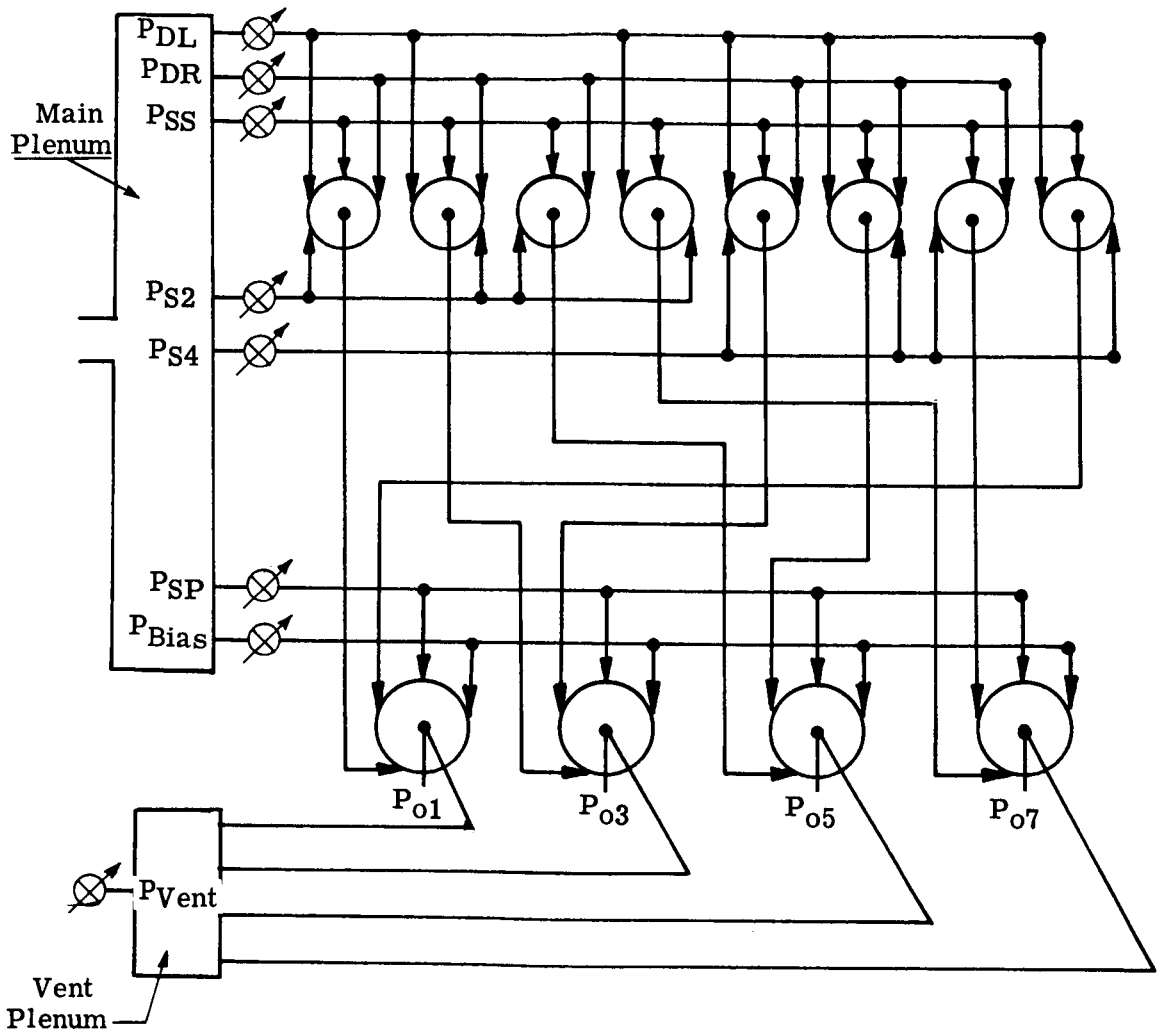

Figure 3-17(a). Model Commutation Circuit - Fixed Orifices

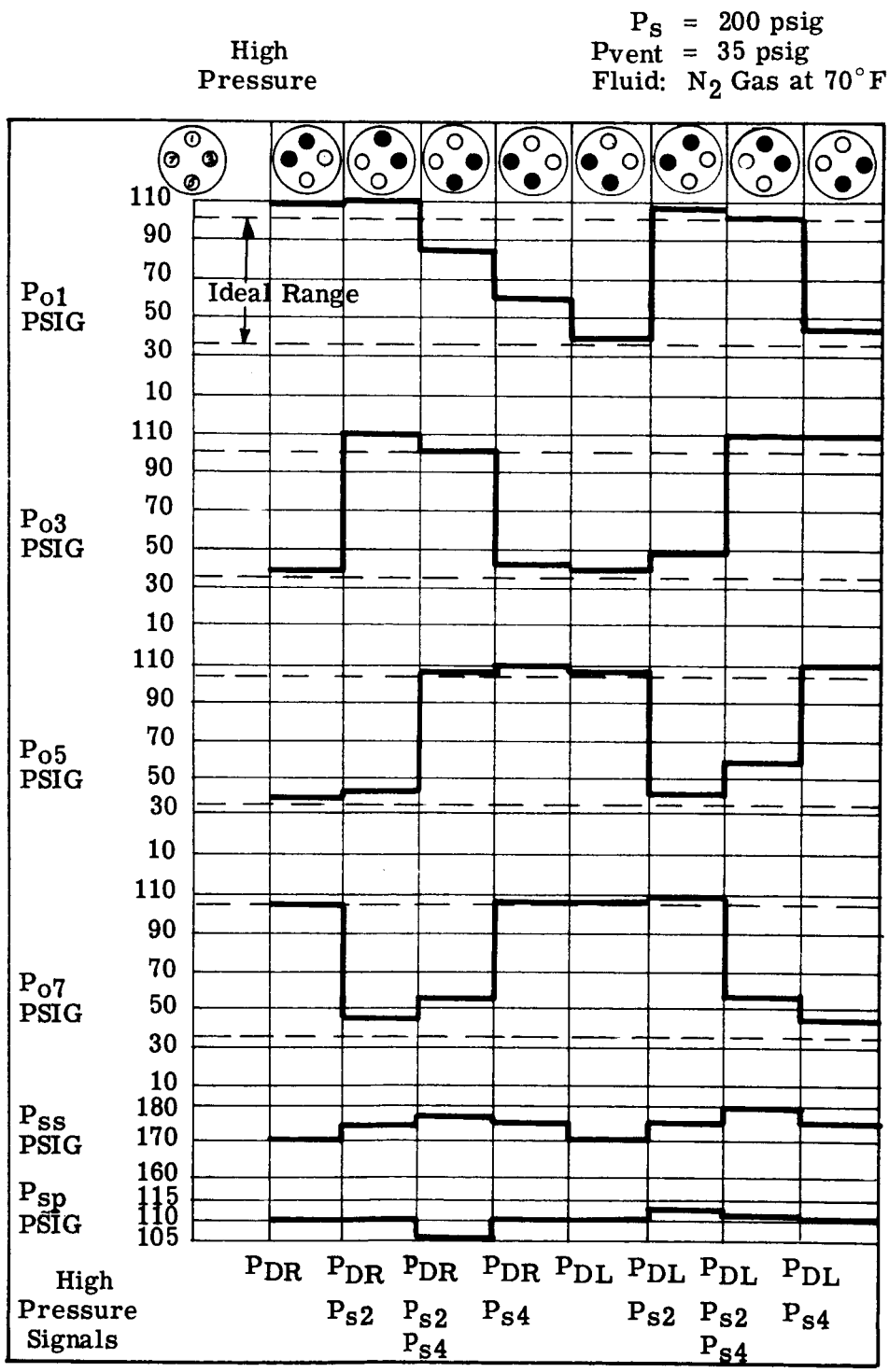

Figure 3-17(b). Model Commutation Circuit - Fixed Orifices

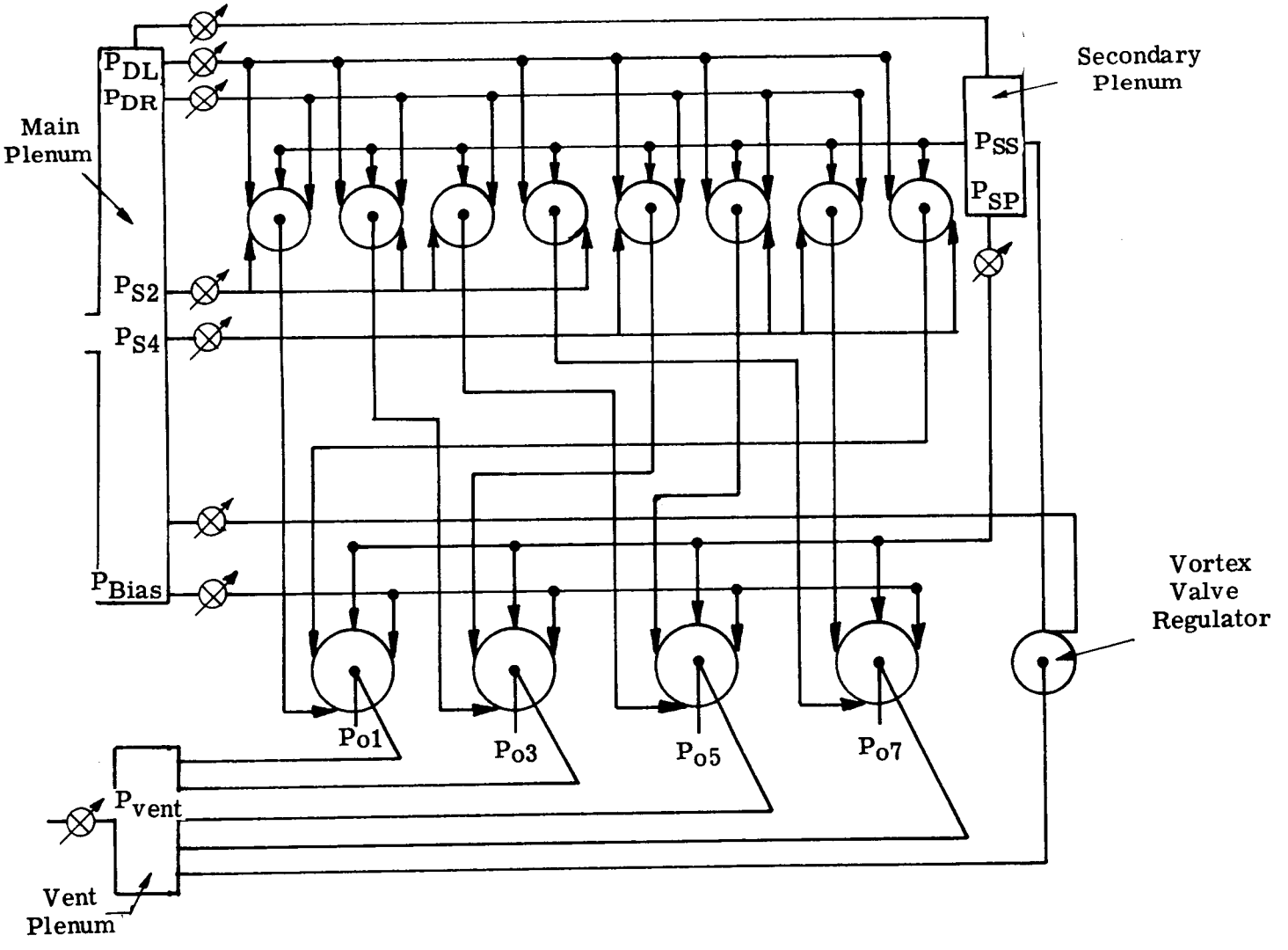

Figure 3-18(a). Model Commutation Circuit - Fixed Orifices with Internal Regulation

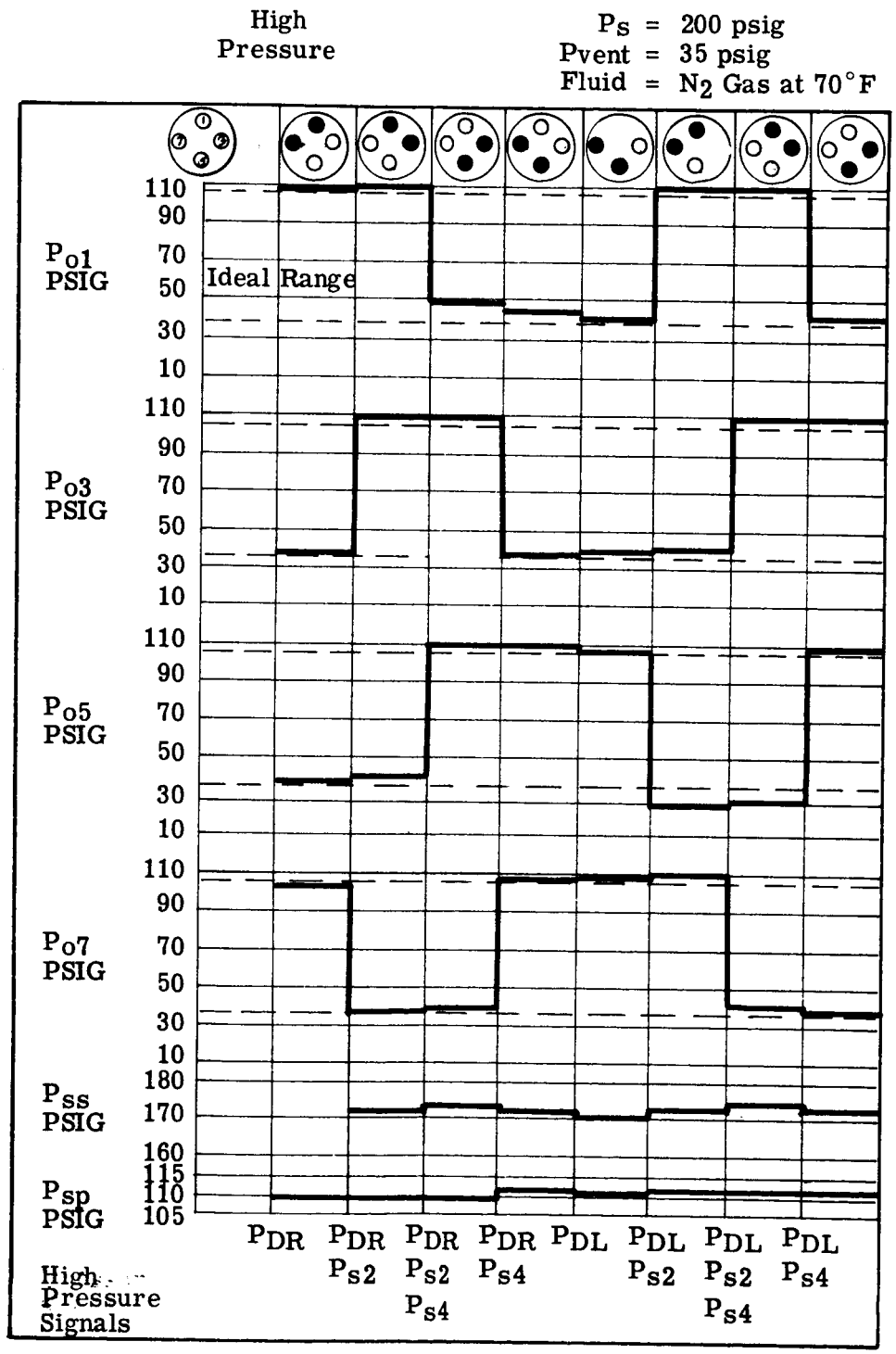

Figure 3-18(b). Model Commutation Circuit - Fixed Orifices with Internal Regulation

In order to minimize the effects of these pressure variations, the selector and power valve supply pressures were obtained by series orifices from the plenum chamber. A vortex pressure regulator was also incorporated across the selector supply pressure to minimize the flow variations. The modified circuit is shown in Figure 3-18(a) and the test results obtained are shown in Figure 3-18(b). The circuit modifications materially reduced the P_O pressure variations, and provided a performance comparable to the ideal regulated system of Figure 3-16(b).

Further development of the circuit allowed a pressure level reduction of P_{SS} from 117 n/cm^2 (170 psig) to 113.5 n/cm^2 (165 psig) and P_{Sp} from 75.6 n/cm^2 (110 psig) to 72.2 n/cm^2 (105 psig). The reduction in supply pressure levels reduces the pressure recovery requirement of the directional amplifier.

It should be remembered that the test results shown in Figures 3-16(b), 3-17(b) and 3-18(b) are shown with the signal pressures (P_{S2} and P_{S4}) either fully "on" or fully "off". In the actual motor commutation, a proportional phasing occurs between these conditions. The circuit is therefore proportional in action rather than on-off, as might be inferred from the above mentioned figures.

3.3.2 Directional Amplifier

A small bi-stable flip-flop was obtained from the Bendix Research Laboratories Division. Although this unit did not have sufficient flow output to control the directional signals for the breadboard logic circuit, tests were conducted to ensure that latching could be obtained under the required pressure level conditions. The amplifier was tested with a supply pressure of 131 n/cm^2 (190 psig) and a vent pressure of 103 n/cm^2 (150 psig). The receiver pressures obtained were 121 n/cm^2 (176 psig) and 113 n/cm^2 (164 psig). This pressure level and pressure differential was determined to be adequate for directional control of the commutation circuit. Switching occurred with an average control pressure level of 113 n/cm^2 (164 psig) and a hysteresis band of 3.1 n/cm^2 (4.5 psi).

From the flow calibration obtained at these conditions it was determined that an area scale factor of 18 would provide the required flow to control the complete logic circuit. A scaled version of the bi-stable amplifier was then manufactured by the Research Division and incorporated in the circuit. Test results of the complete system are given in Section IV.

3.4 FABRICATION AND TEST ASSEMBLY

3.4.1 Circuit Arrangement

The complete commutation circuit was fabricated from eight plates, 20 cm. (7.9 in.) in diameter and varying in thickness from 1.58 mm (.062 in.) to 14.2 mm(.56 in.). These plates are stacked behind the bellows end plate (see Figure 2-4) and held together by 44 studs. One plate contains the eight power valve chambers and is positioned directly behind the bellows end plate. A second plate contains the sixteen selector valves. The remaining plates contain the necessary channeling to connect the circuit. Considerable care was taken to minimize the length and volume of the connecting passages, to ensure a maximum system response. Since any two selector valves which have a common direc-

tional input, supply the control for power valves 180° apart, a large number of channel crossovers occur. These crossover points largely determine the number of plates required.

3.4.2 Plate Sealing Techniques

Due to the large surface area of the commutation plates, it was anticipated that problems would arise in maintaining adequate sealing between the various channels and ports. A small test plate assembly was fabricated consisting of two plates. One plate had four concentric annular grooves, each 6.35 mm (0.25 in.) wide and spaced at a radial distance of 2.5 mm (0.10 in.). The second plate contained pressure fittings to each groove. The plates were bolted together to obtain the same unit loading as would be obtained by the commutation plates. The tests consisted of pressurizing one slot and observing the rate of change of pressure in the deadended remaining slots. The following tests were performed:

a. Plates machined to a 16 RMS finish and 0.51 mm(.002 in.) flatness. High Leakage.

b. Plates hand lapped. High Leakage.

c. Spray coated with "Krylon" coating. Negligible Leakage.

d. Plated with .013 mm(.0005 in.) silver, bolted together and inserted in oven for four hours at 810°K (1000°F). No Leakage.

The configuration (d) was then tested at 75°K (-325°F) and 560°K (+550°F). A temperature shock test was also performed. At no time was any leakage detected. The plates were then broken apart, and are shown in Figure 3-19.

The plates were then relapped and procedure (d) was repeated. Again, no leakage occurred and visual inspection of the mating faces indicated that the seal was uniform.

From the above tests, it was tentatively decided to use the Krylon coating for room temperature tests and adjustment. When the circuit operation is satisfactory, the silver plating procedure (d) would be used to effect a semi-permanent bond.

3.4.3 Circuit Test Assembly

The circuit plates were ground and assembled on a test rig. Aluminum test plates were inserted between certain commutation plates to allow monitoring of the circuit intermediate pressures. The pressure pickoffs were simulated by a partial ring which could be rotated to cover the pickoff holes. The test assembly is shown in the drawing of Figure 3-20.

The complete commutator test stand is shown in Figure 3-21. All fixed orifices as well as the directional signals and pressure error valve output signal were initially simulated by hand valves.

Initial testing indicated an unsatisfactorily high leakage. Krylon coating,

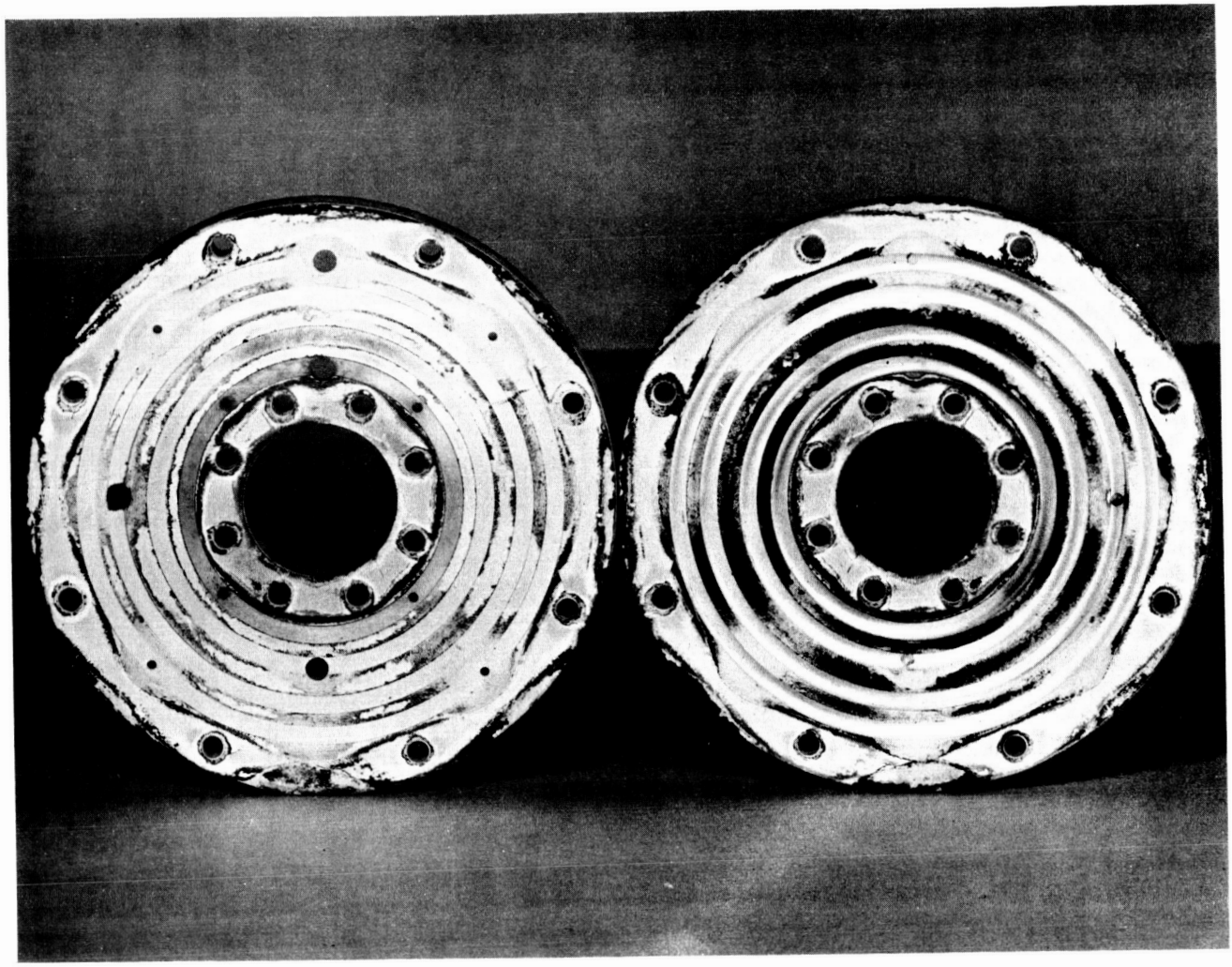

Figure 3-19. Seal Test Fixture

although it gave good results on the smaller plates and test assemblies, did not appreciably improve the sealing of the large plates. The coating also caused considerable difficulty in disassembly. The use of a light vacuum grease coating gave a reasonably good seal but caused clogging in certain of the critical passages.

The plates were then lapped flat and plated with silver. This procedure provided an extremely good seal without channel clogging, and greatly facilitated disassembly. The plates have since been disassembled on numerous occasions without any noticeable deterioration in the sealing quality.

Figures 3-22(a) through 3-22(g) show the assembly procedure of the main logic elements on the base plate of the actuator. A detailed description of the pressure channels for each plate is given in Appendix B. The complete assembly is shown in Figure 3-23.

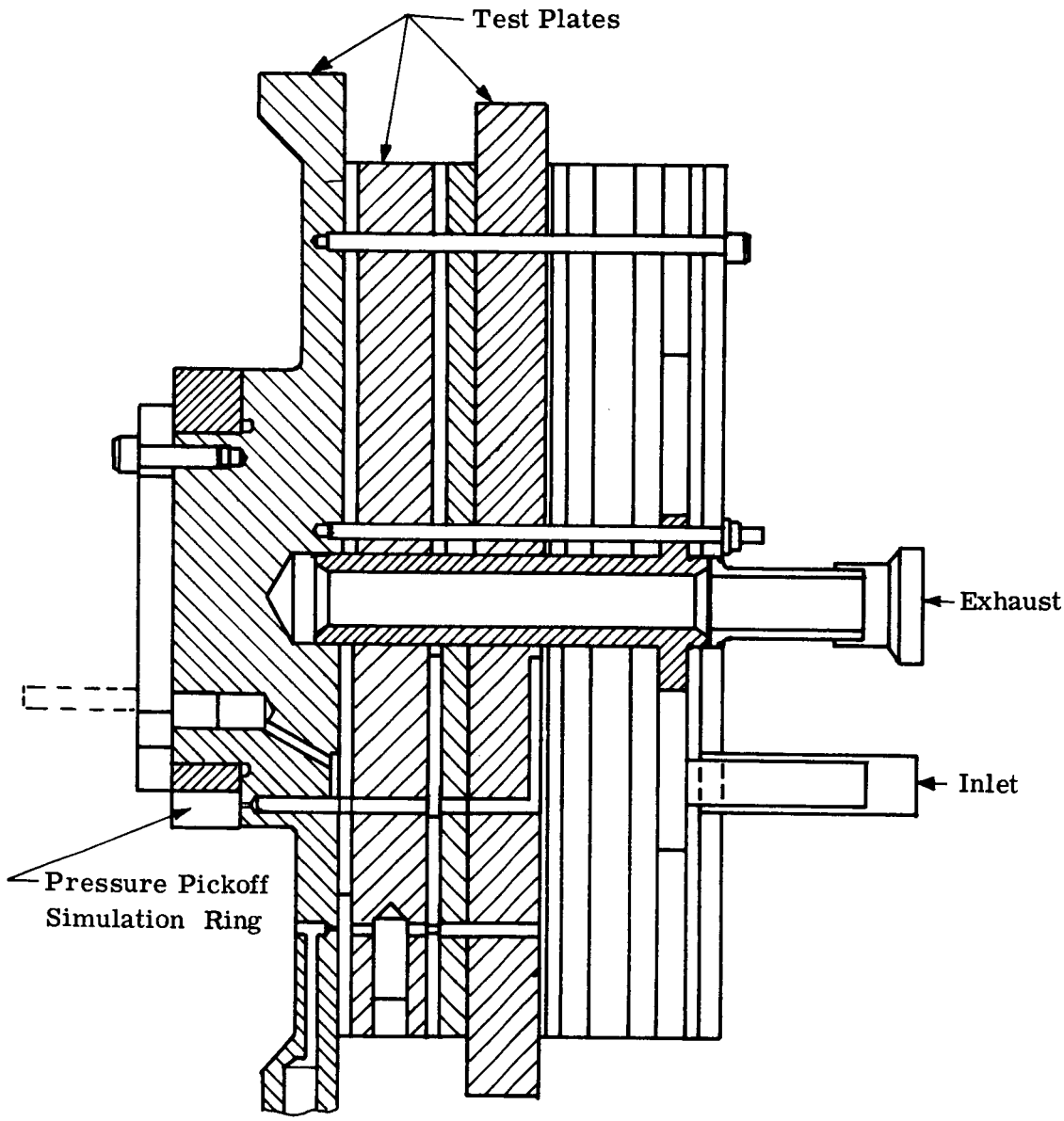

Figure 3-20. Assembly of Commutation and Test Plates

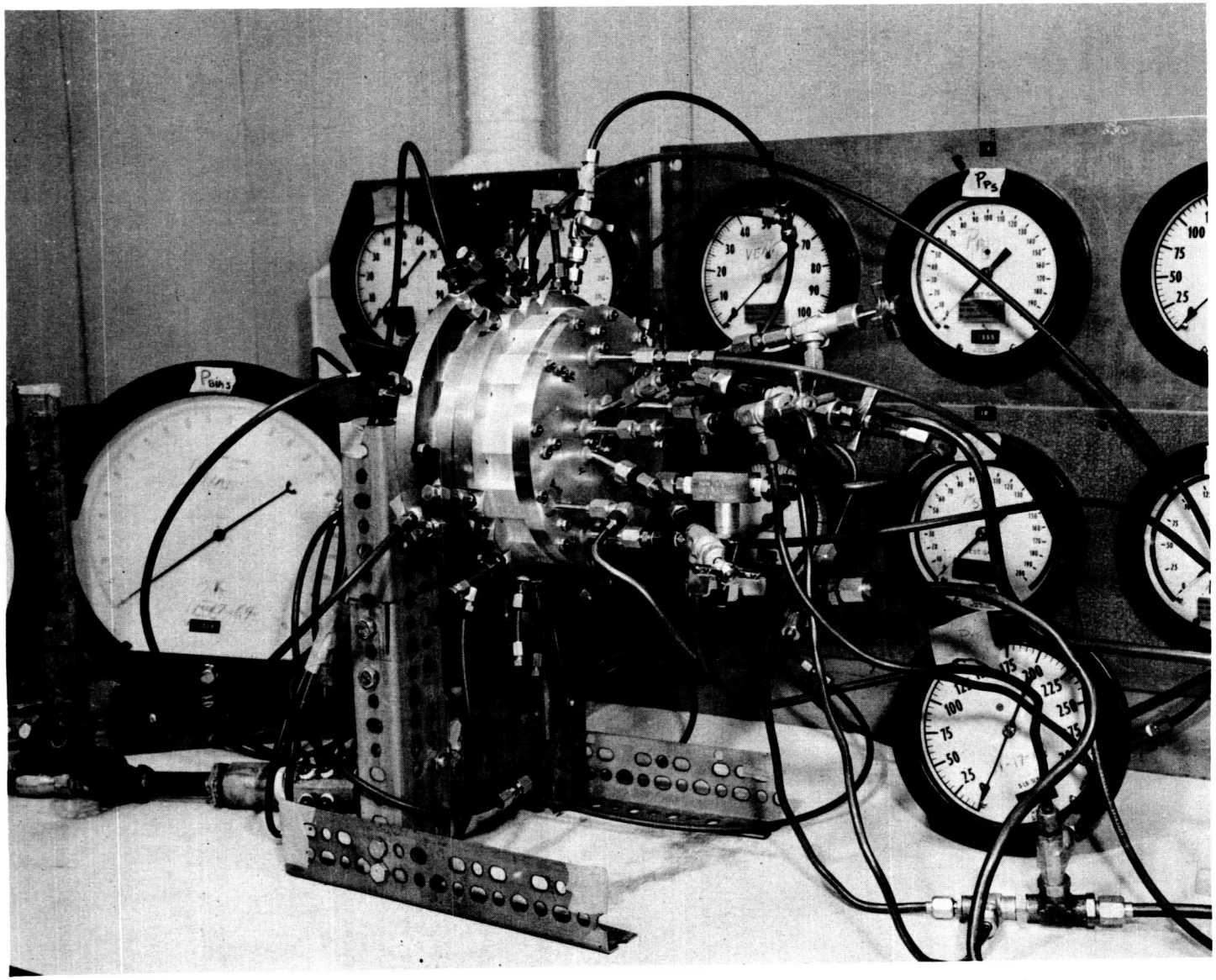

Figure 3-21. Commutation Plate Test Setup

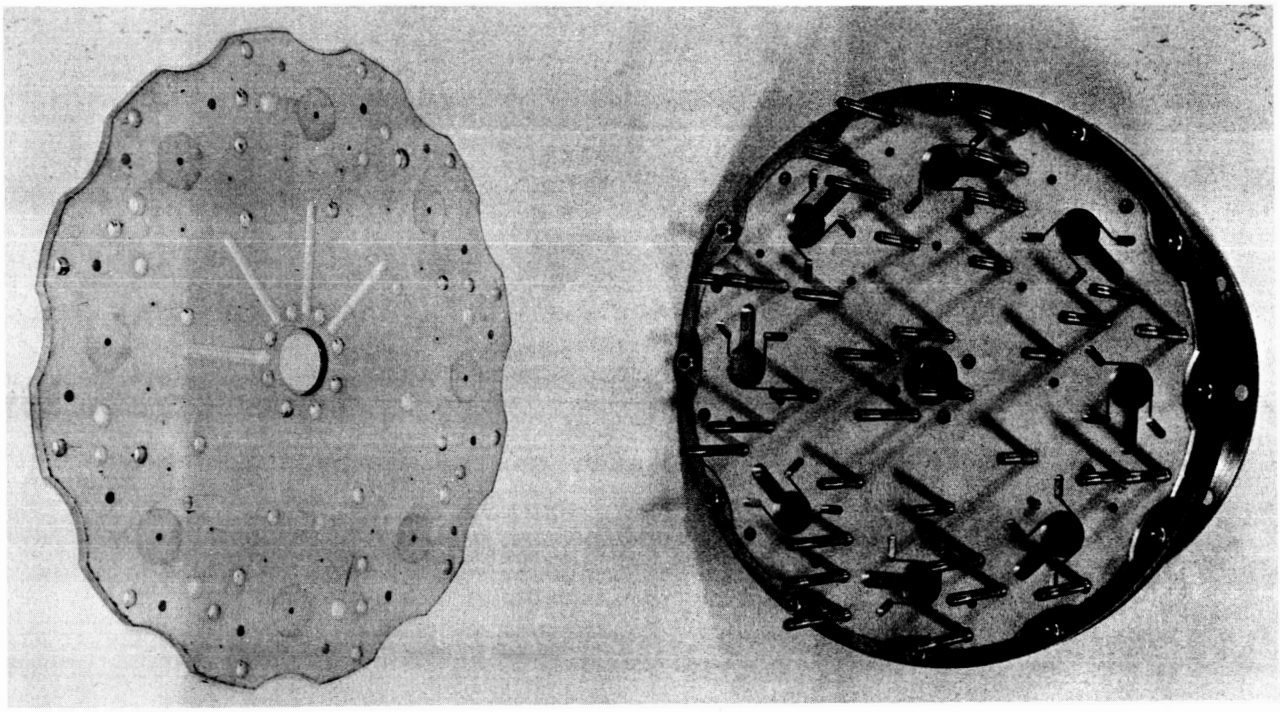

Figure 3-22(a). Power Valve Plate

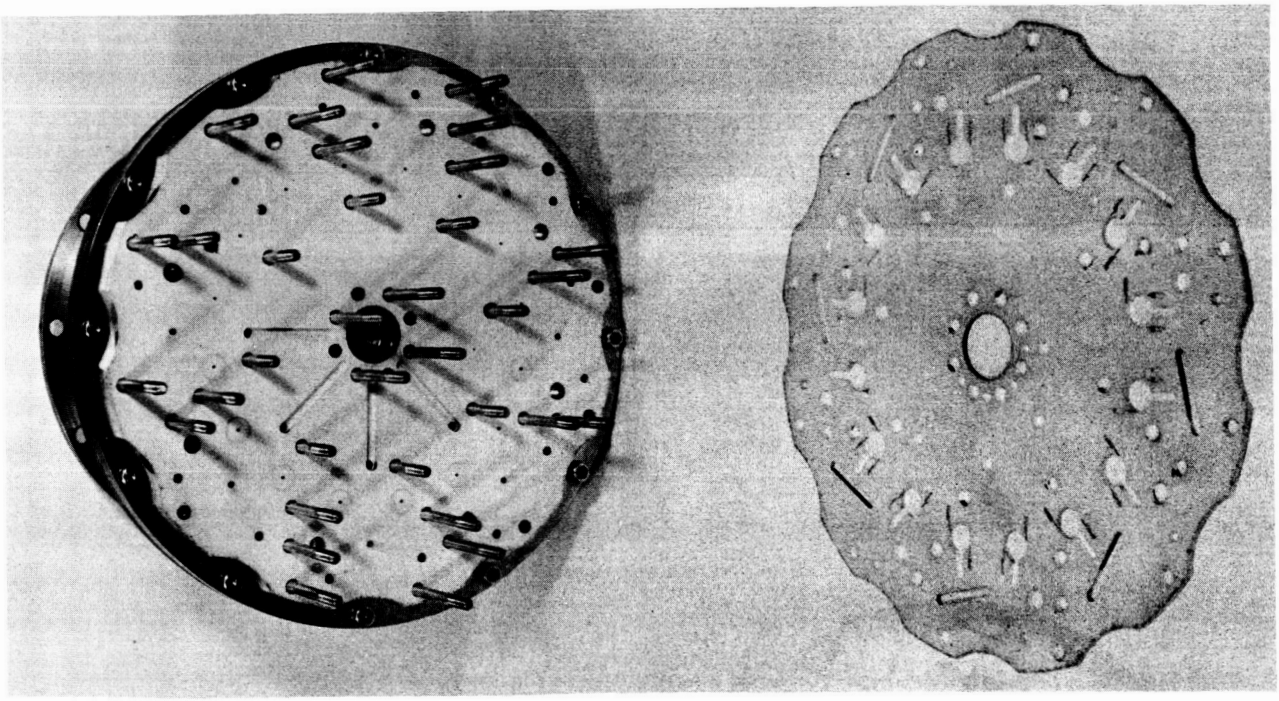

Figure 3-22(b). First Transfer Plate

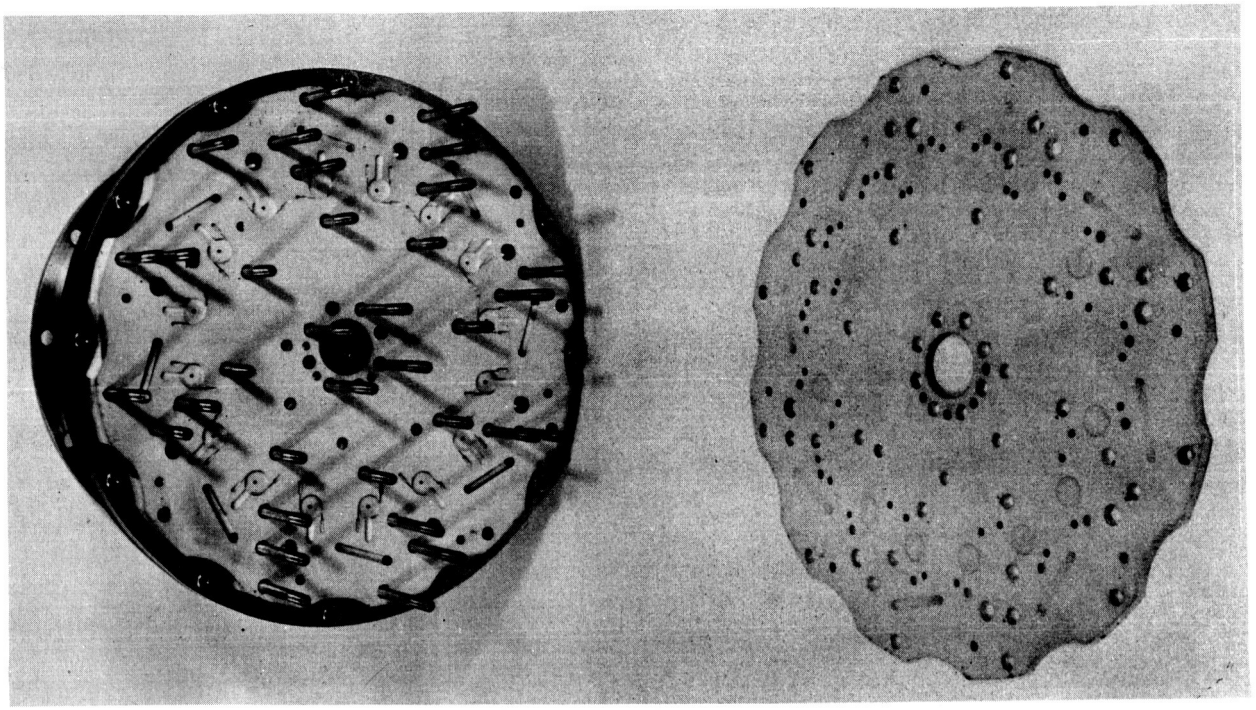

Figure 3-22(c). Selector Valve Plate

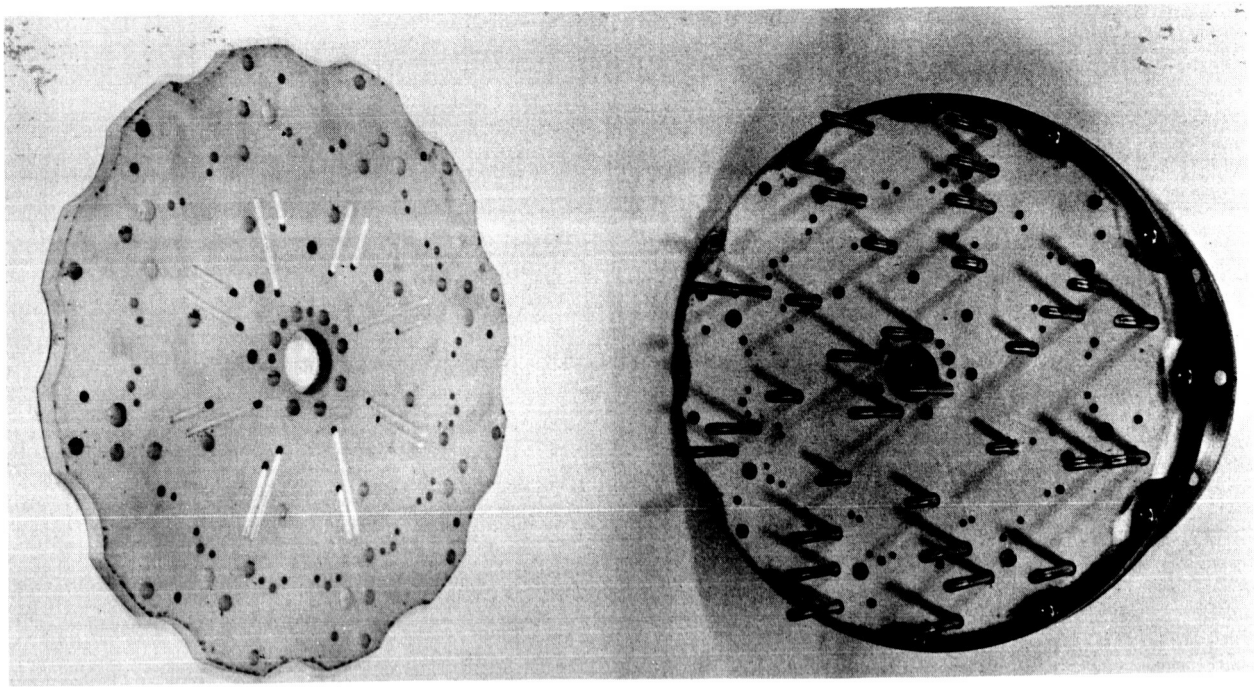

Figure 3-22(d). Second Transfer Plate

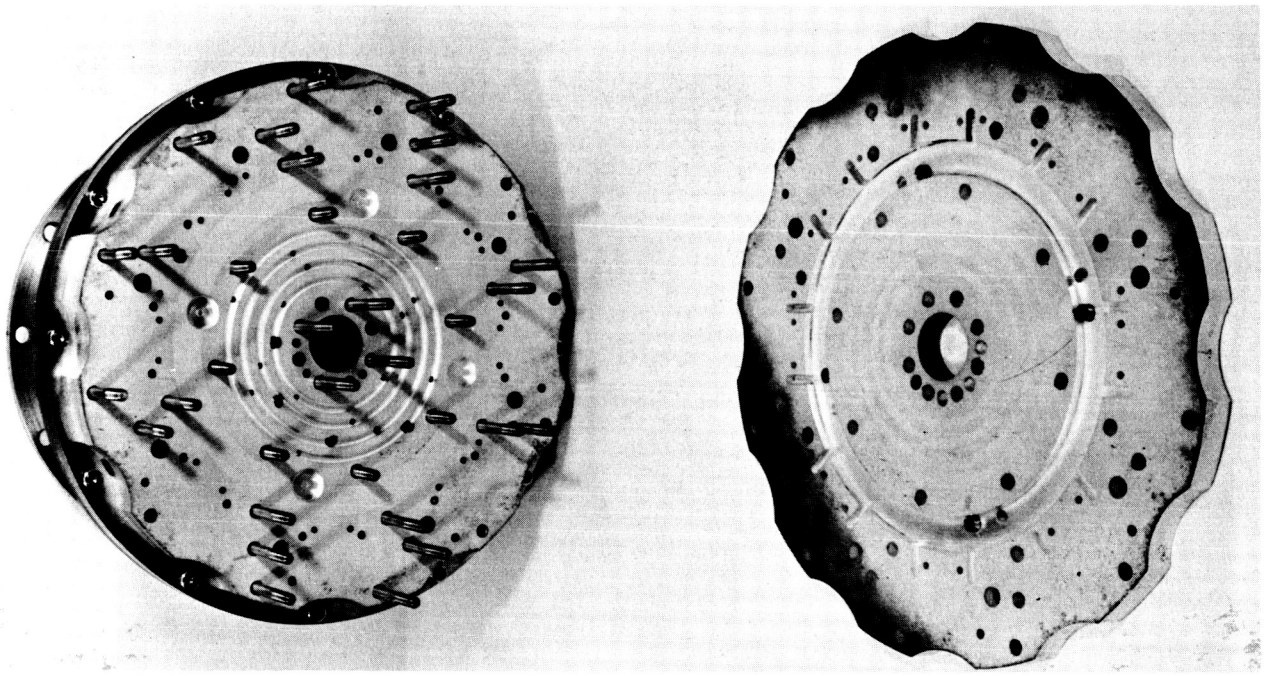

Figure 3-22(e). First Pressure Distribution Plate

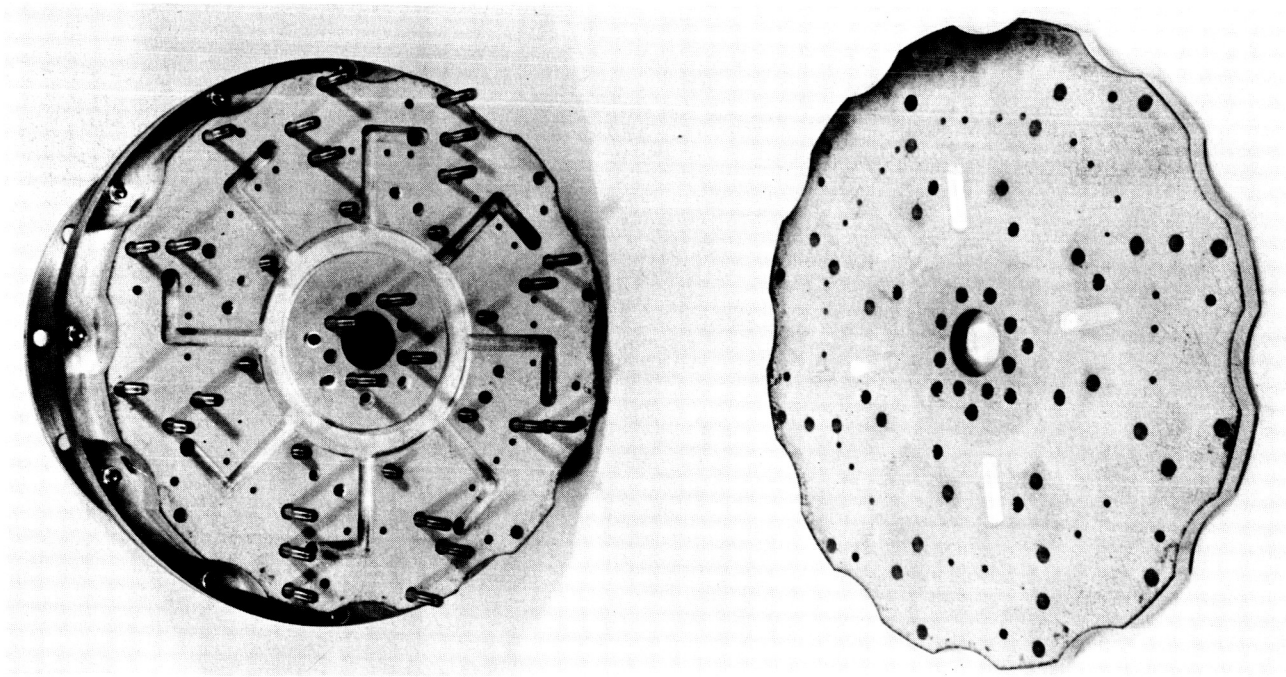

Figure 3-22(f). Second Pressure Distribution Plate

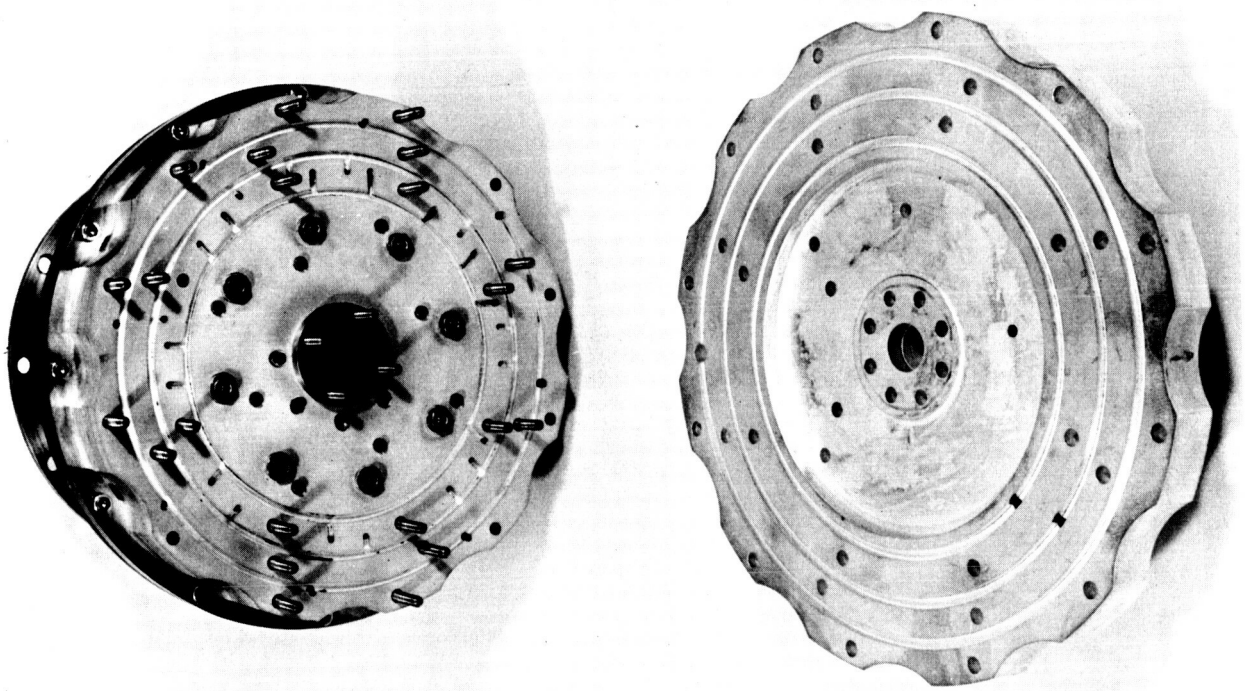

Figure 3-22(g). Third Pressure Distribution Plate

3.4.4 Circuit Optimization

3.4.4.1 Logic Circuit

With the silver plated commutation plates and the various aluminum test plates assembled on the static test stand, a study was made of the effects of various bleed sizes in each of the supply lines. Many combinations of bleeds were tested with data recorded for each set. It was impossible, however, to obtain an optimum bleed combination in this manner. All bleeds were then replaced with adjustable hand valves and the circuit performance was optimized. The pressure level settings were found to be quite critical. The hand valves were replaced by bleeds of exactly equivalent size. After each bleed was inserted the performance was checked to determine if any deterioration of operation occurred.

3.4.4.2 Directional Valve

The signal pressure which determines the direction of rotation is obtained from the bi-stable directional valve. The directional flow requirement of the logic circuit was measured as .004 kg./sec. (.0088 lb./sec.) when operating on nitrogen.

Initial testing indicated that the pressure in the two vents of the directional amplifier would have to be maintained at a high level. It was also found that the vents could not be interconnected, and required individual impedance orifices in order to obtain the required flow recovery.

3.4.4.3 Pressure Error Valve

The pressure error valve converts the command pressure differential to a non directional bias flow for the logic circuit power valves. The required bias flow ranges from .0132 kg./sec. (.029 lb./sec.) at zero actuator torque, to .0177 kg./sec. (.039 lb./sec.) at maximum output torque.

Plastic vortex amplifiers were used initially to breadboard a pressure error valve to meet these requirements and maintain compatibility with the directional amplifier control impedance.

The best flow gain was obtained by using both the vent and the P_O tap. Two vortex valves were plumbed in parallel with a bypass line to maintain minimum flow as in Figure 3-24. It was found, however, that in actual conditions the bypass line was not necessary. The plates for the pressure error valve were designed with the same critical dimensions as the breadboard model. Incorporated with the plates is a provision for mounting an electromechanical torque motor to generate the input differential pressure. The plates making up the pressure error valve were all lapped and silver plated in order to minimize leakage.

The pressure error valve and directional bi-stable valve are shown in Figure 3-25. These valves mount directly on the end plate shown in Figure 3-23. Both valves draw their required power supply from the main supply plenum.

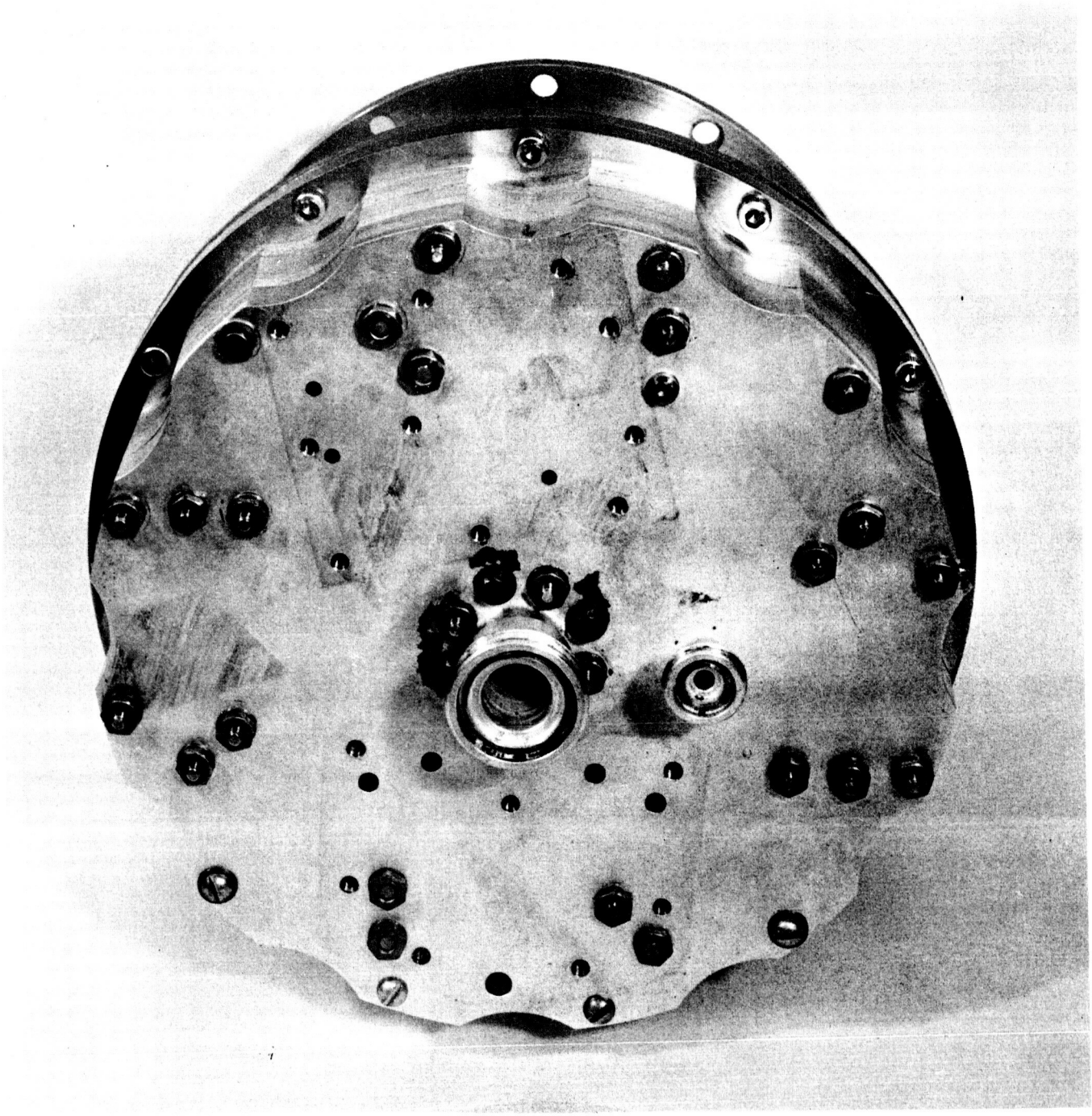

Figure 3-23. Assembled Commutation Logic Unit

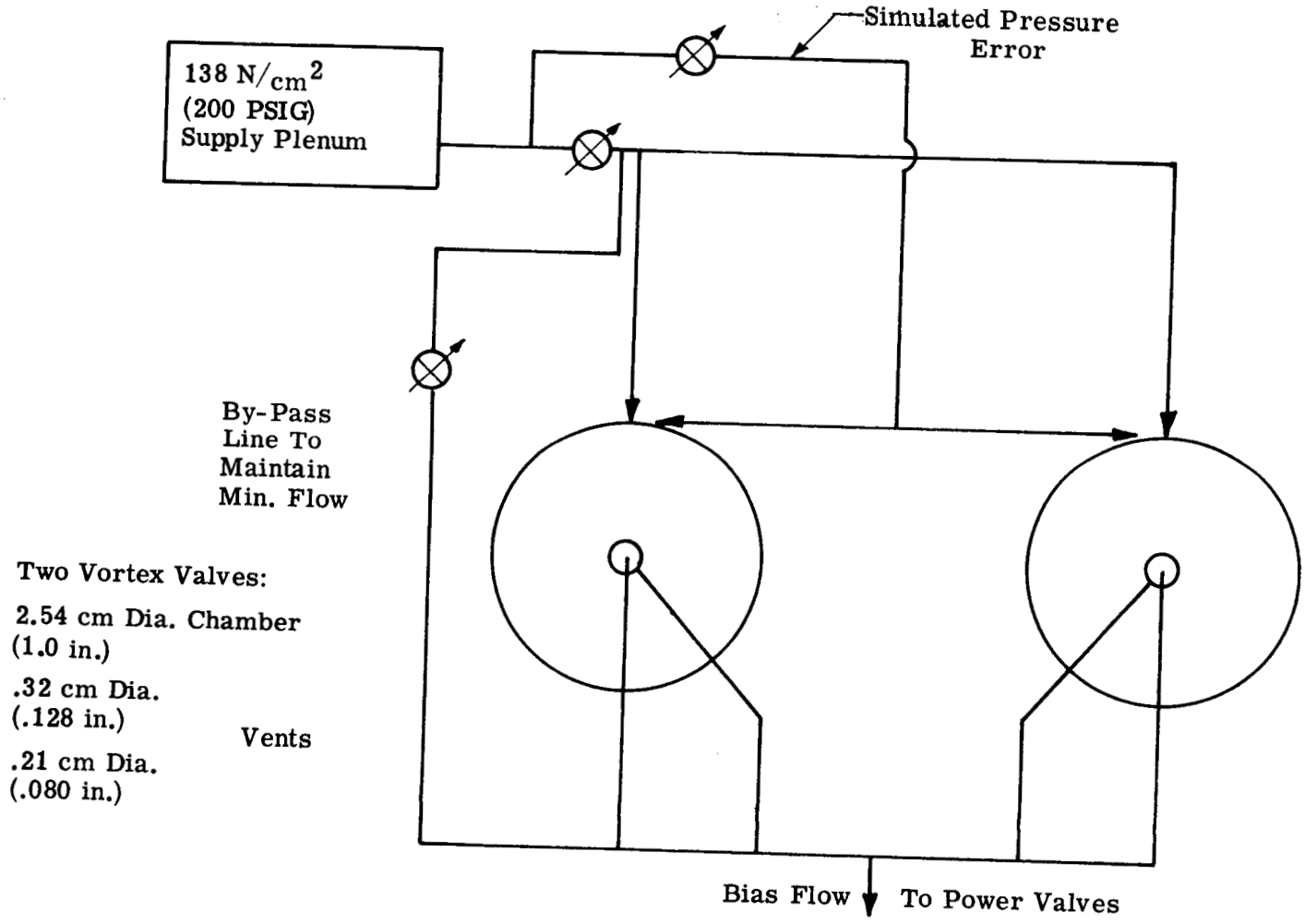

Figure 3-24. Pressure Error Valve - Schematic

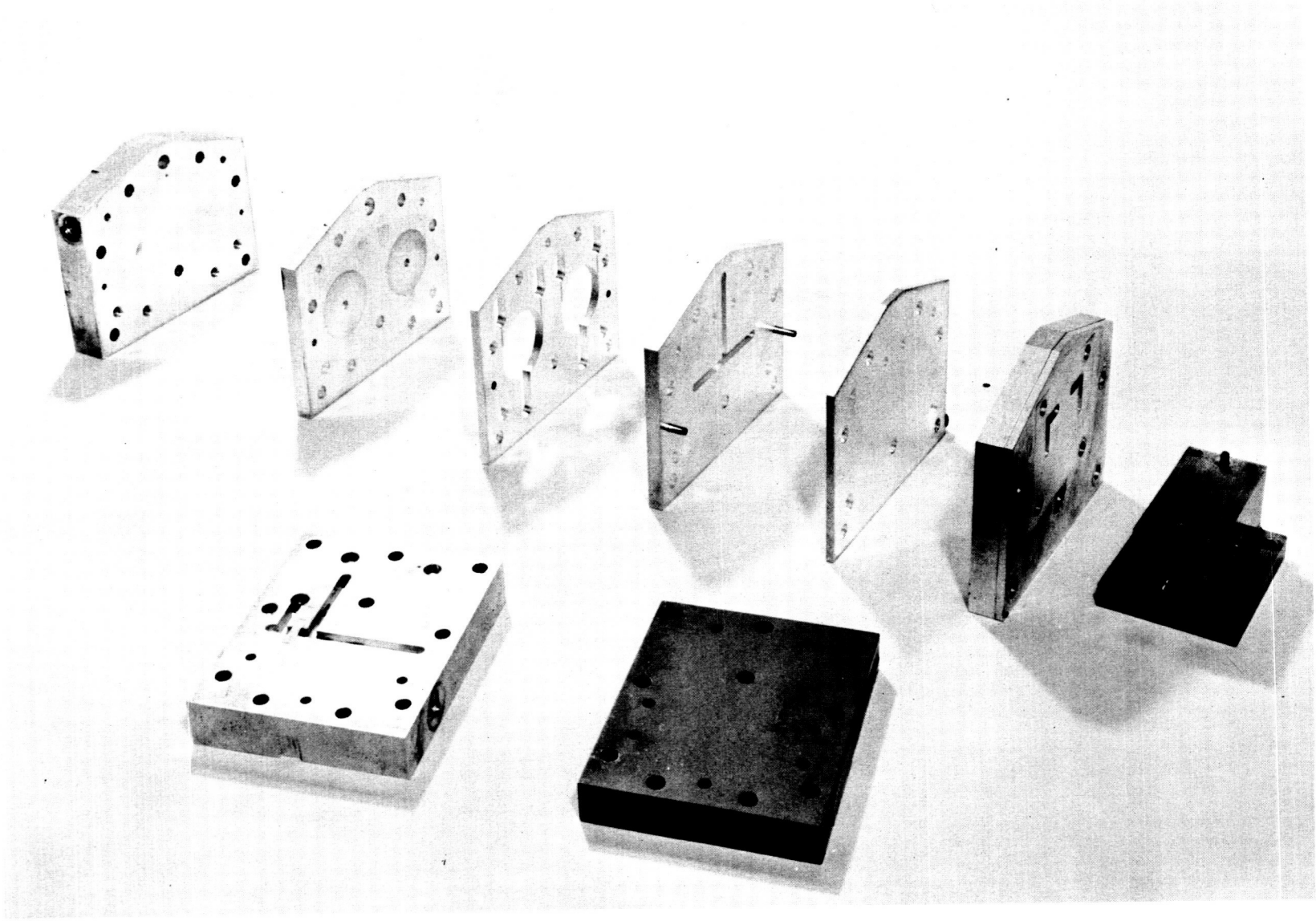

Figure 3-25. Pressure Error and Directional Valve Components

3.4.5 Assembly of Pressure Error and Directional Valves

The pressure error valve consists of eight plates, NPX-104-81 through NPX-104-88. Plate 81 is the base plate and contains the supply orifices for both the pressure error valve and the torque motor. Plates numbered 82, 83, and 84 are a pinned assembly containing two vortex valves in parallel which generate the bias signal to the commutation circuit. The remaining plates are pressure transfer plates.

The torque motor mounting block, NPX-104-80, is assembled on top of the pressure error valve stack, and has provisions for a torque motor or an externally supplied input differential pressure.

Each plate has an arrow etched on the edge; these arrows must be in line and pointing away from the end plate for proper assembly.

The plates assemble in the following sequence:

NPX-104-79
NPX-104-81
NPX-104-82
NPX-104-83
NPX-104-84
NPX-104-85
NPX-104-86
NPX-104-87
NPX-104-88
NPX-104-80

The directional block, NPX-104-88, also mounts directly on the end plate, and the directional amplifier mounts on top of it. The directional block contains two orifices for the vents and provisions for orifices in each of the directional signals.

The input differential pressure which enters the pressure error valves through the torque motor mount must be transfered externally to the directional amplifier as is shown in Figure 3-26. The vent from the directional amplifier must be connected externally with the main vent line.

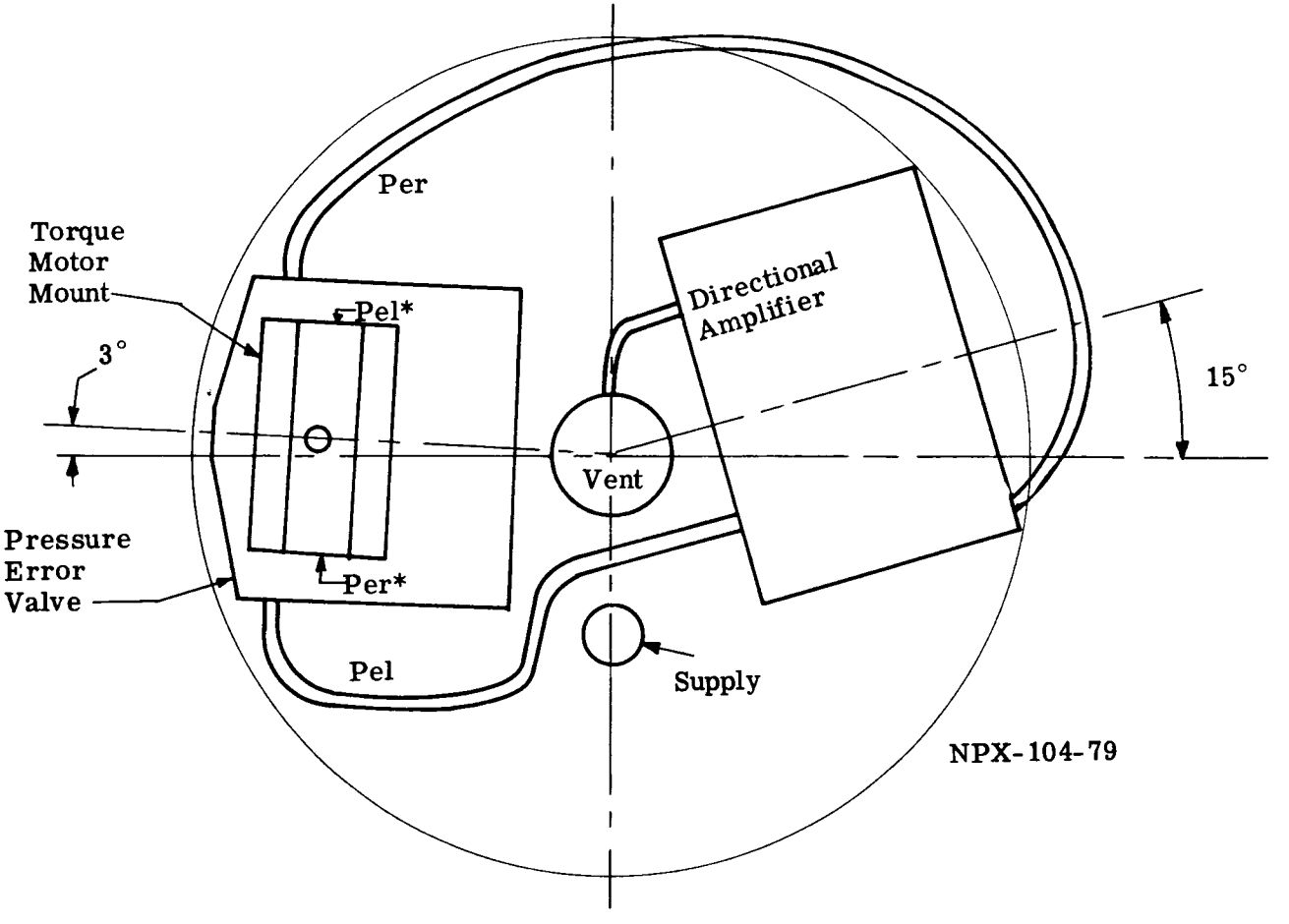

* Input Differential Pressures

Figure 3-26. Assembly Arrangement of the Pressure Error and Directional Valves

SECTION IV

ACTUATOR ASSEMBLY AND TEST

4.1 ACTUATOR ASSEMBLY

The mechanical portion of the actuator is assembled as per assembly drawing NPX-104-A1. Detailed assembly and set-up procedure for the critical components is described below.

4.1.1 Brake Band and Snubber Assembly

a. The brake bands must be assembled before the nutating gear.

b. Loosen the brake bands to assemble the snubber (the snubber must be pushed out from the bottom side of the plate to disassemble it).

c. With the brake bands loose record the torque of the snubber thru its 15° travel.

d. Tighten the brake bands until they add 0.46 meter kilograms (40 in.-lbs.) torque to the snubber.

4.1.2 Scram Spring Assembly

a. The scram spring can be assembled with the outer loop over any one of the four pins in the housing.

b. The gear plate on the output shaft must be removed so the spring can be guided over one of the pins while the bearings are being pressed into the housing.

c. The preload on the scram spring should be set to approximately 0.69 meter kilograms (60 in.-lbs.).

d. The spring load must be checked over the range of the free travel of the output shaft to insure that the spring is operating in the linear range and is not beginning to bind between the coils.

4.1.3 Pickoff Spring Adjustment

a. Check each spring to see that it will seal 124 N/cm^2 (180 PSIG) when the pad covers the pickoff hole completely. Leakage can be minimized by slightly

bending the spring to allow the pad to sit flat over the hole.

b. Block the gear ring parallel to the base plate.

c. Using mechanical commutator plate, pressurize one pickoff orifice at a time.

d. With pressure at 117 N/cm^2 (170 PSIG) set spring so that flow is 4.4×10^{-4} kg./sec. (9.7×10^{-4} lb./sec.).

e. After all 4 are set, all pickoffs can be moved equal amounts by changing the shims under the anchor pins.

Gear travel can be kept constant by changing shims between the outer casing by the same amount as above.

4.1.4 Procedure for Obtaining Gear Concentricity

a. Assemble the gear with the anchor screws only finger tight.

b. Lockwire the screws - so that the vibration will not force them out.

c. Using the mechanical commutator, operate the unloaded actuator in one direction for at least two to three revolutions of the output shaft. The natural tendency of the two gears to center themselves will then force the input gear to "walk" to the correct position.

d. Separate the two gears, remove the lockwire, and tighten the anchor screws.

e. Re-lockwire the anchor screws and pin the assembly.

The assembly procedure for the commutation circuit is described in Section III.

The complete actuator is shown in Figure 4-1.

4.2 ACTUATOR PERFORMANCE EVALUATION

The majority of the testing performed on the actuator was done with the actuator and output adaptor driving a Vickers Magneclutch through a Lebow torque transducer. The output of the Magneclutch was attached to the test stand to provide a magnetic frictional load on the actuator. The output torque was read on a digital voltmeter.

The inertia of the drive system is within 10% of the specified load inertia and therefore allowed a realistic evaluation of the scram system.

The actuator, mounted on the test stand, is shown in Figure 4-2.

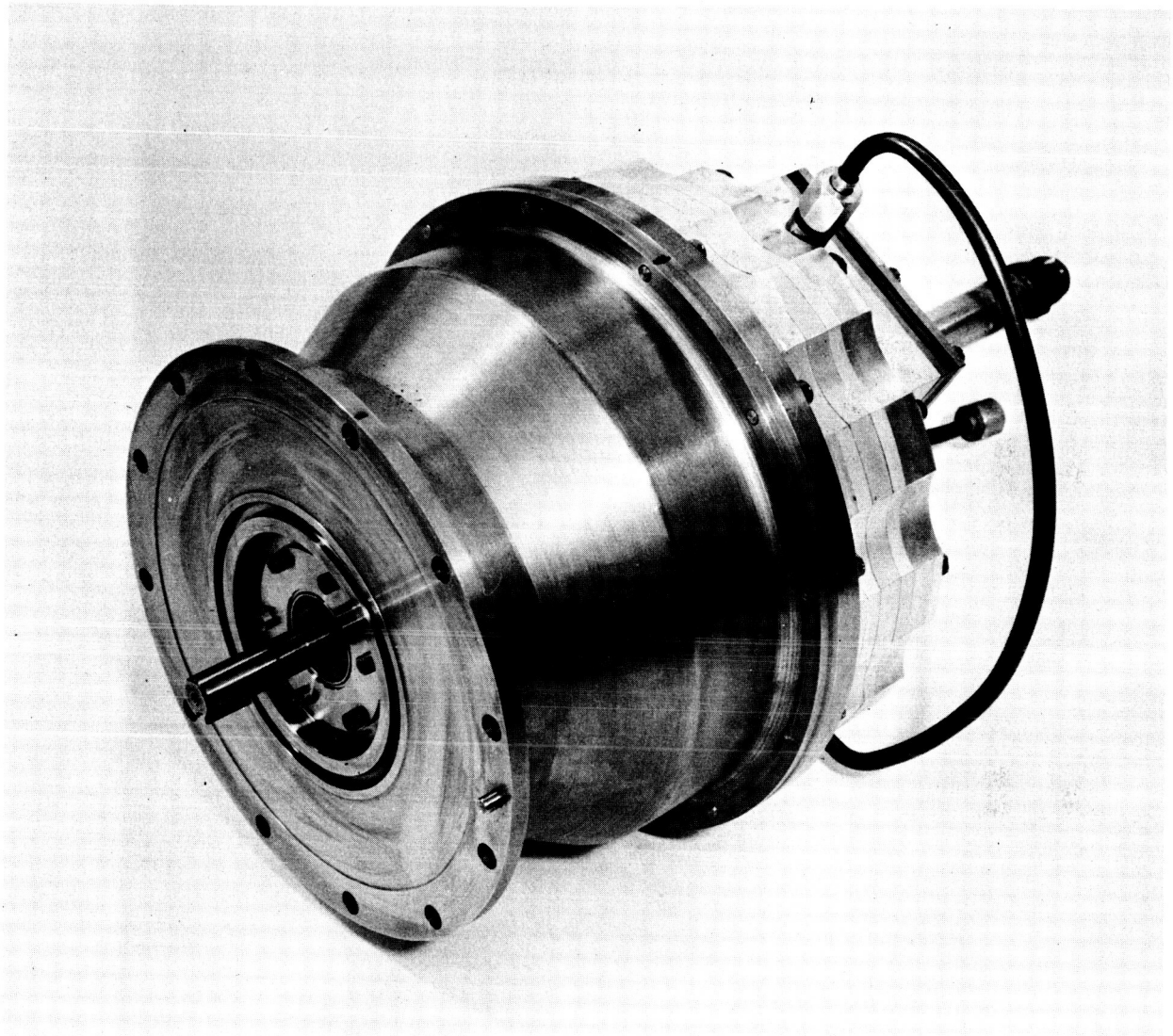

Figure 4-1. Pneumatic Nutator Actuator Motor

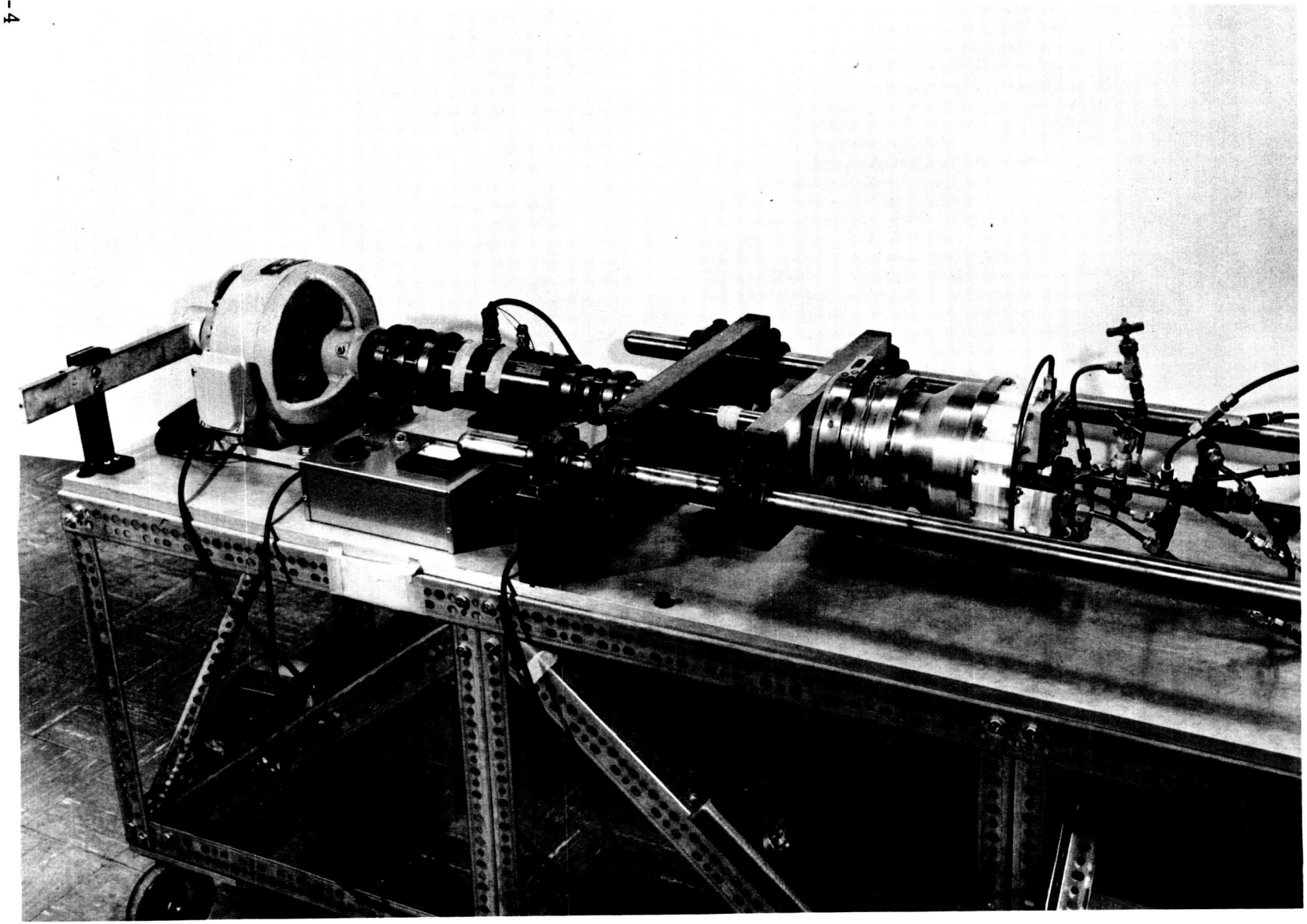

Figure 4-2. Actuator Mounted on Load Test Fixture

Initial testing consisted of obtaining the optimum sizing for the various fixed orifices in the commutation circuit, the optimum setting for the pressure pickoffs and the optimum clearance between the input and output gears.

It was found that considerable increase in output stall torque could be obtained by increasing the clearance between the gears (with the input gear in the neutral plane) from the design value of .33 mm (.013 in.) to .61 mm (.024 in.). Increasing the gap beyond this value caused erratic commutation and loss of stall torque. Assuming that the design meshing of the gears is correct, the total stroke of the input gear was increased from ± 1.52 mm (± .060 in.) to ± 1.80 mm (±.071 in.).

The hole diameter for the commutation pickoffs was set at .76 mm (.030 in.) to provide one sequence of commutation in 45° of input nutation. The increase in the nutation angle causes the bellows pressure sequencing to occur in less than 45°. This causes the torque angle (angle between the gear mesh point and the bellows force centroid) to vary. This variation would be expected to produce an uneven output torque. Since the test results indicated a smoother torque output with increased nutation angle, it has been assumed that the bevel gears are not meshing to the design depth.

The maximum speed obtained from the actuator (unloaded and without the scram spring preload) was 11 degrees/sec. in one direction and 7 degrees/sec. in the opposite direction. The maximum speed reduced to 10 degrees/second and 6 degrees/second with the preloaded scram spring installed (see acceptance test results Para. 4.3).

The actuator could be stalled and back driven without causing the teeth to disengage. The maximum stall torque obtained varied between 2.89 meter kilograms (251 in.lb.) and 1.39 meter kilograms (121.in lb.) depending on the method used to apply the load. If the load is applied rapidly, a high value of stall torque can be obtained. The variations in stall torque with commutation position can also be seen by observing the variation in maximum speed of the unloaded output.

In order that the sequencing of the commutation logic could be studied in more detail, the mechanical portion of the actuator was driven by the mechanical commutator. The commutation circuit was mounted separately on a test stand and the circuit output pressures were monitored. The commutation circuit was controlled from the pressure pickoffs in the actuator. By opening the loop in the commutation circuit in this manner, it was possible to observe the output of the commutation circuit relative to the pressures applied to the input bellows.

These tests indicated that the commutation sequencing was not occurring uniformly over the required 45° of nutation. For certain positions of the input gear, the commutation circuit output indicated five high pressure outputs. At a different gear position the number of high pressure outputs reduced to three. The circuit in general sequenced the pressures correctly, and the variations described above occurred over extremely small input positional increments. These variations, however, will cause changes in both the applied torque angle and the magnitude of the applied input force. It is felt that the non-uniform sequencing affects both the magnitude of the stall torque and the maximum speed obtained.

Methods recommended for providing a uniform pressure sequencing are discussed in Section VI.

4.3 ACCEPTANCE TEST RESULTS

The final tests performed on the actuator, complete with scram spring, dynamic seal, and snubber system were as follows.

4.3.1 Torque Speed Characteristic

With maximum input pressure differential, the output shaft position was recorded (vs. time) for various output loads. The torque speed curve obtained is shown in Figure 4-3. The maximum stall torque for various input pressure differentials is shown in Figure 4-4. The scatter obtained in the test points is indicative of the variation discussed in Para. 4.2 above.

4.3.2 Scram Characteristics

Scram tests were performed with the actuator on the test fixture shown in Figure 4-2 and with the actuator mounted on the drum test fixture. The drum test fixture provides the correct inertia simulation and allows pressurization of the output shaft dynamic seal. Frictional loading, however cannot be correctly simulated. The actuator on the drum test fixture is shown in Figure 4-5.

The scram condition was simulated by energizing a solenoid valve in the actuator pneumatic supply line. Loss of supply pressure causes the input gear to disengage and lie in a plane parallel to the output gear. The output assembly is then free to rotate to the zero shaft position.

Traces of output shaft position and solenoid current against time are shown in Figure 4-6. Figure 4-6(a) shows the time taken to reach zero degrees with .35 meter kilograms (31 in./lbs.) frictional torque. Figure 4-6(b) shows the time taken with no frictional torque, but with the dynamic shaft seal pressurized at 448 N/cm^2 (650 psig). Further tests indicated that the friction generated by the pressurized shaft seal was negligible. Also the shaft seal leakage was too small to obtain an accurate reading.

4.3.3 Input Flow and Pressure Requirements

All the above described tests were performed with room temperature gaseous nitrogen as the working fluid. Total required input flow is 35.5 g/sec (.078 lb./sec.). Measurement of the main plenum supply pressure indicated that the 1/4 in. O.D. inlet supply line had a pressure drop of 29.5 N/cm^2 (44 psi). Since the reduction of this pressure drop represents a relatively minor modification, it was decided not to penalize the overall performance by this drop. The upstream supply pressure was therefore set at 168 N/cm^2 (244 psig).

The input pressures required to operate the actuator are 126 $\pm$ 14 N/cm^2 (180 $\pm$ 20 psig) and the input flow varies from zero to 4.05 g/sec. (.0089 lb./sec.).

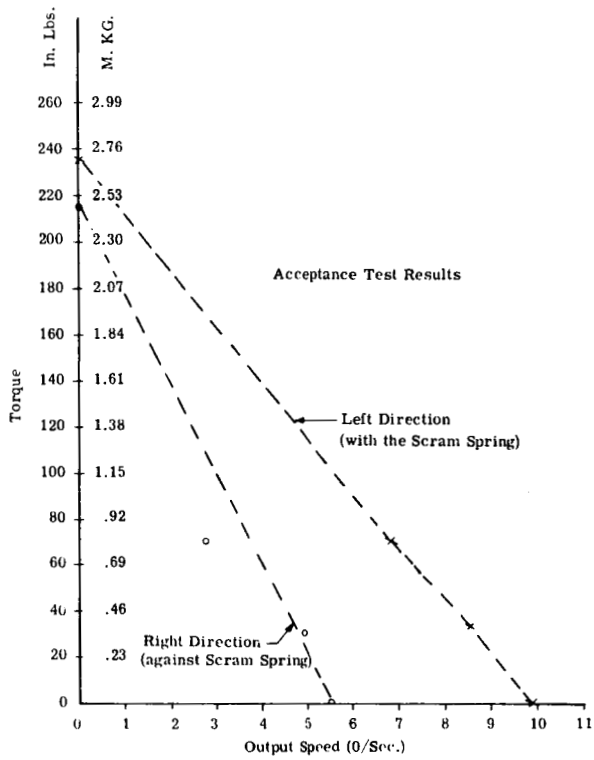

Figure 4-3. Torque vs. Speed Characteristic

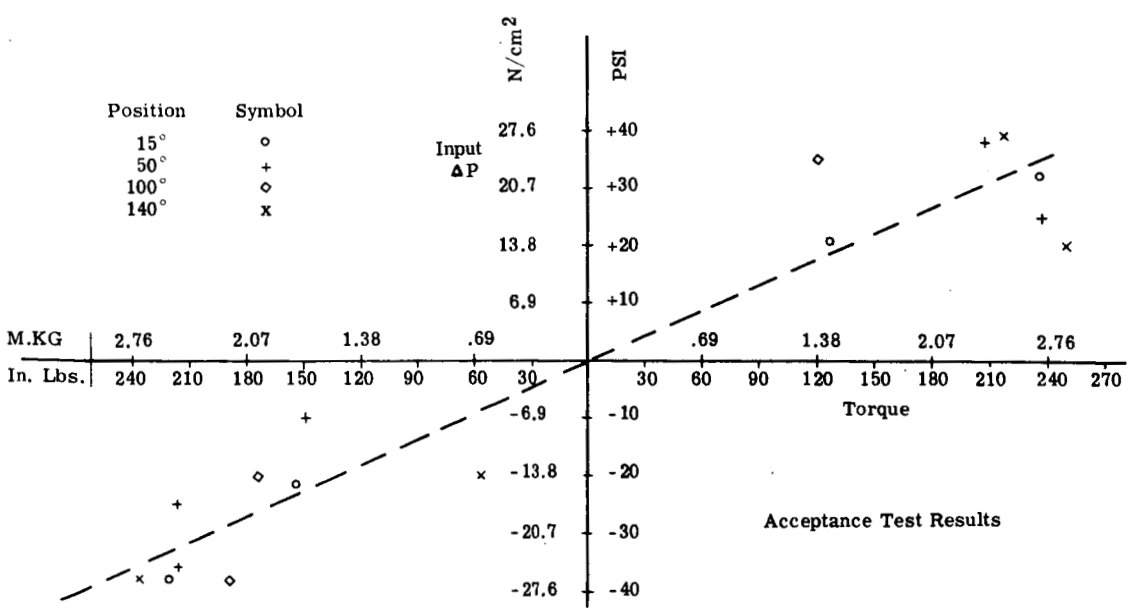

Figure 4-4. Stall Torque vs. Input Pressure Differential

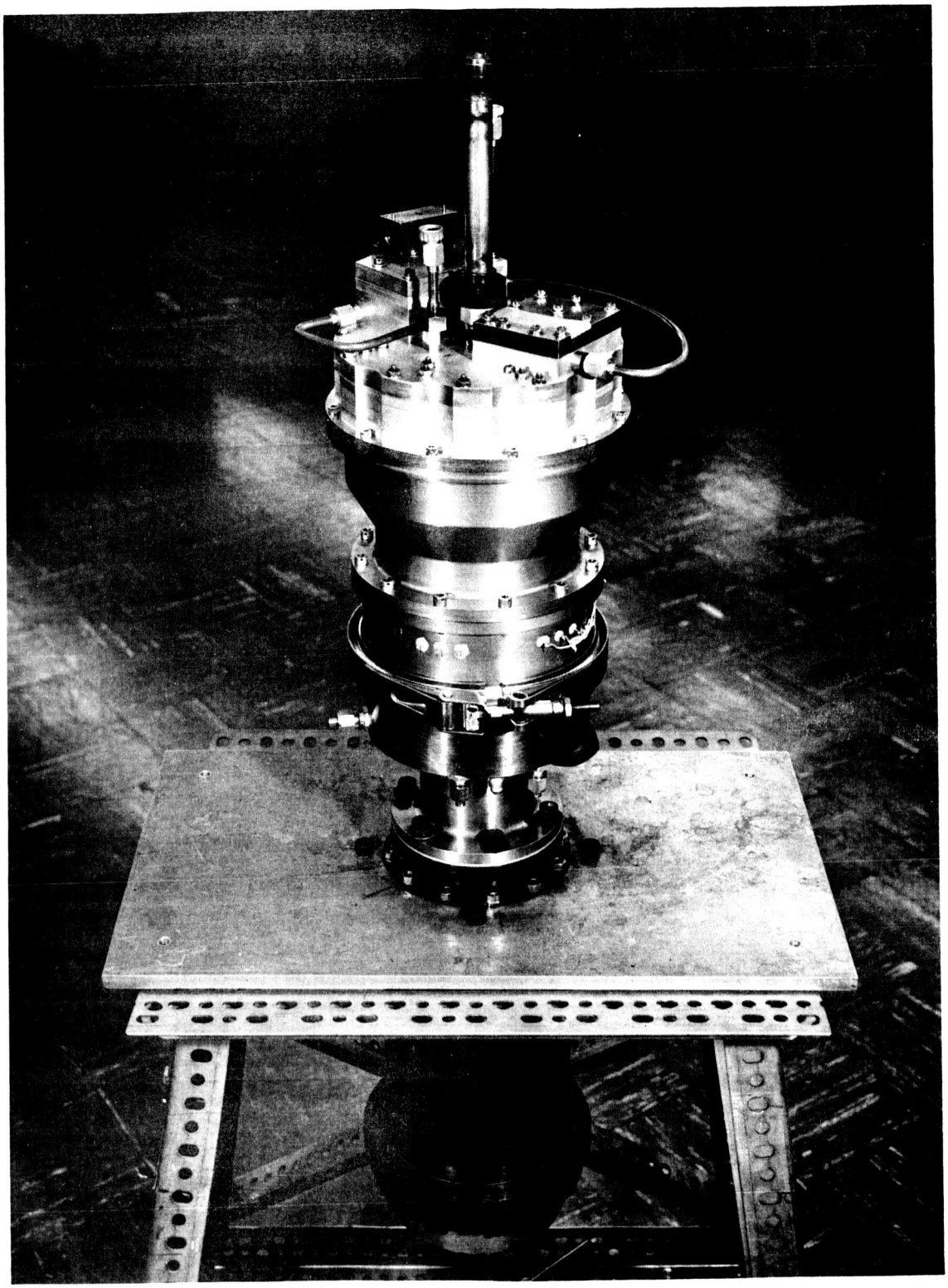

Figure 4-5. Actuator Mounted on Drum Test Fixture

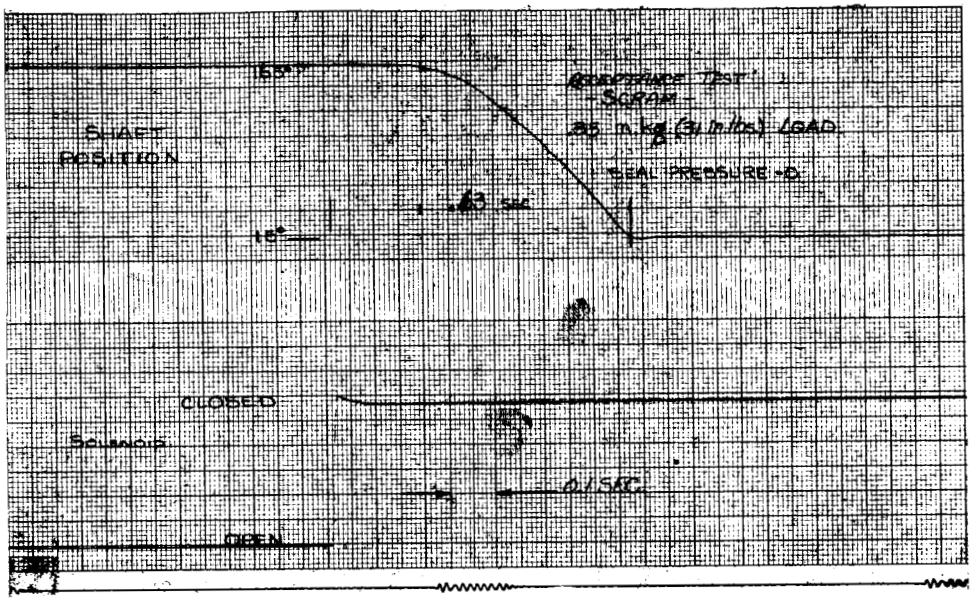

(a) Scram Characteristic with Friction Loading

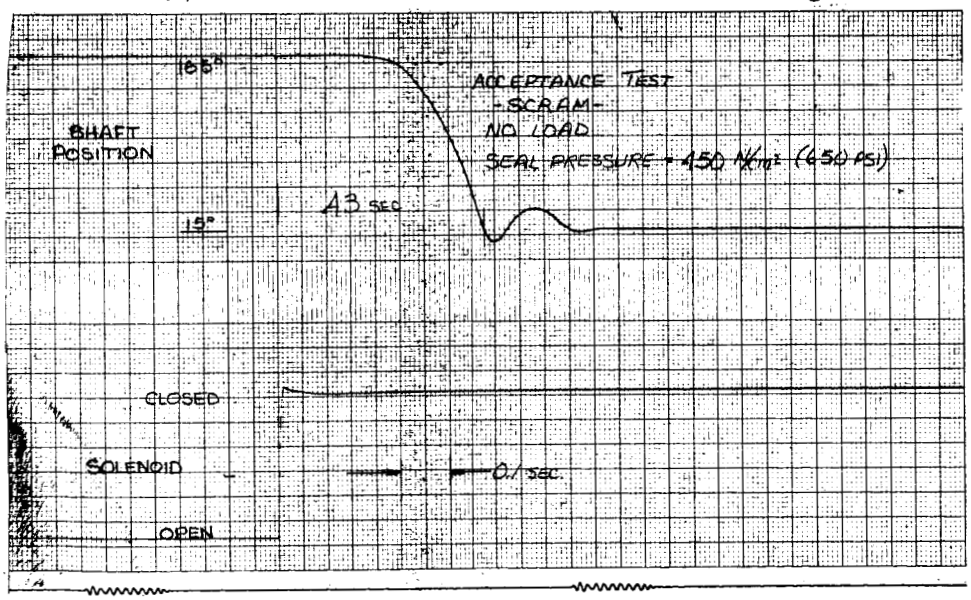

(b) Scram Characteristic without Friction Loading

Figure 4-6. Scram Characteristics

4.3.4 Helium Tests

Preliminary testing was performed using helium gas at room temperature as the working fluid to demonstrate the ability of the logic circuit to operate with gases of different gas constants. The stall torques obtained were identical to those of Figure 4-3. Slight adjustment of the input differential was required. The reason for this adjustment is not presently known.

The maximum speed obtained was 24 degrees/sec. with the scram spring aiding. Tests with the input opposing the scram spring were inconclusive.

SECTION V

COMPARATIVE PERFORMANCE WITH CONVENTIONAL ACTUATORS

The discussion which follows is a relative comparison of the advantages and disadvantages of four types of pneumatic motors, their servo valves, and their transmissions when used as a portion of the forward section of an electropneumatic closed loop reactor drum control system.

It is assumed that the application of the motors is not for a maximum initial torque on-off type of control system, but rather for a continuous control system where the motor input flow and pressure drop are infinitely variable by means of a torque motor and pneumatic servo valve.

5.1 GEAR MOTOR

A typical high performance gear motor consists of two pinions and a center gear. Each gear is supported at each end by ball bearings. The center gear and pinions are held in place axially by carbon plates. The carbon plates are supported in a fixed position at the ends of the center body by the motor end plates. The motor output shaft is an extension of the center gear.

The motor is used in conjunction with a four way two stage spool type pneumatic valve with equal inlet and exhaust areas. The motor is made reversible by connecting diametrically opposite gas chambers together and to the valve P_1 and P_2 ports as shown in Figure 5-1.

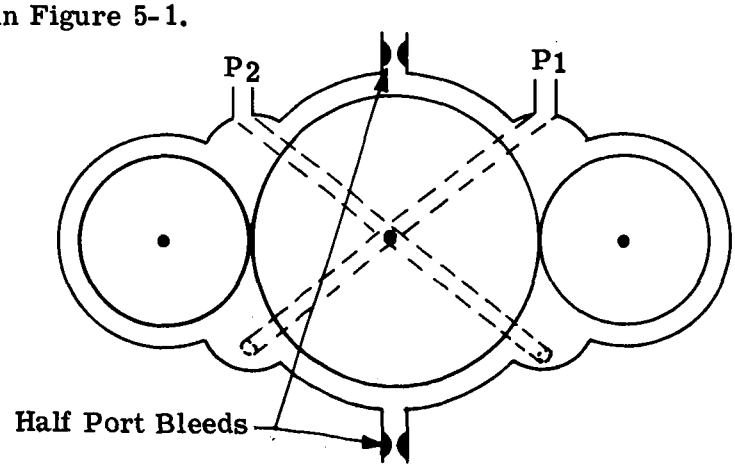

Figure 5-1. Pneumatic Gear Motor Schematic

When the gear motor is totally enclosed, except for the output shaft and its bearing, and operated in conjunction with a symmetrical four way spool valve, its performance is very poor. The resolution is poor, the stall torque sensitivity through null is low, and the wear debris from the carbon plates is considerable.

The low torque sensitivity through null is caused by a low pressure build-up across the motor as a function of the valve displacement, and is primarily the result of gas leakage from the high pressure (P_1) chamber to the low pressure (P_2) chamber, and the inability to exhaust this gas through the valve P_2 orifice without a significant pressure drop across it.

In order to reduce the flow into the P_2 chamber, the leakage is diverted to atmosphere through a low impedence path by means of a fixed orifice or half port bleed. The orifice is placed in center body on opposite sides of the center gear teeth as shown in Figure 5-1. This modification has been found to be adequate in linearizing the generated stall torque curve through null. However, the total gas flow to the motor is increased, and the initial break frequency is reduced.

The motor is basically unsymmetrical due to the single ended output shaft. With the slight variation in clearance at each end of the gear and pinions, a pressure drop results along the gear axis, and the gear and pinions ride against a single carbon plate rather than float in between them. This usually causes an increase in motor internal friction and, due to carbon plate wear, an increase in the axial clearance.

To minimize the axial pressure drop, the pressure in the bearing cavities is equalized by interconnecting the cavities through slots and hollow shafts. The resulting gas flow is discharged to atmosphere through large orifices at each bearing.

In summary, the disadvantages of the gear motor are:

1. The close tolerances required between moving parts.
2. The meticulous care required during assembly to ensure alignment between the gears, end plates and center body.
3. The increased flow required to improve the torque characteristics through null.
4. The rapid deterioration of the gears when they become contaminated.

The advantages are:

1. The linear torque speed characteristic through null.
2. Ability to operate on low gas pressures.
3. The small and constant volume under compression.
4. The ability to operate satisfactorily over a wide ambient temperature range.
5. The small amount of dry lubrication required.
6. The moving parts are inherently dynamically balanced, allowing high speed operation and consequent reduction in package size.

5.2 VANE MOTOR

The vane motor consists of a rotor with vane slots located on its outer

diameter. In the direction of its axis are contained the vanes, the center body and contoured bore upon which the vanes slide, and the end plates. The rotor is supported at each end by a ball bearing.

The motor is made reversible by interconnecting diametrically opposite chambers to the valve P_1 port, and the adjacent chambers to the P_2 port. The gas entering the P_1 chamber is allowed to expand for approximately one quarter of a revolution and then it is discharged through a large fixed orifice to a low pressure level. After discharge, the gas at the discharge pressure level is recompressed for a portion of a revolution and then discharged through the valve P_2 port.

The motor P_2 chamber is adjacent to the motor P_1 chamber and in the simplest motor configuration the P_1 and P_2 chambers are separated by a single vane. Due to the reciprocating action of vanes, the depth of the vane slot must be slightly greater than the maximum displacement of the vanes. As a result of this volume below the vane, there must be a clearance between the vane and the slot of such size as to allow this entrapped volume to charge and discharge when the motor is operating at its maximum speed. Also, at high motor speeds the heat generated by the vane rubbing against the sides of the vane slot and center body bore causes the vane to expand relative to the rotor, this requires an additional clearance in the vane slot as well as between the ends of the vane and the motor end plates.

When the vanes have a pressure drop across them, they seat against the top edge of the slot. Most of the leakage from P_1 to P_2 occurs at the ends of the vanes and rotor. To reduce this cross port leakage it would be desirable to discharge this leakage prior to it reaching the P_2 chamber. Due to the small thickness of the vane, the space available is limited. Generally, to the interest of simplicity and reliability, the leakage is controlled by the clearance allowed between the rotor and the end plates, and the gas is discharged through a valve with an exhaust area gain greater than the inlet.

At null when P_1 is equal to P_2, the vane separating the two chambers has no net force acting on it.

It is then possible for the vane to float in its slot. When P_1 is greater than P_2, the net radial force on the vane tends to seat the vane tip against the bore or cam surface, and the net tangential force tends to move the vane towards the P_2 chamber. Both movements of the vane occur simultaneously when the pressure drop is greater than is required to overcome the friction forces.

The average pressure on the rounded vane tip surface is less than the pressure applied to the bottom of the vane. The net force is then in a direction to move the vane towards the bore. During this transition two leakage paths from P_1 to P_2 are evident, across the vane tip, and between the vane faces and the vane slot. Since there is friction involved, a finite P_1 to P_2 pressure drop is required to seat the vane tip against the bore. Sometimes a low rate spring is placed in the slot below the vane to insure proper vane tip seating.

The vane also tends to pivot about the upper edge and wedge in place. When

a reduction in output torque is required, the P_1 pressure would have to be lowered an amount corresponding to that required to unwedge the vane, since the friction force caused by the wedging action now reverses and acts in the same direction as the P_1 pressure force on the face of the vane. The net result is a large hysteresis in the stall torque characteristics.

Also during the transition period, the P_1 to P_2 leakage is detrimental to the build-up of the motor pressure drop through null.

The net effect of the P_1 to P_2 leakage and the friction forces is a stall torque characteristic with a low gain through null and a large hysteresis band.

Since the vane motor has the same problem as the gear motor with respect to axial pressure drop across the rotor, the solution by equalizing the pressures in the bearing cavities is equally applicable.

As the motor rotates, the vanes reciprocate in the vane slots, but they do not remain exactly midway between the ends of the slots. They move in a manner such as to cause an unsymmetrical but rhythmic wear pattern on the surface of the end plates. The width of the worn area is equal to the height of the vane plus the length of the vane stroke. What causes the vanes to move in this manner is not thoroughly understood, but the results are a degradation of motor stall torque and an accumulation of wear debris in the bearings.

In summary, the disadvantages of the vane motor are:

1. The large number of sliding parts, and the resultant lubrication problem.
2. The low stall torque sensitivity through null.
3. The complex porting arrangement required to exhaust the leakage flow.
4. The requirement for an unsymmetrical servovalve.
5. The wide hysteresis deadband.

The advantages of the vane motor are:

1. Its relatively high volumetric efficiency.
2. A small number of critical tolerance parts.
3. A reduction in the number of high density parts, resulting in a good power to weight ratio.
4. Ease of assembly.

5.3 LINEAR PISTON

The linear piston motor can be used with either a pressure or flow control valve. In order to minimize the phase shift due to the entrapped volume and the low bulk modulus of the gas, a pressure type control valve is generally used.

Because of its large volume under compression, the piston-cylinder actuator is usually operated at higher pressures to maintain a reasonable open loop natural frequency.

The push-pull linear actuator is very similar to the gear and vane motors with respect to generated stall torque. All are sensitive to P_1 to P_2 or cross port leakage. The piston-cylinder actuator relies on a piston seal to minimize leakage as contrasted to controlled clearance and vane tip seals for the vane motor and controlled clearance for the gear motor. Because of the greater use of sliding seals, the piston-cylinder actuator has the highest internal friction followed by the vane motor and then the gear motor.

The piston-cylinder actuator has a reasonably linear generated stall torque through null, but due to the relatively high coulomb friction of the piston seal its resolution or dead band is considerably wider than the others.

The piston-cylinder motor generally uses only dynamic seals for leakage control. As a result it has a higher performance deterioration rate than either the vane or the gear motor. The use of dynamic seals does however offer some advantages. It is necessary, when using controlled clearances, that close tolerances be held during the machining and assembly operations. Consequently, the manufacturing cost is the least for the piston actuator. Also, the piston-cylinder motor because of its smaller cross port leakage has the lowest gas consumption.

In summary, the disadvantages of the piston motor are:

1. Large volume under compression and hence reduced response characteristics.
2. High internal friction resulting in large deadband at null.
3. More rapid degeneration of performance.

The advantages are:

1. Highest power to weight ratio.
2. Simple and economical to manufacture.
3. Low gas consumption.

5.4 SERVOVALVES

Gear and vane motors have both been operated in conjunction with open center four way spool type valves with a good deal of success. These valves have operated in excess of 300 hours without significant deterioration in performance. The spool and sleeve are made of materials such as stellite which, when heated in an oxygen containing atmosphere, produces a durable, low friction coefficient oxide coating.

The disadvantage of this type of servovalve is the small clearances involved and the added complexity of stabilizing the pilot stage with damping tanks and bleeds.

Due to the spool to sleeve clearance and the resulting leakage, this type of valve does not lend itself to a pressure type control as readily as bellows operated poppet valves or combination bellows and spool sleeve valve. The pressure type control valve is similar to the flow or area control valve with negative pressure feedback. The effect of the negative pressure feedback is a reduction in the phase shift caused by the volume under compression, and a decrease in the stiffness of the control. When the open loop resonant frequency requirements are met, the resolution of the piston

actuator is generally less than desired. This problem is difficult to overcome without raising the supply pressure or introducing a frequency dependent pressure feedback such that the static stiffness is much greater than that obtained with a fixed amount of pressure feedback.

5.5 TRANSMISSIONS

In order to match the motor output to the load requirements, some form of transmission is required. The piston-cylinder motor requires a conversion from linear to rotational motion with a relatively small transmission ratio. This can be readily obtained with a simple rack and pinion, and is by far the least complex of the three.

The gear and vane motors have essentially the same transmission requirements. Because of their high output speeds, they require a rather large transmission ratio, which can be obtained with either a planetary or nutator transmission. The planetary transmission is advantageous in that it is inherently dynamically balanced with a low input inertia, and can be contained in a reasonably small package. Unfortunately, these advantages are offset by the considerable number of gears and bearings required, and consequently its questionable reliability.

From a reliability standpoint, the nutator transmission is superior to the planetary transmission. The nutator transmission is a unique means of obtaining a large transmission ratio with a single pair of bevel gears.

The nutator transmission is not inherently dynamically balanced. When balanced, its input inertia is greater than that of the planetary transmission, but not prohibitively high for this application. Its obvious advantage is the few gears and parts required to obtain a large transmission ratio. In addition, the package size for a given transmission ratio and power capability is less than the equivalent planetary transmission.

5.6 NUTATOR MOTOR

Since the nutator motor developed under this contract provides a uniform torque speed characteristic proportional to an input pressure differential, the actuator can be compared directly with gear, vane or piston and cylinder concepts.

Although the commutation circuit of the nutator motor is considerably more sophisticated than the conventional spool valves, the lack of any moving parts gives the circuit an inherently high reliability. The circuit construction lends itself to conventional production techniques such as chemical or tape controlled milling. The absence of flow grinding requirements will greatly reduce the manufacturing costs.

The use of bellows to provide the pneumatic pressure to mechanical force conversion eliminates any inherent problems of controlled leakage paths, friction in high speed rotating and sliding components, and critical manufacturing tolerances. The use of only two bearings to support the output shaft simplifies the construction, reduces the mechanical power losses and minimizes the hysteresis due to stiction effects.

Since there are no high speed rotating components, the input inertia is low, consisting only of the nutating gimbal ring and the negligible bellows mass. The frequency response is therefore determined directly by the commutation circuit response.

The design concept of the nutator motor provides a combined pneumatic pressure to mechanical force conversion and high torque amplification in one integral unit. It is then possible to obtain a package size and weight which is smaller and lighter than a conventional actuator of comparable performance. When the motor is not supplied with pneumatic power, the input gear is automatically disconnected from the output. This disconnect feature is particularly desirable in the control of a nuclear reactor, since a scram condition can be obtained without the requirement of clutches or the necessity to backdrive high speed components.

The basic design of the mechanical portion of the nutator actuator allows operation as an analog motor or, by changing the commutation circuitry, a pneumatic pulse input will provide an accurate stepped increment in output shaft position. The versatility of operation is unique in an actuator design.

SECTION VI

SUMMARY AND RECOMMENDATIONS

6.1 SUMMARY

The pneumatic nutator actuator provides a low speed high output torque device with a minimum number of moving parts. The lack of high speed rotary components and minimum volume under compression gives the concept design an inherently high reliability and wide closed loop frequency response. Since the basic actuator can be used as either an analog or digital stepping motor, depending on the commutation circuit employed, the concept provides a versatility which is unusual in pneumatic actuator design.

The development program performed under this contract successfully demonstrated the feasibility of the pneumatic nutator actuator concept. The operation of the commutation circuit demonstrates the ability of vortex type fluid amplifier to operate in a complex combination of series and parallel logic sequence.

During the course of the program, unforeseen development problems were encountered which could not be solved under the scope of the contract. The results obtained, however indicated the actuator's potential and gave an indication of the direction of effort required to obtain the design performance.

6.2 RECOMMENDATIONS FOR FURTHER DEVELOPMENT

The main areas of investigation should be concentrated on obtaining the design stall torque and a higher maximum speed (or slew velocity). Of secondary importance is an investigation of the gas constant sensitivity.

The test fixtures used during this initial contract provide the ability to operate the commutation circuit and the mechanical portions of the actuator either separately or in an open loop mode. Investigations performed with these fixtures were qualitative in nature and have been discussed in Section IV. In order that the actuator performance be improved, it is necessary that a quantitative investigation be made of both the static and dynamic operation of the commutation circuit and the mechanical hardware.

It is therefore recommended that the following evaluation tests be performed to determine the maximum potential capabilities of the developed actuator:

a. Using a sinusoidal input forcing function determine the dynamic characteristics of the commutation circuit both in terms of pressure error input and position pickoff input.

b. With the mechanical commutator, determine the static and dynamic potential of the bellows force elements and the effects of input inertia.

c. Evaluate the fluctuations in bellows pressure due to power supply variations.

d. Evaluate various position pickoff bleed configurations to obtain the optimum timing sequence.

From these evaluation tests, the critical areas affecting performance can be determined. Corrective action can then be initiated to obtain the full design capability of the actuator.

APPENDIX A

DESIGN CALCULATIONS

APPENDIX A

DESIGN CALCULATIONS

A-1 GEAR FORCE ANALYSIS

Let,

F_p = Resultant force applied by bellows

F_s = Separating force of gear set

γ = Nutation angle

ζ = An angle between F_p and F_s which is a function of the system torque (force angle).

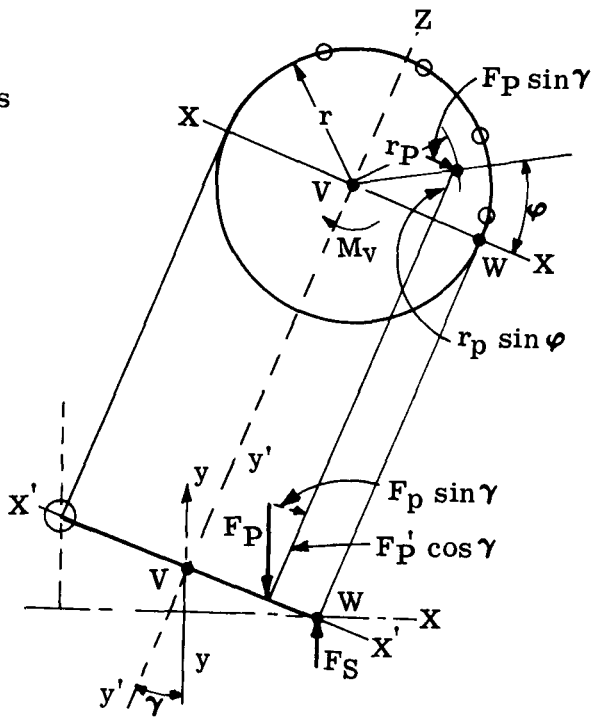

Moment created by Applied Force F_p:

Consider a disc in a rectangular coordinate system oriented so that the axis of the disc (y' - y') is at an angle (γ) with the y-y axis. The disc is instantaneously supported at points V and W in the x-y plane and is free to rotate about the instant axis (x' - x'). A force (F_p) is applied at some radius (r_p) and some angle (ζ) from the x-x axis. This force is parallel to the y-y axis and can be resolved into two components,

$F_p \sin\gamma$ and $F_p \cos\gamma$.

The component $F_p \sin\gamma$ will produce a moment (M_v) about the y'-y' axis.

Let N = transmission ratio.

Then, $M_v = (F_p \sin\gamma)\ r_p \sin\zeta$ (input torque)

Or $\boxed{M_t = N(F_p \sin\gamma)\ r_p \sin\zeta}$ (output shaft torque) (1)

Equation (1) is the general equation which describes the relationship between moment (M_v) and the angle of force application (ζ). Thus, when $M_v = 0$, $\zeta = 0$ and, neglecting all other considerations, M_v maximum occurs when $\zeta = 90°$. The torque produced by the force acts in a direction opposite to the motion of the disc. Including an overall efficiency factor (η),

$$\boxed{\text{Shaft Torque} = M_t = N\eta\,(F_p \sin\gamma)\; r_p \sin\zeta} \qquad (1\text{-a})$$

Separating Moment:

The separating force (F_s) acting at the gear tooth mesh is related to the shaft load torque (M_t) by the following expression,

$$\tan\phi = \frac{F_s}{F_t} = \frac{F_s\, r_g}{M_t} \qquad \text{(tooth pressure angle)}$$

or

$$F_s = \frac{M_t}{r_g} \tan\phi$$

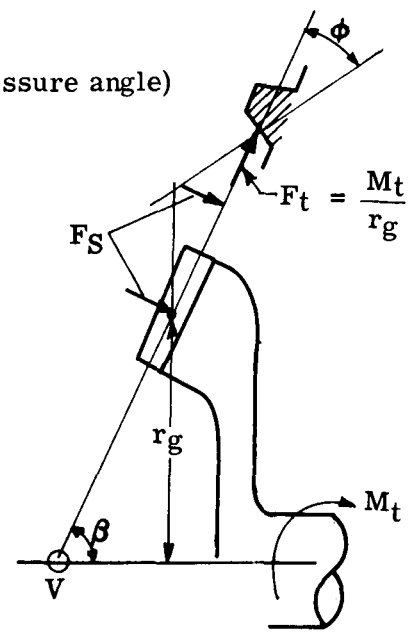

Then, the moment acting about the vertex (v) due to the separating force (F_s) is,

$$M_s = F_s\left(\frac{r_g}{\sin\beta}\right)$$

Substituting the expression for F_s into the above equation gives,

$$\boxed{M_s = M_t\left(\frac{\tan\phi}{\sin\beta}\right)} \qquad (2)$$

The moment created by the force F_p tending to hold the gears in mesh is,

$$\text{(Meshing moment)} = \boxed{M_m = F_p\, r_p \cos\zeta} \qquad (3)$$

Shaft torque (M_t) related to separating angle(ζ_{max})

The nutating gear set will tend to separate (jump out of mesh) when the separating moment (M_s) is equal to, or greater than the meshing moment (M_m) created by the applied force (F_p). Thus, by equating (2) and (3),

$$F_p\, r_p \cos \zeta_{max} = M_t \left(\frac{\tan \phi}{\sin \beta} \right)$$

Or

$$\boxed{\text{Cos } \zeta_{max} = \frac{M_t}{F_p\, r_p} \left(\frac{\tan \phi}{\sin \beta} \right)} \qquad (4)$$

Also, substituting equation (1) into (4),

$$\text{Cos } \zeta_{max} = \frac{N\,(F_p \sin \gamma)\, r_p \sin \zeta_{max}}{F_p\, r_p} \left(\frac{\tan \phi}{\sin \beta} \right)$$

$$\boxed{\tan \zeta_{max} = \frac{\sin \beta}{N \tan \phi \sin \gamma}} \qquad (5)$$

Equation (5) indicates that the separation angle is independent of the applied force (F_p) and the effective radius (r_p). It is solely dependent on gear set parameters (pressure angle, transmission ratio, half-cone angle, and nutation angle.)

Using the actuator design figures,

β = cone angle = 75° $\qquad$ $\sin \beta = 0.966$

γ = nutation angle = 1° 8' 21.2" $\qquad$ $\sin \gamma \approx \gamma = .0198$ radians

N = transmission ratio = 180

ϕ = tooth pressure angle = 14 1/2°

Substituting in Equation (5).

$$\tan \zeta_{max} = \frac{\sin \beta}{N \tan \phi \sin \gamma} = \frac{0.966}{180(.259)(.0198)} = 1.04$$

$$\boxed{\zeta_{max} \approx 46° = \text{separation angle}}$$

Therefore the gears will separate if the input force is applied at an angle of 46° or greater to the mesh point of the gears.

A-2 BELLOWS AREA DESIGN

Pressure Force Centroid

Bellows Unit Force = F

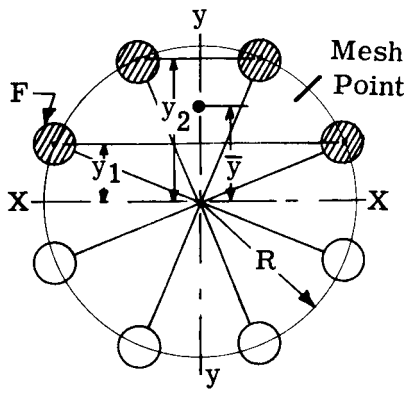

$$4F\bar{y} = 2Fy_1 + 2Fy_2$$

$$\bar{y} = \frac{2F(y_1 + y_2)}{4F}$$

$$\bar{y} = \frac{y_1 + y_2}{2}$$

$y_1 = R \sin 1/2 \left(\frac{360°}{N}\right)$ when N = total number of bellows.

$y_2 = R \sin 3/2 \left(\frac{360°}{N}\right)$

For N = 8

$y_1 = R \sin 22.5° = .383R$

$y_2 = R \sin 67.5° = .924R$

then $\bar{y} = \frac{y_1 + y_2}{2} = \frac{1.307R}{2} = 0.653R$

Design: M_t = 360 in-lb. r_g = 2.175 inches

R = 3 inches

$\bar{y}$ = 0.653R = 1.959 inch **Use $\bar{y}$ = 1.96 inch**

Separating Force, $F_s = \frac{M_t}{r_g} \tan\phi = \frac{360}{2.175} (.259) = 42.9$ lb. max.

Separating Moment = $M_s = F_s \left(\frac{r_g}{\sin\beta}\right) = 42.9 \left(\frac{2.175}{.966}\right) = 96.5$ in-lb. max.

Applied Force Required (F_p):

Known: Max. shaft torque = M_t = 360 in-lb.

Nutation angle = γ = 1^0 8' 21.2" $\quad \sin\gamma \approx \gamma = .0198$ radians

Force angle = ζ = 45° $\quad \sin\zeta = .707$

Transmission ratio = N = 180:1

From Equation (1)

$$F_p = \frac{M_t}{N(\sin\gamma)\, r_p \sin\zeta} \qquad r_p = \bar{y} = 1.96 \text{ inch}$$

$$= \frac{360}{180(.0198)(1.96)(.707)} = 73 \text{ lb.}$$

Bellows force $F_\beta = \left(\frac{F_p}{4}\right) = \frac{73}{4} = 18.3$ lb.

Maximum pressure differential across bellows = ΔP = 70 psi

$$\therefore \text{ Bellows area (ideal)} = \frac{F_\beta}{\Delta P} = \frac{18.3}{70} = 0.26 \text{ inch}^2$$

This is the minimum effective bellows area required based on 100 percent mechanical efficiency and a maximum pressure drop of 70 psid across the bellows.

Allowing an over-all efficiency and pressure drop factor of 60 percent, we will obtain an effective bellows area of,

$$A_b = \left(\frac{0.26}{0.6}\right) = 0.435 \text{ inch}^2$$

A-3 GEAR DESIGN SUMMARY

Number of teeth input gear N = 181
Number of teeth output gear n = 180
Input gear cone angle $\beta = 75°$
Output gear cone angle $\alpha = 73° 51' 39''$
Nutation angle $= 1° 8' 21''$
Clearance angle $= 31' 40''$
Minimum gear tooth clearance 0.018 inch
Stubbing ratio K = 0.50
Tooth average pressure angle = 14 1/2°
Tooth bending stress = 23,100 psi
Hertz stress = 3,680 psi
Allowable Hertz stress = 142,000 psi (BHN = 382)

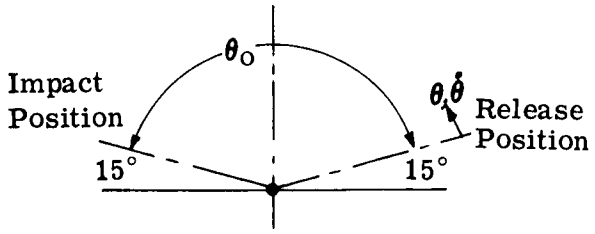

A-4 SCRAM SYSTEM ANALYSES

(a) Friction (M_f): The seal friction is assumed to be 15 in-lb. and the load friction is 32 in-lb max. For design calculations, assume a value of $M_t = 15 + \frac{32}{2} = 31$ in-lb.

(b) Inertia (J_L): The load inertia is set @ 0.246 in-lb-sec^2. The inertia of the actuator output shaft and gear is estimated at 0.014 in-lb-sec^2. For design calculations, assume a value of $J_L = 0.26$ in-lb-sec^2.

(c) Spring "Installed Load" (M_s): The maximum friction in this system can be 32 + 15 = 47 in-lb., allowing 3 in-lbs. over this maximum to permit a slight margin above the friction load. Let $M_s = 50$ in-lb.

(d) Torsional Spring Rate (K): For this application, K should be low. For design, let K = 4 in-lb./rad.

(e) Release Angle (θ_0): For a total travel of 180° with a soft stop at 15° from either end, $\theta_0 = 150°$ (2.618 radians)

System Constants:

$$\omega = \sqrt{\frac{K}{J_L}} = \sqrt{\frac{4.0}{.26}} = \sqrt{15.4} = 3.8 \text{ sec}^{-1} \qquad \omega^2 = 15.4 \text{ sec}^{-2}$$

$$a = \left(\frac{K\theta_0 + M_s - M_f}{J_L}\right) = \left[\frac{4(2.618) + 50 - 31}{.26}\right] = \left(\frac{29.5}{.26}\right) = 113.5 \text{ sec}^{-2}$$

Kinetic Energy at Impact (V_i):

The kinetic energy at impact is,

$$V_i = 1/2\ J_L\ \dot{\theta}^2$$

where

$$\dot{\theta} = \left(\frac{a}{\omega}\right) \sin\ \omega t \quad \text{and} \quad t \approx \sqrt{\frac{2\theta}{a}}$$

Substituting, $t \approx \sqrt{\frac{2(2.618)}{113.5}} = \sqrt{\frac{5.23}{113.5}} = \sqrt{.046} = 0.214$ sec.

$$\dot{\theta}_{max} = \left(\frac{113.5}{3.8}\right) \sin\ (3.8)(.214) = 29.9 \sin\ .813$$

$$= 29.9(.727)$$

$$= 21.7 \text{ rad/sec.}$$

Then

$$V_i = 1/2\ J_L\ \dot{\theta}^2 = 1/2(0.26)(21.7)^2 = 90.5 \text{ in-lb.}$$

$\boxed{V_i = 90.5 \text{ in-lb.}}$ This is the kinetic energy at impact for 150° release position.

Rebound (θ_R)

The specification allows a rebound of 1/4 of the incoming release-to-impact travel. For a perfectly elastic impact (no energy absorbed),

$$\left(\frac{M_f + M_s}{K}\right) = \left(\frac{31 + 50}{4}\right) = \left(\frac{81}{4}\right) = 20.2 \qquad \left(\frac{2V_i}{K}\right) = \frac{181}{4} = 45.2$$

$$\theta_R = \left(\frac{M_f + M_s}{K}\right) - \sqrt{\left(\frac{M_f + M_s}{K}\right)^2 - \frac{2V_i}{K}} = 20.2 - \sqrt{408 - 45.2} = 20.2 - 19.1$$

$$\theta_R = 1.1 \text{ radian } (63°)$$

Allowable rebound

$$\theta_{all} = \frac{\theta_o}{4} = \frac{2.618}{4} = 0.65 \text{ radian}$$

So that

$$\theta_R > \theta_{all}$$

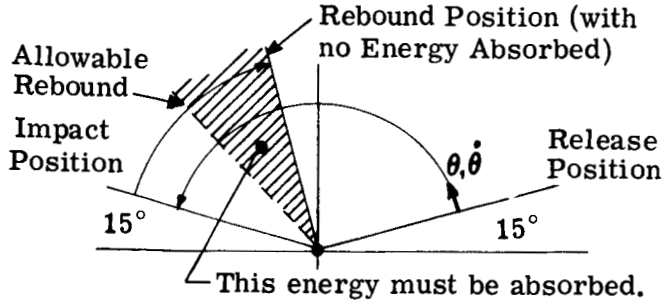

Energy Absorbed By Snubber (Vs)

(Impact Energy = Rebound energy + Energy absorbed by snubber)

or $V_i = V_R + V_S$

If the allowable rebound is $\theta_{all} = \frac{\theta_o}{4} = \frac{2.618}{4} = 0.65$ rad, then the energy associated with this becomes,

$$V_R = 1/2K\ \theta_{all}^2 + (M_s + M_f)\ \theta_{all}$$

$$= 1/2(4)(.65)^2 + (31 + 50)(.65) = .846 + 52.7 = 53.5 \text{ in-lb.}$$

Then, the energy that must be absorbed by the snubber becomes,

$$V_S = V_i - V_R = (90.5 - 53.3) = 37 \text{ in-lb.}$$

Summary of Energy Balance

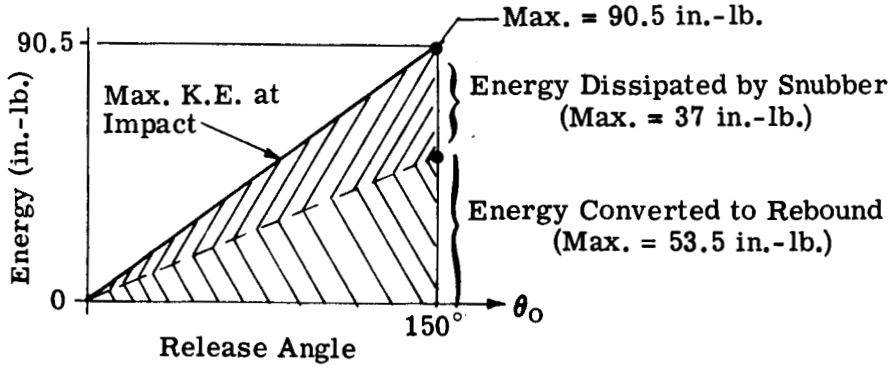

Deceleration Rate ($-\ddot{\theta}$):

The specification limits the deceleration to $\ddot{\theta} = -2000$ rad/sec^2. Using the expression,

$$\ddot{\theta}_{max} = \left(\frac{r}{\delta}\right) \dot{\theta}^2_{max}$$

$$\therefore \left(\frac{r}{\delta}\right) = \frac{\ddot{\theta}_{max}}{\dot{\theta}^2_{max}} = \frac{2000 \text{ rad/sec}^2}{(21.7 \text{ rad/sec})^2} = \left(\frac{2000}{472}\right) = 4.25$$

where r = radius from actuator to snubber centerlines

δ = snubber stroke (in.)

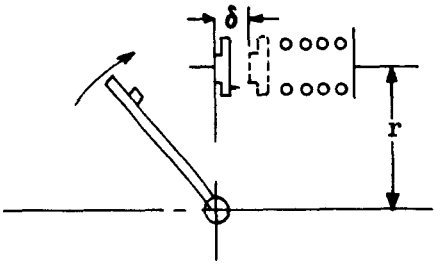

Energy Dissipation (Considering a friction device)

The heat generated is a measure of the amount of kinetic energy being absorbed by the snubber,

$$H_g = \frac{\overline{V}_s}{778} \quad \text{Btu/min.}$$

where $\overline{V}_s$ = The rate of kinetic energy to be absorbed $\left(\frac{\text{ft-lb}}{\text{min}}\right)$

Also, the heat generated is equal to the rate of frictional work or,

$$H_g = \left(\frac{p\, A_c\, f v}{778}\right)$$

where p = average contact pressure (psi)

A_c = contact area (in^2)

f = coefficient of friction

v = velocity (ft/min)

Then,

$$\overline{V}_s = p\, A_c\, f\, v$$

Or

$$p\, A_c = \left(\frac{\overline{V}_s}{f\, v}\right)$$

Friction coefficients for sintered - Metallic Materials = 0.1 - 0.2
for Metal - ceramic materials = 0.2 - 0.4

Assume $f = 0.2$, $V_s = 37$ in-lb. $= 3.1$ ft-lb.

$$v = r\dot{\theta} \approx \frac{2 \text{ in } 21.7 \text{ rad} \times 60 \text{ sec. ft.}}{\text{sec. } 12 \text{ in. } \text{min}} = 217 \text{ ft/min.}$$

$$\overline{V}_s = \frac{V_s}{t} = \frac{3.1 \text{ ft-lb.}}{.214 \text{ sec}} \times \frac{60 \text{ sec}}{\text{min.}}$$

$$= 870 \text{ ft-lb/min.}$$

Then

$$p\, A_c \approx \frac{870 \text{ ft-lb/min}}{(.2)\ 217 \text{ ft/min}} = 20 \text{ psi-in}^2$$

Using a contact area of 3.76 in^2, the contact pressure is 5.32 psi, which is satisfactory for the metal-ceramic material selected. The brake band is then adjusted to a torque of $T = p\, Ac\, fv$ or $T = 20 \times .2 \times 1.2 = 4.8$ in-lb.

A-5 SNUBBER SPRING

The snubber spring must absorb 54 in-lb. of kinetic energy while deflecting through 15°. The spring must deflect 15° in both directions.

Assume spring will be made of 17-4 PH Steel.

$F_{tu} = 190$ Kpsi $\qquad G = 10.5 \times 10^6$ psi

$F_{ty} = 170$ Kpsi $\qquad F_{su} = 120$ Kpsi

$E = 28.5 \times 10^6$ psi

Comparison of Spring Types

The comparison will be based on the gravimetric elastic efficiency (η_w) which is a measure of the energy per unit volume capability of the spring in (in-lb/lb.).

(a) Constant-Strength Cantilever:

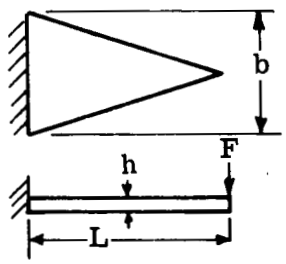

$$\eta_w = \left(\frac{S_B^2}{6E\rho}\right)$$ where:

S_B = Bending stress (psi)

ρ = Specific weight of material ($\#/in^3$)

(b) Straight Round Bar (Solid)

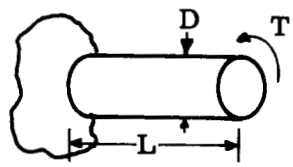

$$\eta_w = \left(\frac{S_s^2}{4G\rho}\right)$$

(c) Straight Round Bar (Hollow)

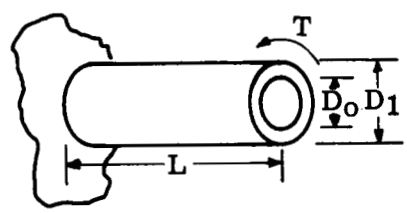

$$\eta_w = \left(\frac{S_s^2}{4G\rho}\right)\left(\frac{D_1^2 - D_0^2}{D_1^2}\right)$$

(d) Straight Rectangular Bar (Solid)

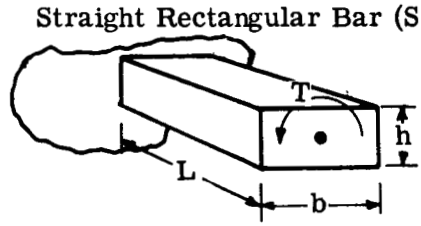

$$\eta_w = \left(\frac{S_s^2}{4G\rho}\right)\left(\frac{b^2h^2}{C}\right)$$

where $C = 9b^4 + 3.24h^4 + 10.8(bh^3 + b^3h) + 12.24\, b^2h^2$

Comparing (a) and (b) assume S_B = 150 ksi S_s = 100 ksi ρ = .28

for (a) $$\eta_w = \frac{(150 \times 10^3)^2}{(6)(30 \times 10^6)(.28)} = \frac{22{,}500}{50.3} = 447 \text{ in-lb./lb.}$$

for (b) $\eta_w = \dfrac{(100 \times 10^3)^2}{(4)(10.5 \times 10^6)(.28)} = \dfrac{10{,}000}{11.8} = 850$ in-lb./lb.

for (c), let $D_1 = 1.5\, D_0$ $\dfrac{D_1^2 - D_0^2}{D_1^2} = \dfrac{2.25\, D_0^2 - D_0^2}{2.25\, D_0^2} = \dfrac{1.25}{2.25} = 0.55$

for (c) $\eta_w = 850(.55) = 470$ in-lb/lb.

for (d), let $b = 6h$

$\therefore\ C = 11{,}700\, h^4 + 3.24h^4 + 10.8(6h^4 + 216h^4) + 450\, h^4 = 14{,}400\, h^4$

and $\dfrac{b^2h^2}{C} = \dfrac{36\, h^4}{14{,}400\, h^4} = \dfrac{1}{400}$

for (d) $\eta_w = (850)\dfrac{1}{400} = 2.1$ in-lb./lb.

Thus, the best choice is (b): Straight Round Bar (Solid).

To reduce the torsion bar length, a solid bar and hollow cylinder combination was selected. The design stress levels were calculated as follows:

The torsion bar can be drawn as follows (for ease in visualization)

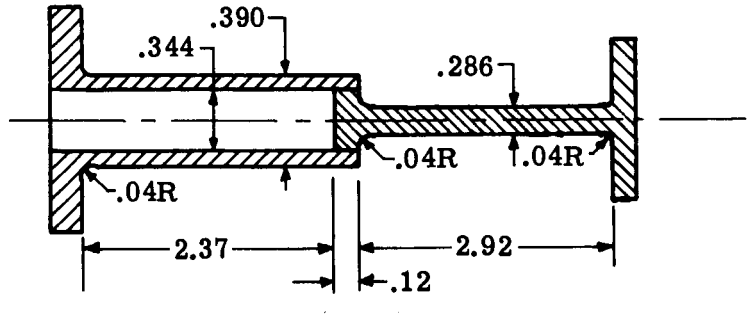

For solid shaft, $\tau = \dfrac{16M_t}{\pi d^3}$

For hollow shaft, $\tau = \dfrac{16M_t\, d_0}{\pi (d_o^4 - d_i^4)}$

Assume maximum M_t = 415 in-lb.

Solid shaft: $d = 2.86 \times 10^{-1}$, $d^3 = 23.4 \times 10^{-3}$

$$\therefore \tau = \frac{(16)(415)}{\pi 23.4 \times 10^{-3}} = 90{,}500 \text{ psi}$$

Hollow shaft: $d_o = 3.90 \times 10^{-1}$, $d_o^4 = 232 \times 10^{-4}$

$d_i = 3.44 \times 10^{-1}$, $-d_i^4 = \dfrac{140 \times 10^{-4}}{92 \times 10^{-4}}$

$$\therefore \tau = \frac{16(415)(3.90 \times 10^{-1})}{\pi\, 94 \times 10^{-4}} = 88{,}000 \text{ psi}$$

Angle of twist:

For solid shaft: $\theta = \dfrac{584\, M_t L}{G d^4}$

For hollow shaft: $\theta = \dfrac{584\, M_t L}{G(d_o^4 - d_i^4)}$

Maximum M_t = 415 in-lb.

$G = 11.7 \times 10^6$ psi

$$\text{let } K = \frac{584\, M_t}{G} = \frac{(5.84)(4.15) \times 10^4}{11.7 \times 10^6} = 2.07 \times 10^{-2}$$

Solid shaft: $L = 2.84$ in. $d = 2.86 \times 10^{-1}$, $d^4 = 67 \times 10^{-4}$

$$\therefore \theta = \frac{KL}{d^4} = \frac{2.07 \times 10^{-2} \times 2.84}{67 \times 10^{-4}} = 8.8^\circ$$

Hollow shaft: $L = 2.33 \qquad d_o^4 - d_i^4 = 92 \times 10^{-4}$

$$\therefore \quad \theta = \left(\frac{KL}{d_o^4 - d_i^4}\right) = \frac{2.07 \times 10^{-2} \times 2.33}{92 \times 10^{-4}} = 5.25°$$

A-6 STOP PIN STRESS ANALYSIS

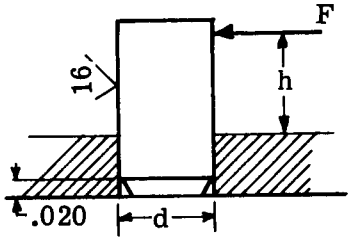

Maximum deceleration $\ddot{\theta} = 2{,}000$ rad/sec^2 (max.)

$$J\ddot{\theta} = \Sigma T = FR$$

For $R = 1" \qquad J = .246$ in-lb-sec^2

$$F = \frac{J\ddot{\theta}}{R} = \frac{(.246)(2{,}000)}{1} = 492 \text{ lb. (max. impact force)}$$

Assume $F = 500$ lb.

Maximum Moment arm on pin = 0.2 inch = h

Stud Diameter = d = 0.25 inch

The maximum combined stress in the stud is,

$$\sigma_{max} = \sqrt{\sigma_s^2 + \sigma_b^2 + \sigma_p^2} \quad \text{where}$$

σ_s = shear stress

σ_b = bending stress

σ_p = pressing stress

$$\sigma_s = \frac{F}{A} = \frac{500}{\pi(.125)^2} = 10{,}400 \text{ psi}$$

$$\sigma_b = \frac{32M}{\pi d^3} = \frac{(32)(500)(.2)}{\pi(.25)^3} = 65{,}000 \text{ psi}$$

$$\sigma_{p_{max}} = \frac{Ee_{max}(r_2^2 - r_1^2)}{r_2 r_1} \quad \text{where}$$

r_2 = distance from $\mathbb{C}_L$ of stud to edge of plate containing stud

r_1 = radius of stud

e_{max} = max radial int. fit (in)

Assume r_2 = 1 inch, e = 0.0005 (.001 dia. int. fit)

$$\sigma_{pmax} = \frac{30(10^6)(5 \times 10^{-5})(1 - .125^{-2})}{(1)(.125)} = \frac{1500\ (.98)}{.125} = 12{,}000\ (.98) = 11{,}800 \text{ psi}$$

$$\sigma_{max} = \sqrt{(1.04)^2 + (6.5)^2 + (1.18)^2} \times 10^4 = 67{,}000 \text{ psi}$$

$$f_s = \frac{S_e S_y}{\sigma_r S_y + \sigma_a S_e}$$

$$\sigma_r = \text{variable stress} = \frac{\sigma_{max} - \sigma_{min}}{2} = 67{,}000 \text{ psi}$$

$$\sigma_a = \text{angular stress} = \frac{\sigma_{max} + \sigma_{min}}{2} = 0 \text{ psi}$$

Assume $\{S_e$ = endurance limit = 80,000 psi (minimum)

Factor of safety $f_s = \frac{S_e}{\sigma_r}$

$$f_s = \frac{80}{67} = 1.2 \text{ (minimum)}$$

Typical chrome-ni steels have an endurance limit of 80,000 psi for 100,000 cycles.

A-7 BEARING LOADS

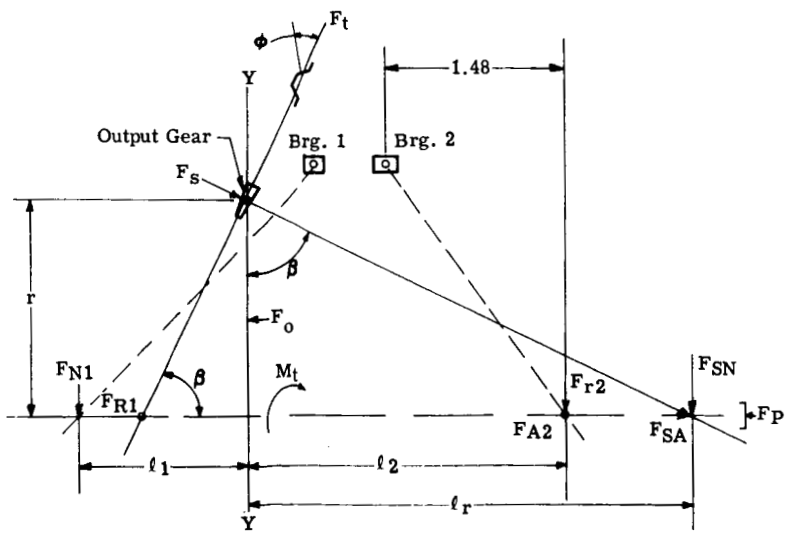

The output torque (M_t) acts at center of the pitch line of the gear tooth to produce a tangential force (F_t)

$$F_t = \frac{M_t}{r}$$

The separating force (F_s) = $F_b \tan\phi$

Resolving $F_{(s)}$ into normal component (F_{sN}) and axial component (F_{sA}), project to intersection with shaft centerline at distance ℓ_r from y-y axis

$$F_{sN} = F_s \cos\beta = F_t \tan\phi \cos\beta$$

$$F_{sA} = F_s \sin\beta = F_t \tan\phi \sin\beta$$

Forces transferred to shaft.

Radial forces due to (F_s)

$$\Sigma M_1 = 0 \quad F_{N2}(\ell_2 + \ell_1) = F_{sN}(\ell_r + \ell_1)$$

$$F_{N2} = F_{sN}\left(\frac{\ell_1 + \ell_r}{\ell_1 + \ell_2}\right)$$

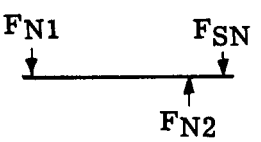

$$\Sigma F = 0 \quad F_{N1} = F_{N2} - F_{sN}$$

Radial forces due to F_t (at 90° to those for F_s) call F_{R1} and F_{R2}

$$\Sigma M_1 = 0 \quad F_t \ell_1 = F_{R2}(\ell_1 + \ell_2)$$

$$F_{r2} = F_t\left(\frac{\ell_1}{\ell_1 + \ell_2}\right)$$

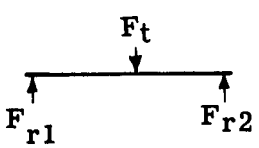

$$\Sigma F = 0 \quad F_{r1} = F_t - F_{r2}$$

Total radial force on bearings ($\overline{F}_{R1}$ and $\overline{F}_{R2}$)

$$\overline{F}_{R1} = \sqrt{F_{N1}^2 + F_{R1}^2}$$

$$\overline{F}_{R2} = \sqrt{F_{N2}^2 + F_{R1}^2}$$

Assumed Requirements:

Life - 150 hours - 200 in-lbs. at 33 1/3 RPM

Thrust load due gas pressure (F_p) = 520 lb.

$\beta = 75°$ $M_t = 200$

$\phi = 14.5° = .2586$

$\tau = 2.175$

Find F_t (Tangential force)

$$F_t = \frac{M_t}{\tau} = 92.2 \text{ lb.}$$

Find F_s (Separating force)

$$F_s = F_t \tan\phi = 92.2 \times .2586 = 23.85 \text{ lb.}$$

Resolve F_s

$$F_{sN} = F_s \cos\beta = 23.85 \times .259 = 6.18 \text{ lb.}$$

$$F_{sA} = F_s \sin\beta = 23.85 \times .966 = 23 \text{ lb.}$$

Find ℓ_r

$$\ell_r = \tau \tan\beta = 2.175 \times 3.73 = 8.1$$

Let $\ell_1 = 0.9$

$\ell_2 = 3.15$

$\ell_r = 8.1$

Find radial forces on bearing

(1) Due to separating force $F_{(s)}$

$$F_{N2} = F_{sN}\left(\frac{\ell_1 + \ell_2}{\ell_1 + \ell_2}\right) = 6.18\left(\frac{0.9 + 8.1}{0.9 + 3.15}\right)$$

$$F_{N2} = 6.18\left(\frac{9}{4.05}\right) = 13.72 \text{ lb.}$$

$$F_{N1} = F_{N2} - F_{sN} = 13.72 - 6.18 = 7.54 \text{ lb.}$$

(2) Due to tangential force (F_t)

$$F_{R2} = F_t\left(\frac{\ell_1}{\ell_1 + \ell_2}\right) = 92.2\left(\frac{0.9}{4.05}\right)$$

$$F_{R2} = 20.5 \text{ lb.}$$

$$F_{R1} = F_t - F_{R2} = 92.2 - 20.5$$

$$F_{R1} = 71.7 \text{ lb.}$$

(3) Summation radial load

$$\bar{F}_{R1} = \sqrt{F_{N1}^2 + F_{R1}^2} = \sqrt{7.54^2 + 71.7^2}$$

BRG No. 1	$\bar{F}_{R1} = 72.1$ lb.

$$\bar{F}_{R2} = \sqrt{F_{N2}^2 + F_{R2}^2} = \sqrt{13.72^2 + 20.5^2}$$

BRG No. 2	$\bar{F}_{R2} = 24.6$ lb.

Axial Bearing Load.

BRG No. 1 Maximum axial load condition is with $F_p = 0$
But with 65 psi back pressure (F_s) axial force (F_B)
$= 65 \times .8 = 52.0$ lb.

BRG No. 2 Maximum axial condition is 650 psi shaft pressure (F_p), no back pressure, no separating force

$$F_p = 650 \text{ psi} \times 0.850 \text{ in.} = 520 \text{ lb.}$$

Bearing Selection (Using Kaydon Engineering catalog S200)

(1) Establish equivalent bearing loads

Bearing No. 1 Radial load = 72.1 lb.
Axial load $= F_B + F_{sA} = 52 + 23 = 75$ lb.

Therefore the axial load is predominant

$$E_t = \ell_t + 30\, \ell_r$$

$$E_t = 75 + (3 \times 72.1) = 291.3$$

Bearing No. 2 Radial load = 24.6 lb.
Axial load = 520 lb.

$$E_t = \ell_t + 30\, \ell_r$$

$$E_t = 520 + (3 \times 24.6) = 593.8 \text{ lb.}$$

Required basic capacity (C)

$$C = \frac{L \times F_L}{F_s}$$

where

L = Load on bearing
F_L = Life Factor, F_s = Speed factor
L = 593.8 lb.

$$F_L = .626$$

$$F_s = 1.44$$

$$C = \frac{593.8 \times .626}{1.44} = 258 \text{ lb.}$$

Factor for dry lubrication

Increase C by a factor of 10 for lubrication.

$$C_1 = 2580 \text{ lb. thrust.}$$

Kaydon Bearing KC 47 AR has dynamic thrust capacity of 2600 lb.

A-8 FEEDBACK LEAF SPRING DESIGN

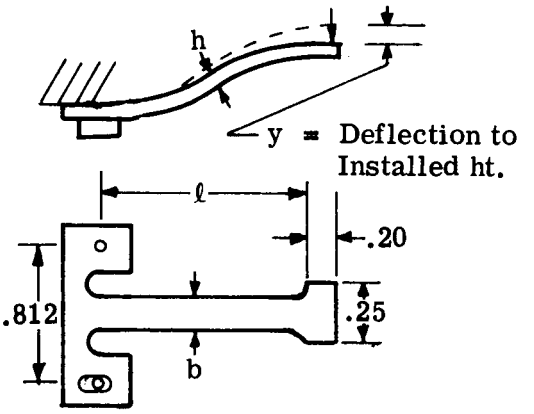

Use 17-7 per AMS 5529
HT. 1 hr.@900°F

Let

ℓ = .7 in.
h = .015 in.
b = .13 in.
y = .06 = deflection to installed ht.

Then,

$$F = \frac{yEbh^3}{4\ell^3} = \frac{(.06)\,(30\text{x}10^6)\,(.13)\,(1.5\text{x}10^{-2})^3}{4\,(7\text{x}10^{-1})^3} = \frac{.79}{1.372} = 0.58 \text{ lb.}$$

$$\sigma = \frac{6F\ell}{bh^2} = \frac{(b)\,(.58)\,(.7)}{.13\,(1.5\text{x}10^{-2})^2} = \frac{2.44}{.29\text{x}10^{-4}} = 84{,}000 \text{ psi}$$

A-9 MISCELLANEOUS

The output shaft and shaft key were designed per the ASME code, based on an allowable stress of 24,300 psi for AMS 5616 heat treated to R30-38.

The actuator base plate thickness was calculated to give a maximum deflection of 0.003 inch under the pressure differential of 650 psi. This deflection must be minimized to maintain an adequate dynamic seal surface.

A first approximation was made of the natural frequency of the bellows and gimbal ring configuration. A value of 50 cps was calculated. It is expected that the system will be overdamped, due to the frictional action of the pickoff springs and the pumping action of the bellows.

Various methods of analysis were employed to evaluate the orifice size required to fill the bellows in the allowable time. Since each method of approaching the problem required certain assumptions, no final method was evolved. It was generally agreed, however, that an orifice diameter between 0.030 inch and a 0.040 inch would pass the required flow rate of 4.75 in^3/sec to give a no load output speed of 65°/sec. This speed should be obtainable with room temperature nitrogen gas or with hydrogen gas at -360°F.

An analysis was also made of the feasibility of replacing the bellows with pistons and cylinders. The results indicated that a volumetric efficiency of 92% or better (depending on gas temperature) could be obtained with a frictional power loss less than 0.1%. The inertial forces could be kept low, and the Hertz stress at the gimbal ring

interface would be acceptable for a dry running environment. The use of pistons and cylinders would be considered for high temperature or hydraulic fluid applications.

A-10 SCALING FACTORS FOR ACTUATOR DESIGN

The following equations and graphs are derived to provide first approximations of the size and configuration of a pneumatic or hydraulic nutator actuator designed to provide any given output torque for a selected bellows pressure differential. The maximum diameter of the actuator is determined by the gear reduction required, the gear stress levels and/or the number of pressure elements employed.

No estimate is made of the actuator length, which is determined mainly by the bearing load design and the complexity of the commutation circuit. Variations in length can be considered to be small relative to diameter variations.

Strength of Straight Bevel-Gear

Teeth (Ref: Faires "Machine Design")

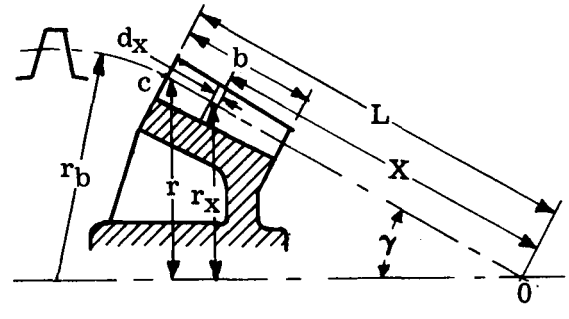

From the Lewis equation:

$$\left(F = \frac{sbY}{P_d}\right) \text{ we get,}$$

$$dF_x = \frac{sYdx}{P_{dx}} \quad \text{where } P_{dx} \text{ is the diametral pitch @dx.}$$

Multiply both sides of equation by r_x,

$$\int r_x dF_x = \int \frac{sYr_x d_x}{Pd_x} = \text{torque transmitted by gear} = T$$

Also, the circular pitch (P_c) varies inversely as the diametral pitch, so that,

$$\frac{P_{cx}}{P_c} = \frac{x}{L} = \frac{P_d}{P_{dx}} \quad \text{or} \quad P_{dx} = P_d\left(\frac{L}{x}\right)$$

Also, from similar triangles,

$$\frac{r_x}{r} = \frac{x}{L} \quad \text{or} \quad r_x = r\left(\frac{x}{L}\right)$$

Then,

$$T = \frac{sYr}{P_d L^2} \int_{L-b}^{L} X^2 d_x = \frac{sYrb}{P_d} \left[1 - \frac{b}{L} + \frac{b^2}{3L^2} \right]$$

since $\frac{b^2}{3L^2}$ is small,

$$\boxed{T = \frac{sYrb\,(L-b)}{P_d L}}$$

where s = endurance strength of material

Y = form factor based on virtual no. of teeth

P_d = diametral pitch

Based on practice, the max face width (b) of a bevel gear should be 1/3 the cone distance (L) or,

$$b = \left(\frac{L}{3}\right)$$

Also, from the geometry (See sketch)

$$L = \frac{r}{\sin \gamma}$$

For bevel gears, the diametral pitch is related to the virtual number of teeth (N_v) by the following expression,

$$P_d = \frac{N_v}{2r_b} \quad \text{and since } N_v = \frac{N}{\cos \gamma} \quad \text{and } r_b = \frac{r}{\cos \gamma}$$

$$P_d = \frac{N}{2r}$$

Substituting these expressions into the torque equation,

$$T = \frac{sYrv2r}{3 \sin \gamma N} \left(\frac{L - b}{L} \right) \qquad \frac{L - b}{L} = \frac{L - \frac{L}{3}}{L} = \frac{2L}{3L} = \frac{2}{3}$$

$$\boxed{T = \left(\frac{4sY}{9 \sin \gamma N} \right) r^3} \qquad (6)$$

Let $K = \left(\frac{4sY}{9 \sin \gamma N} \right)$ and select typical values to establish a value for K.

If,

S = endurance strength of material = For 17-4PH (38-42R_c) S_u = 190 ksi

$$\text{then } S = S_n = .5S_u = 95 \text{ KSI.}$$

Y = Form factor (based on virtual number of teeth) for N = 150

$$N_v = \frac{150}{\cos \gamma} = \frac{150}{.259} = 580$$

$$\text{let } \gamma = 75°, \sin \gamma = .966, \cos \gamma = .259$$

$\therefore$ $Y \approx 0.54$
$N = 150$

$$\text{Then } K = \frac{(4)(95 \times 10^3)(.54)}{(9)(.966)(150)} = 157$$

Thus, for a typical gear set (having a transmission ratio of 150:1), equation (6) can be rewritten as

$$r_{min} = \sqrt[3]{\frac{T}{157}}$$

$$r = \frac{D}{2}$$

where T = transmitted torque (in-lb)
r = pitch radius (in)
D = pitch diameter (in)

$$\text{or} \quad \boxed{D_{min} \approx \sqrt[3]{\frac{T}{20}}} \tag{7}$$

A plot of Equation (7) is shown on the next page.

Considering Hertz's Stress in gear tooth, from Shiglay "Machine Design", page 351,

$$\sigma^2 = \frac{0.7W\left(\frac{1}{D_1} + \frac{1}{D_2}\right)}{b \sin\phi \left(\frac{1}{E_1} + \frac{1}{E_2}\right)} \tag{8}$$

where W = tooth load (#)
E = mod. of elasticity
b = face width of tooth
ϕ = pressure angle
D_1 = pinion dia.
D_2 = gear dia.

First, assume that the gear and pinion are essentially the same dia. and made of the same material, so that

$$D_1 = D_2 = D \text{ and } E_1 = E_2 = E$$

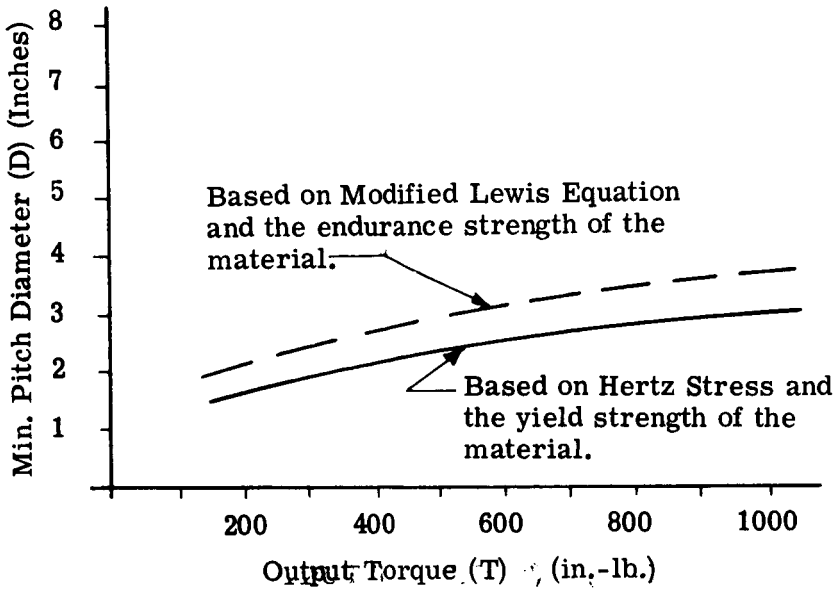

Equation (8) becomes $\sigma^2 = \dfrac{0.7W\ E}{b \sin\phi\ D}$ (9)

Also, in terms of torque at the output shaft,

$$T = rW = \frac{D}{2} W \quad \text{or } W = \frac{2T}{D}$$

$$\text{let } b \approx \frac{D}{6}$$

Then, $\sigma^2 = \dfrac{0.7\ (2T)6\ \ E}{D\ D \sin\phi\ D} = \dfrac{8.4\ TE}{D^3 \sin\phi}$

Or $D = \sqrt[3]{\left(\dfrac{8.4\ E}{\sigma^2 \sin\phi}\right)T}$

For 17-4PH (38-42R_c), S_y = 175 K psi

$E = 30 \times 10^6$ psi

$\phi = 20°$, $\sin\phi = .342$

Then $K_1 = \left(\frac{8.4E}{\sigma^2 \sin\phi}\right) = \frac{8.4 \times 30 \times 10^6}{3.1 \times 10^{10} \times .34} = 240 \times 10^{-4} = 0.024$

And $D_{min} \approx \sqrt[3]{.024\ T} \approx \sqrt[3]{\frac{T}{40}}$

Considering the relationship between shaft torque, pressure, and bellows (or piston) location.

Output Torque = $T = N_\eta\ (F_p \sin\gamma)\ r_p \sin\zeta$

Where,

N = transmission ratio
η = overall efficiency
F_p = resultant force applied by bellows (or pistons)
γ = nutation angle
r_p = radius @ which F_p is applied $\approx \frac{D}{3}$
ζ = "separation" angle

If N = 150
η = 0.6
$\sin\gamma = \gamma$ = .03 radians (approx. 1.5°)
$\sin\zeta$ = sin 45° = 0.7

Then,

$$T = 150\ (.6)\ F_p\ (.03)\frac{D}{3}\ (0.7)$$

or

$$T = .63\ F_pD$$

The resultant force applied by the bellows can be expressed as,

$$F_p = \Delta p\ A_b\ \bar{n}$$

Where

Δ_p = pressure drop acting on bellows (psi)
A_b = effective area of bellows (in^2)
$\bar{n}$ = No. of bellows pressurized at any time.

Then

$$T \approx .63\ \Delta p A_b\ \bar{n}\ D$$

Since the torque output is directly proportional to the bellows area, let the bellows area be equal to 1 in^2. Also, let the total number of bellows be eight and the number pressurized ($\bar{n}$) be four. Then,

$$T \approx 2.5\ \Delta pD \quad \text{or} \quad D = \frac{T}{2.5\ \Delta p} \tag{10}$$

A plot of equation(10)is shown below.

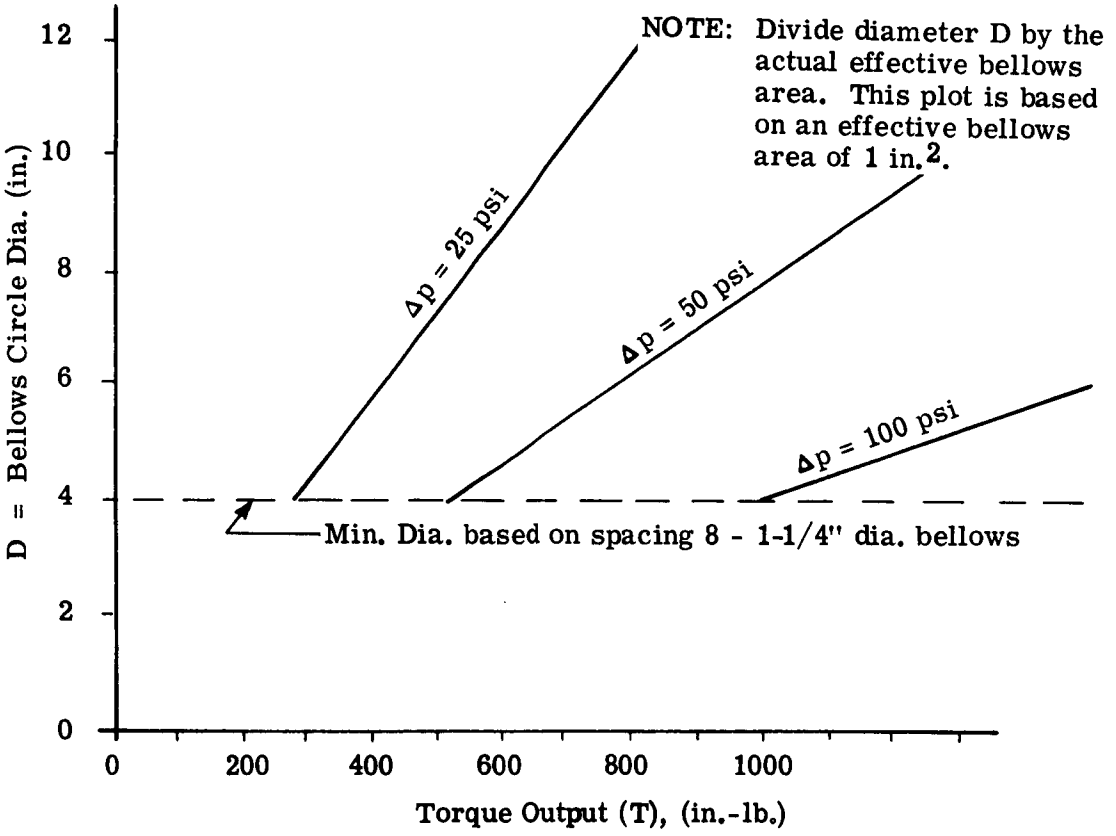

For hydraulic powered applications, the pressures will be higher - thus permitting smaller values for effective piston area (A_b). Let,

$$A_b = 0.1\ in^2 \qquad \bar{n} = 4 \text{ (8 piston unit)}$$

Then

$$T \approx .25\ \Delta pD \quad \text{or} \quad D = \left(\frac{4T}{\Delta p}\right) \tag{11}$$

A plot of equation(11)is shown below.

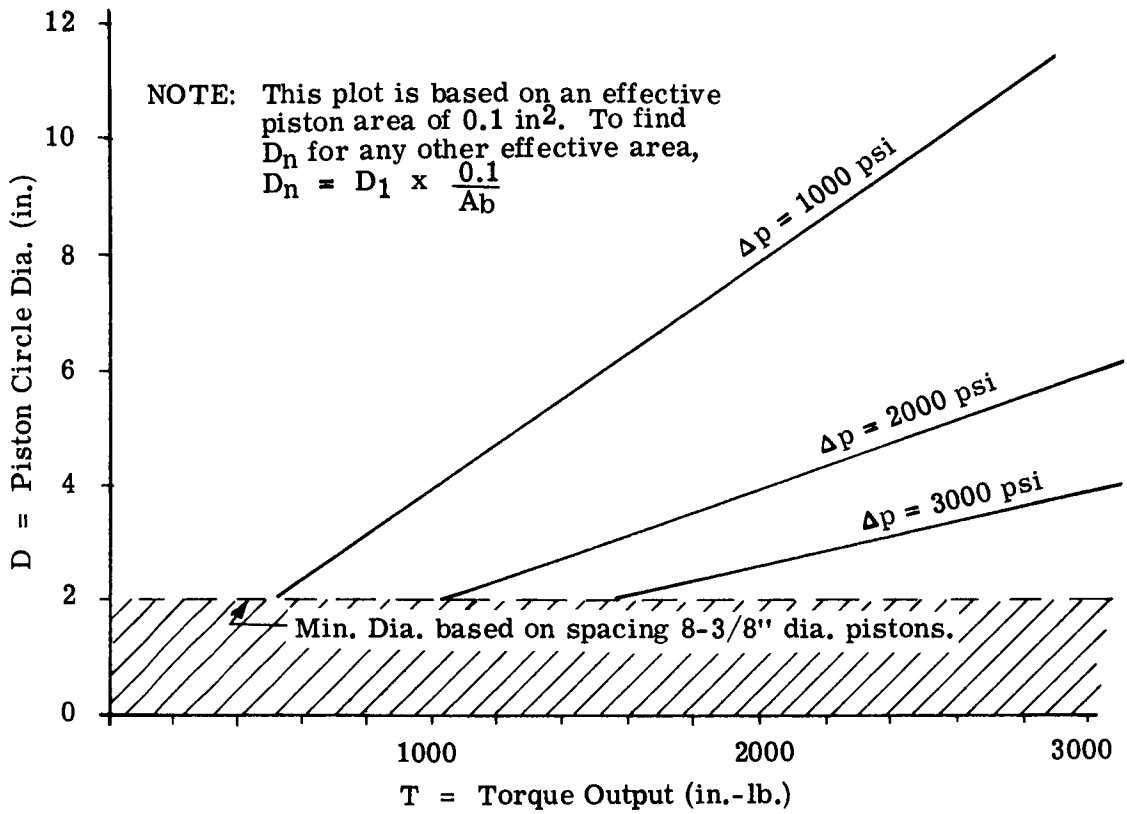

When estimating the size of a complete actuator-motor, it will be necessary to add one piston or bellows diameter plus housing allowance onto the diameter obtained from these curves. This will give a good approximation of the overall diameter.

Pressure element spacing: Based on eight units (bellows or pistons)

$$D = \frac{8(d+s)}{\pi} = 2.55\,(d+s)$$

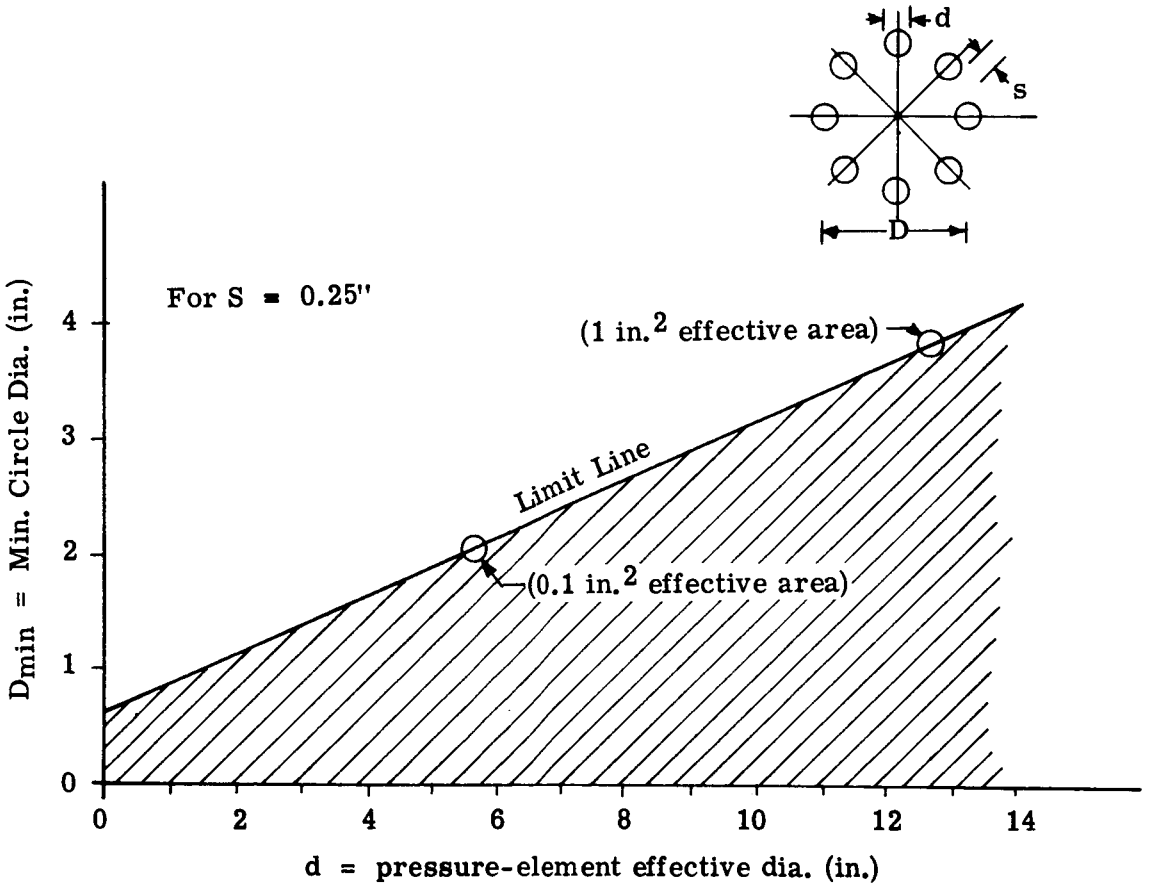

APPENDIX B

COMMUTATION CIRCUIT PLATE IDENTIFICATION

COMMUTATION CIRCUIT PLATE ORIENTATION

AND PRESSURE SEQUENCING INFORMATION

B-1. For purposes of identification, plate NPX-104-66 will be known as the bottom plate of the assembly, and plate NPX-104-74 will be known as the top plate of the assembly. Thus the top and bottom side of the individual plates and the assembly are established. On the edge of each plate appears a number and arrow. The number is the last number of the NPX designation. This number can be used to identify the individual plates and correlate them with the drawings. The arrow on the edge of each plate points toward the top of the plate. Unless otherwise specified, when the plates are assembled, the arrows should all point the same direction and be in line with each other. This is illustrated in Figure B-1(a). Also, when specifying a direction of rotation, it is specified looking downward on the plate or plates, as illustrated in Figure B-1(b).

B-2. For testing purposes, the plates will be stacked as follows, from bottom to top:

TYPE OF PLATE	PLATE NO.
Test	NPX-104-66
Commutation	NPX-104-41
Test	NPX-104-63
Commutation	NPX-104-42
Test	NPX-104-64
Test	NPX-104-65
Commutation	NPX-104-43
Commutation	NPX-104-44
Commutation	NPX-104-45
Commutation	NPX-104-46
Commutation	NPX-104-47
Test	NPX-104-74-B
Test	NPX-104-74-A

For shipping purposes, the plates will be stacked as follows, from bottom to top: NPX-104-27, 41, 42, 43, 44, 45, 46, 47 and the back plate which will have to be designed to incorporate the pressure error valve and the directional amplifier. Each plate used for testing shall be described individually below.

B-3. Test plate NPX-104-66 is identified as shown in Figure B-2. Taps 1 through 8 identify the pressure ports to the bellows. P_1 through P_4 identify the position pickoffs pressure ports.

B-4. Commutation plate NPX-104-41 is the second plate and can be assembled in one way only.

B-5. Test plate NPX-104-63 is assembled next. This test plate has pressure taps which are available in order to read bias, supply, and selector signal pressures for two opposed power vortex valves at a time. So that all the pressures in the power valves can be read, the plate must be indexed. By indexing the plate 45° CCW relative to plate NPX-104-41, two other power valves' pressure may be read. By indexing the test plate 45° CCW with respect to plate NPX-104-41, position 2 is defined. On the edge of plate NPX-104-63 there are markings denoting positions 2 through 4. When the position mark is in line with the arrows, the test plate is in the marked position, as shown in Figure B-3(a) (position 1 is denoted by the arrow). Shown in Figure B-3(b) is the letter designations of the pressure taps. Figure B-4 is a schedule of plate NPX-104-63 position and the pressures read from the lettered taps. Figure B-5 describes the selector valves by number and letter designations, appearing in the centers of the valves.

B-6. Plate NPX-104-42 is identified on the edge by number and arrow.

B-7. Plates NPX-104-65 and NPX-104-65 function as one plate. Therefore when plate NPX-104-65 is rotated, plate NPX-104-65 should also be rotated the same amount. The pressure taps in plate NPX-104-65 are lettered in a clockwise fashion. Primed letters are used to eliminate confusion with those letters of plate NPX-104 -43. The position markings on plate NPX-104-65 appear on the top surface instead of the edge of the plate. The position markings are the same as for plate NPX-104-63 except that at any setting, plate NPX-104-65 taps gain access to four selector valves' pressures. The pressure tap designations for plate NPX-104-65 appears in Figure B-6. A schedule for the position and pressure tap readings appears in Figure B-7. Position pickoff, left directional, and right directional pressures are designated in Figure B-5.

B-8. NPX-104-44 is a flow transfer plate. It is marked on the edge for installation.

B-9. Plate NPX-104-45 is the position pickoff pressure distribution plate. Figure B-8 illustrates the distribution rings and designates them.

B-10. Commutation plate NPX-104-46 is the plate which contains the supply plenums for the power and selector valves.

B-11. Plate NPX-104-47 contains the distribution rings for the right and left directional and the bias pressure. Figure B-9 designates these rings.

B-12. Plate NPX-104-74 is a cover test plate.

B-13. Figure B-10 indicates the pressure schedule for reading input, intermediate, and output pressures. The X's designate high relative pressures and the 0's designate low relative pressures.

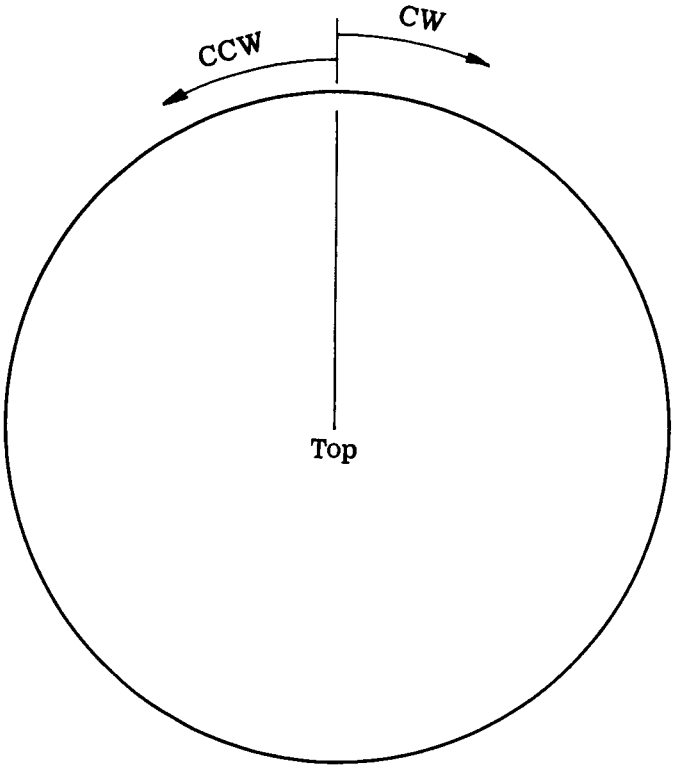

Figure B1(a). Direction Designations

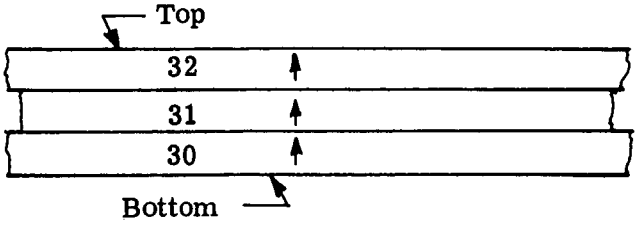

Figure B1(b). Direction Designations

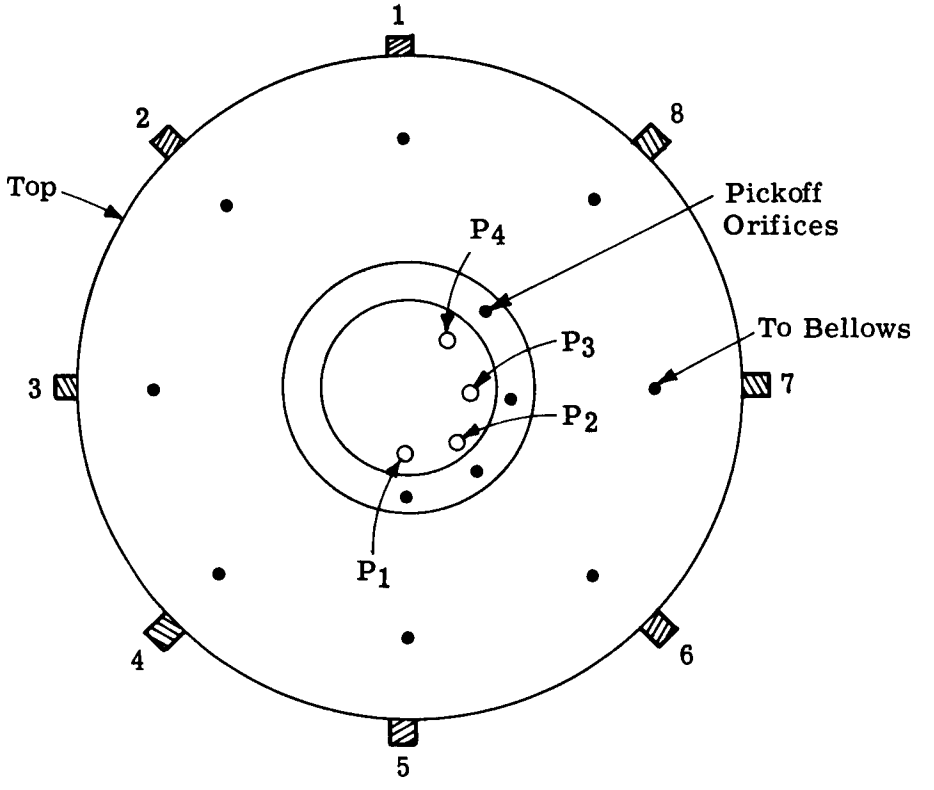

Figure B-2. Plate NPX-104-66

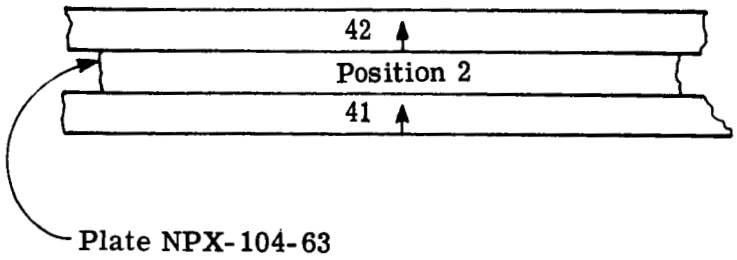

Figure B-3(a). Plate Assembly Showing NPX-104-63 in Position 2

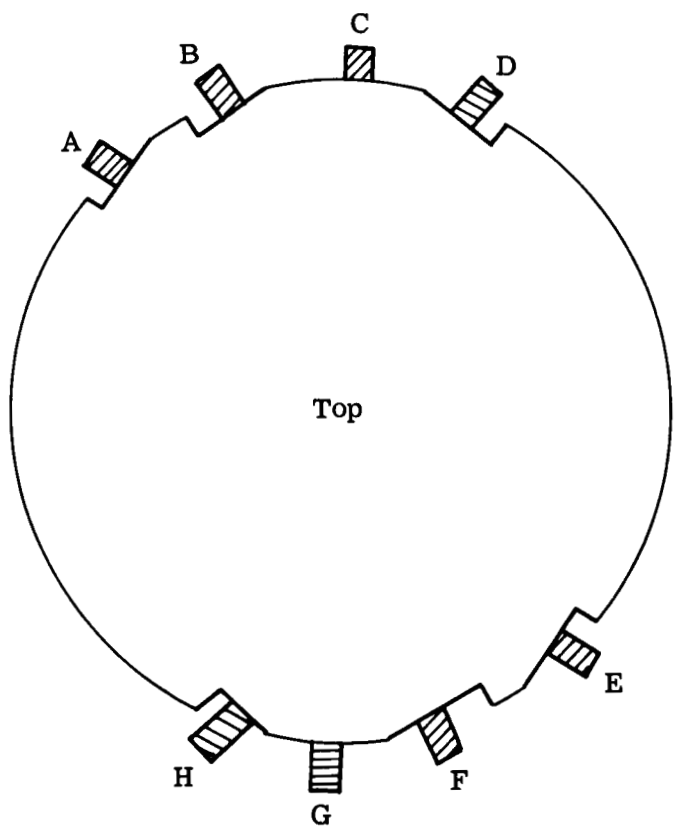

Figure B-3(b). Plate NPX-104-63 Showing Pressure Taps

Position	Pressures Read							
	A	B	C	D	E	F	G	H
1	2A	4D	B1	S1	2C	4B	B5	S5
2 (45° CCW)	1B	3A	B2	S2	1D	3C	B6	S6
3 (90° CCW)	2B	4A	B3	S3	2D	4C	B7	S7
4 (135° CCW)	1C	3B	B4	S4	1A	3D	B8	S8

NOTE: Any pressure designation beginning with a number is a selector valve designation. The selector valves are shown in Figure B-5.

A prefix of S designates supply to the power valve numbered. (Ex:S1 designates supply to power valve 1).

A prefix of B designates bias to the power valve numbered. (Ex: B1 designates bias to power valve 1)

Figure B-4. Positioning Schedule for NPX-104-63

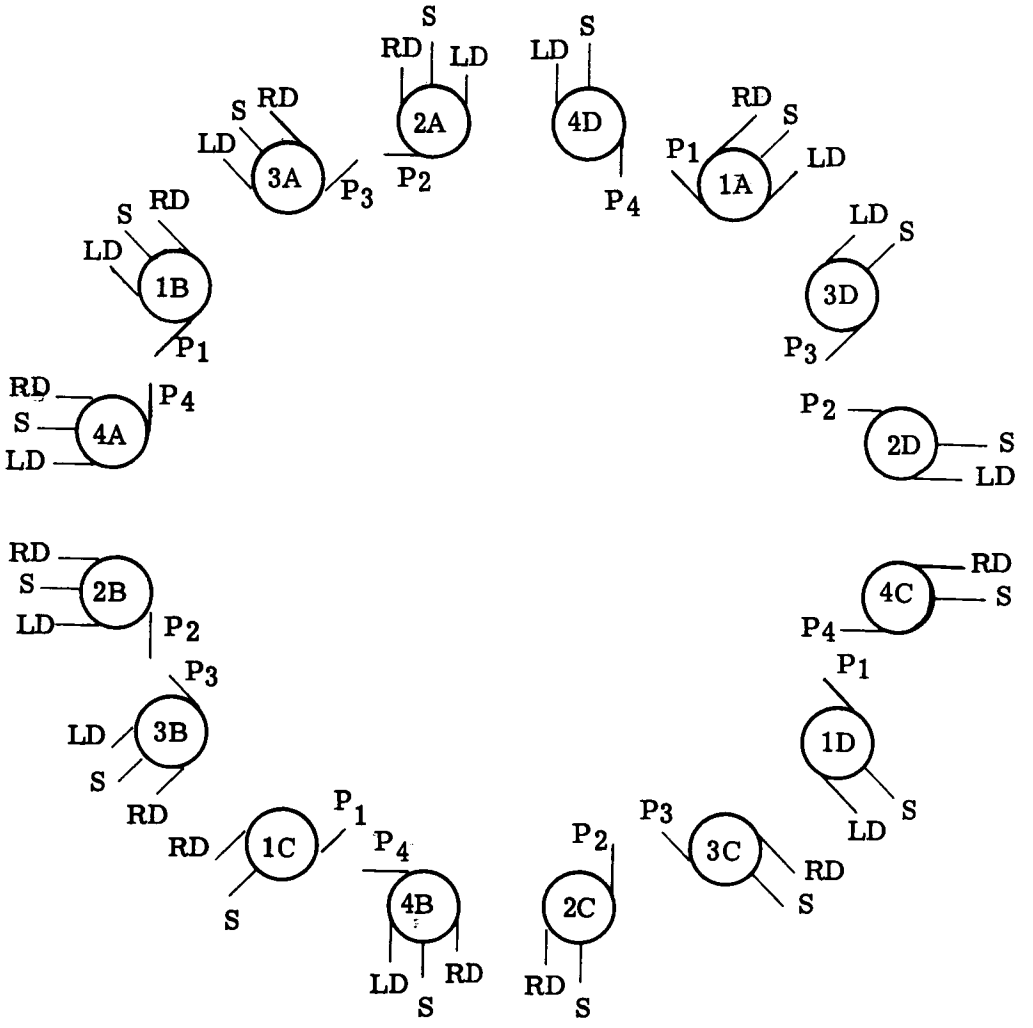

Figure B-5. Selector Valve Designations

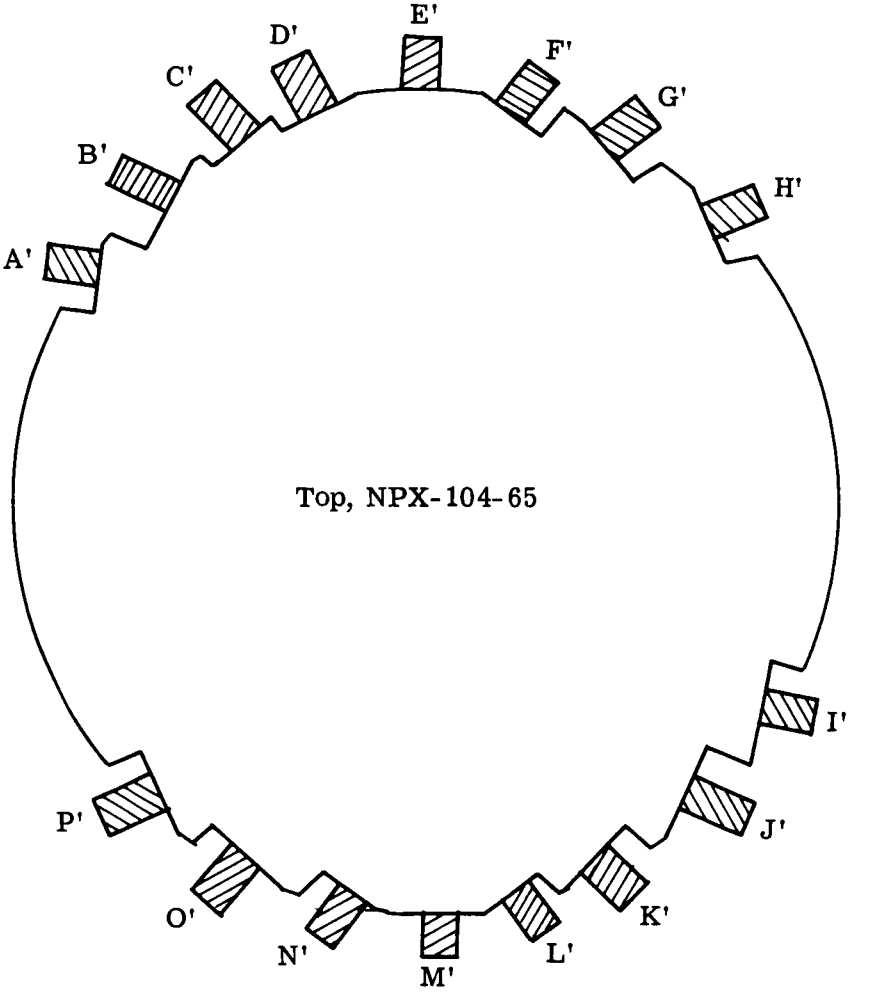

Figure B-6. Pressure Tap Letter Designations for NPX-104-65

Position	Pressure Taps															
	A'	B'	C'	D'	E'	F'	G'	H'	I'	J'	K'	L'	M'	N'	O'	P'
1	$2AP_2$	2ARD	S2A	2ALD	4DLD	S4D	--	$4DP_4$	$2CP_2$	--	S2C	2CRD	4BRD	S4B	4BLD	$4BP_4$
2	$1BP_1$	1BLD	S1B	1BRD	3ALD	S3A	3ARD	$3AP_3$	$1DP_1$	--	S1D	1DLD	3CRD	S3C	--	$3CP_3$
3	$2BP_2$	2BLD	S2B	2BRD	4ALD	S4A	4ARD	$4AP_4$	$2DP_2$	--	S2D	2DLD	4CRD	S4C	--	$4CP_4$
4	$1CP_1$	--	S1C	1CRD	3BRD	S3B	3BLD	$3BP_3$	$1AP_1$	1ARD	S2A	1ALD	3DLD	S3D	--	$3DP_3$

NOTE: An S prefix denotes supply to the designated selector valve. (Ex: S2A is the supply to valve 2A).

All other prefix designations call out the selector valve and the type of control pressure. (Ex: $2AP_2$ means selector valve 2A and position pickoff pressure P_2. 4DLD means selector valve 4D and left directional pressure. 3BRD means selector valve 3B and right directional pressure).

Figure B-7. Pressure Tap Position

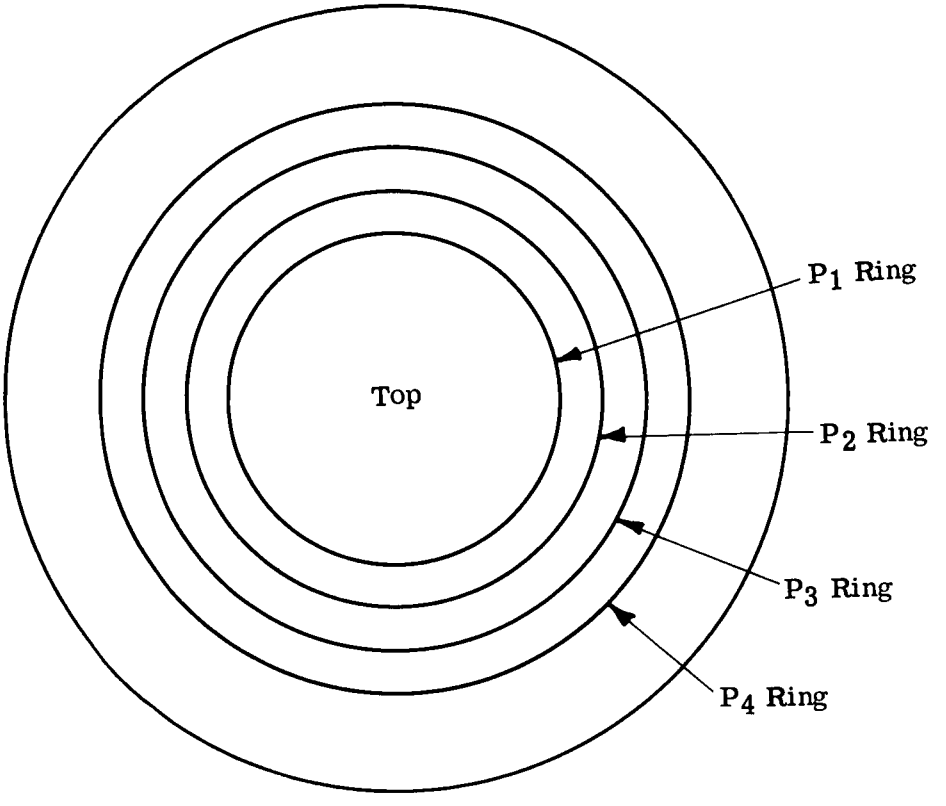

Figure B-8. Plate NPX-104-45

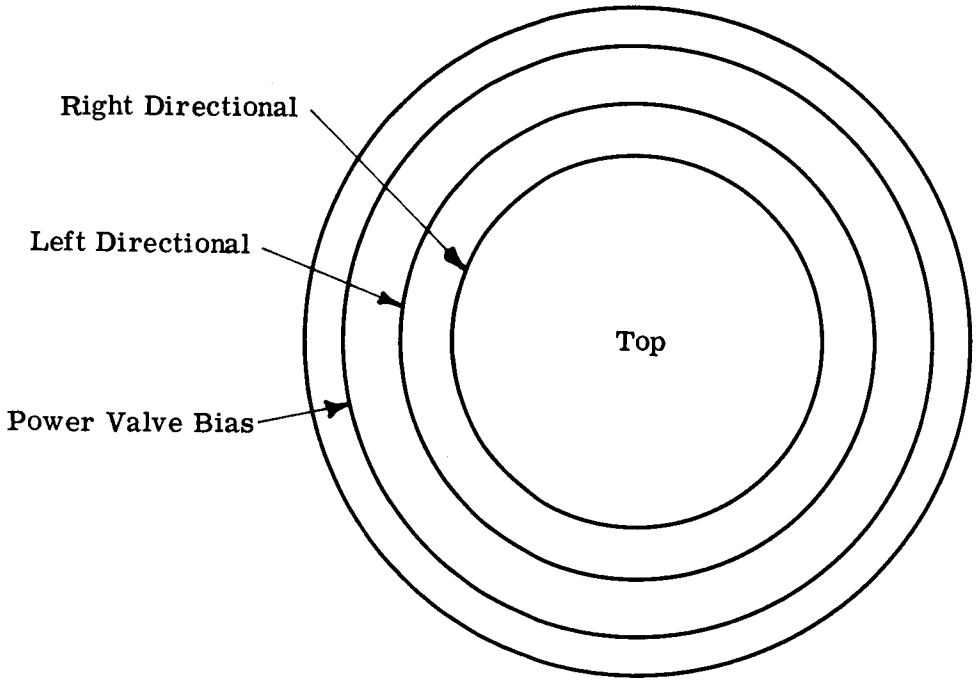

Figure B-9. Plate NPX-104-47

INPUTS						INTERMEDIATE												OUTPUT							
DR	DL	P_1	P_2	P_3	P_4	1A	1B	1C	1D	2A	2B	2C	2D	3A	3B	3C	3D	4A	4B	4C	4D	1	2	3	4	5	6	7	8
x	o	x	x	x	x	o	x	o	o	o	x	o	o	o	x	o	o	o	x	o	o	o	x	x	x	x	o	o	o
x	o	o	x	x	x	o	o	o	x	o	x	o	o	o	x	o	o	o	x	o	o	o	o	x	x	x	x	o	o
x	o	o	o	x	x	o	o	o	x	o	o	o	x	o	x	o	o	o	x	o	o	o	o	o	x	x	x	x	o
x	o	o	o	o	x	o	o	o	x	o	o	o	x	o	o	o	x	o	x	o	o	o	o	o	o	x	x	x	x
x	o	o	o	o	o	o	o	o	x	o	o	o	x	o	o	o	x	o	o	o	x	x	o	o	o	o	x	x	x
x	o	x	o	o	o	o	x	o	o	o	o	o	x	o	o	o	x	o	o	o	x	x	x	o	o	o	o	x	x
x	o	x	x	o	o	o	x	o	o	o	x	o	o	o	o	o	x	o	o	o	x	x	x	x	o	o	o	o	x
x	o	x	x	x	o	o	x	o	o	o	x	o	o	o	x	o	o	o	o	o	x	x	x	x	x	o	o	o	o
o	x	x	x	x	x	x	o	o	o	x	o	o	o	x	o	o	o	x	o	o	o	x	x	x	o	o	o	o	x
o	x	x	x	x	o	x	o	o	o	x	o	o	o	x	o	o	o	o	o	x	o	x	x	o	o	o	o	x	x
o	x	x	x	o	o	x	o	o	o	x	o	o	o	o	o	x	o	o	o	x	o	x	o	o	o	o	x	x	x
o	x	x	o	o	o	x	o	o	o	o	o	x	o	o	o	x	o	o	o	x	o	o	o	o	o	x	x	x	x
o	x	o	o	o	o	o	o	x	o	o	o	x	o	o	o	x	o	o	o	x	o	o	o	o	x	x	x	x	o
o	x	o	o	o	x	o	o	x	o	o	o	x	o	o	o	x	o	x	o	o	o	o	o	x	x	x	x	o	o
o	x	o	o	x	x	o	o	x	o	o	o	x	o	x	o	o	o	x	o	o	o	o	x	x	x	x	o	o	o
o	x	o	x	x	x	o	o	x	o	x	o	o	o	x	o	o	o	x	o	o	o	x	x	x	x	o	o	o	o

Figure B-10. Pressure Schedule

APPENDIX C

DESIGN SPECIFICATIONS

ENGINEERING SPECIFICATION

BELLOWS ASSEMBLY - PNEUMATIC NUTATING ACTUATOR-MOTOR

This bellows assembly is to be used in a cryogenic-nuclear environment to provide an actuating force in a pneumatic mechanism. Following are the specific requirements.

1.0 Medium: Gaseous hydrogen at -350°F to +300°F.

2.0 Pressure Drop Across Bellows:

I.D. = P_1 = 0-150 psig (full range)
O.D. = P_2 = 0-50 psig (full range)
(P_1-P_2) = 70 psi (normal working pressure)

Bellows must withstand any combination of P_1 and P_2.

3.0 Nuclear Environment:

Component is exposed to high level nuclear radiation.

4.0 Effective Area: 0.435 $in.^2$ ± 5%.

5.0 Bellows Assembly: End fitting dimensions per Specification Control Drawing. Bellows assembly shall contain device for reducing P_1 volume (see suggested method on Specification Control Drawing) to a minimum. If can is used, as shown, internal pressure is same as P_2 in Paragraph 2.

6.0 Bellows Motion: Stroke: ± 0.06 inch (about free length position)
Fill Time: 0.015 second (minimum)
Angular Displacement of Ends: ± 1°8' each stroke

7.0 Life Expectancy: 50 x 10^6 cycles at -300°F (±0.06 inch from null = 1 cycle.)

8.0 Spring Rate: 50 lbs./inch (maximum).

9.0 Material: Bellows assembly shall be corrosion resistant and compatible with conditions listed in above paragraph.

ENGINEERING SPECIFICATION

TORSIONAL SCRAM SPRING - PNEUMATIC NUTATING ACTUATOR-MOTOR

This spring is to be used in a cryogenic-nuclear environment. Following are the specific requirements:

1.0 Environment: Hydrogen atmosphere at -350°F to +300°F.

2.0 Nuclear Environment:

Component is exposed to high level nuclear radiation.

3.0 Envelope: Spring must fit unto the envelope requirements as shown on the Specification Control Drawing.

4.0 End Fittings: End fittings shall be as shown on the Specification Control Drawing.

5.0 Installed Torque: The torque supplied by the spring in the installed position shall be 50 inch-pounds (± 5%).

6.0 Deflection: The spring shall deflect 180 degrees (maximum) during operation. The torque supplied by the spring shall increase as the spring is rotated from the installed position.

7.0 Spring Rate: The spring rate shall be 4 in-lbs./rad. (maximum).

8.0 Operating Life: The minimum operating life shall be 10,000 cycles of 0-180°-0 at any temperature between -300°F and +300°F.

9.0 Weight: The weight of the complete spring shall not exceed 1.3 pounds.

10.0 Material: The spring shall be corrosion resistant and compatible with the conditions listed in the above paragraph.

ENGINEERING SPECIFICATION

DYNAMIC SEAL - PNEUMATIC NUTATING ACTUATOR - MOTOR

This seal is to be used in a cryogenic-nuclear environment to seal gaseous hydrogen. Following are the specific requirements:

1.0 Medium: Gaseous hydrogen @ -350°F to +300°F.

2.0 Pressure Drop Across Seal: (working pressures)

Seal I.D. = P_1 = 0-650 psig
Seal O.D. = P_2 = 0-50 psig

Seal must withstand any combination of the P_1 and P_2.

3.0 Nuclear Environment:

Component is exposed to high level nuclear radiation.

4.0 Seal Envelope: As shown on Specification Control Drawing.

5.0 Lubrication Available: None

6.0 Allowable Leakage:

For ($P_1 > P_2$): 0.001 lb./sec. H_2 (0.0037 lb./sec. N_2) maximum
For ($P_2 > P_1$): 0.0001 lb./sec. H_2 (0.00037 lb./sec. N_2) maximum

7.0 Friction Torque: 15 in.-lb. maximum at any pressure drop specified in Paragraph 2.0.

8.0 Shaft Motion: Angular Velocity: 0-360 deg./sec.
Angular Displacement: 0-180 deg.

9.0 Life: 300 hours @ 100 rpm @ -300°F @ 600 psid.

10.0 Mating Surface: To be specified by seal manufacturer.

APPENDIX D

DISTRIBUTION LIST FOR CONTRACT NAS 3-5214 FINAL REPORT

APPENDIX D

DISTRIBUTION LIST

NASA-Lewis Research Center (20)
21000 Brookpark Road
Cleveland, Ohio 44135
Attention: Vernon D. Gebben

NASA-Lewis Research Center (2)
21000 Brookpark Road
Cleveland, Ohio 44135
Attention: Lewis Library

NASA-Lewis Research Center (1)
21000 Brookpark Road
Cleveland, Ohio 44135
Attention: James E. Burnett, Technology Utilization Office

NASA-Ames Research Center (1)
Moffett Field, California 94035
Attention: Library

NASA-Goddard Space Flight Center (1)
Greenbelt, Maryland 20771
Attention: Library

NASA-Marshall Space Flight Center (1)
Huntsville, Alabama 35812
Attention: Michael A. Kalange, R-ASTR-NF

NASA-Western Operations (1)
150 Pico Boulevard
Santa Monica, California 90406

NASA Scientific & Technical Information Facility (6 & Reproducible)
Box 5700
Bethesda, Maryland
Attention: NASA Representative

Harry Diamond Laboratories (2)
Washington 25, D. C.
Attention: Joseph M. Kirshner

NASA-Lewis Research Center (1)
21000 Brookpark Road
Cleveland, Ohio 44135
Attention: C. J. Shannon

NASA-Lewis Research Center (1)
21000 Brookpark Road
Cleveland, Ohio 44135
Attention: Lewis Technical Information Division

NASA Headquarters (2)
Washington, D. C. 20546
Attention: F. C. Schwenk, NPO

NASA-Flight Research Center (1)
P.O. Box 273
Edwards, California 93523
Attention: Library

NASA-Langley Research Center (1)
Langley Station
Hampton, Virginia 23365
Attention: Library

NASA-Marshall Space Flight Center (1)
Huntsville, Alabama 35812
Attention: Roy E. Currie, Jr.
R-ASTR-TN

NASA-Manned Spacecraft Center (1)
Houston, Texas 77001
Attention: Library

Jet Propulsion Laboratory (1)
4800 Oak Grove Drive
Pasadena, California 91103
Attention: Library

Harry Diamond Laboratories (2)
Washington 25, D. C.
Attention: Library

Wright-Patterson Air Force Base (2)
Ohio
Attention: Library

U. S. Atomic Energy Commission (3)
Technical Information Service Extension
P.O. Box 62
Oak Ridge, Tennessee

NASA-Lewis Research Center (2)
21000 Brookpark Road
Cleveland, Ohio 44135
Attention: Nuclear Rocket Technology
Office

NASA Headquarters (2)
Washington, D. C. 20546
Attention: John E. Morrissey, NPO

Army Missile Command (2)
Redstone Arsenal, Alabama
Attention: Library

U. S. Atomic Energy Commission (3)
Technical Reports Library
Washington, D. C.

Los Alamos Scientific Laboratory (3)
Los Alamos, New Mexico
Attention: Joseph Perry, N-4

NASA-Lewis Research Center (1)
21000 Brookpark Road
Cleveland, Ohio 44135
Attention: Alan S. Hintze, SNPO

Case Institute of Technology (1)
Mechanical Engineering Department
Cleveland, Ohio
Attention: Prof. Charles Taft

NASA Headquarters (1)
Washington, D. C. 20546
Attention: Herman H. Lowell, REI

NASA-Marshall Space Flight Center (1)
Huntsville, Alabama 35812
Attention: Jerold Peoples,
R-ASTR-NFM

Army Missile Command (1)
Redstone Arsenal, Alabama
Attention: B. J. Clayton

Army Missile Command (1)
Redstone Arsenal, Alabama
Attention: William A. Griffith

Army Transportation & Research
Command (1)
Ft. Eustis, Virginia
Attention: George W. Fosdick

Bolling Air Force Base (1)
Washington, D. C. 20332
Attention: Major C. R. Wheaton

Wright-Patterson Air Force Base (1)
Ohio
Attention: James F. Hall

NASA-Marshall Space Flight Center (1)
Huntsville, Alabama 35812
Attention: William White,
R-ASTR-TN

NASA-Marshall Space Flight Center (1)
Huntsville, Alabama 35812
Attention: Russel Alcott,
R-ASTR-NFM

Army Material Command (1)
Research Division
Washington 25, D. C.
Attention: Major W. T. Kerttula

Army Missile Command (1)
Redstone Arsenal, Alabama
Attention: T.G. Wetheral

Army Munitions Command (1)
Picatinny Arsenal
Dover, New Jersey
Attention: Silvio J. Odierno

Army Transportation & Research
Command (1)
Ft. Eustis, Virginia
Attention: Robert R. Piper

Kirtland Air Force Base (1)
New Mexico
Attention: Capt. Charles V. Fada

Wright-Patterson Air Force Base (1)
Ohio
Attention: Seth A. Young

Wright-Patterson Air Force Base (1)
Ohio
Attention: Ronald Ringo

Office of Naval Research (1)
Department of Navy
Washington, D. C. 20360
Attention: Stanley Doroff

Bureau of Weapons (1)
Munitions Building
Washington 25, D. C.
Attention: Richard A. Retta

Massachusetts Institute of Technology (1)
Department of Mechanical Engineering
Cambridge 39, Massachusetts
Attention: Forbes T. Brown

Wright-Patterson Air Force Base (1)
Ohio
Attention: Charles Bentz

Office of Naval Research (1)
Washington, D. C. 20360
Attention: Ancel E. Cook

U. S. Atomic Energy Commission (1)
Division of Reactor Development
Washington 25, D. C.
Attention: Frank C. Legler

NASA-Lewis Research Center (2)
21000 Brookpark Road
Cleveland, Ohio 44135
Attention: Nuclear Rocket
Technology Office

NASA Headquarters (1)
Washington, D. C. 20546
Attention: Carl Janow, REC

NASA-Langley Research Center (1)
Langley Station
Hampton, Virginia 23365
Attention: H. Douglas Garner

NASA-Flight Research Center (1)
Edwards, California 93523
Attention: Wilton Lock

NASA-Ames Research Center (1)
Moffett Field, California 94035
Attention: E. Perkins

NASA-Manned Spacecraft Center (1)
Houston, Texas 77058
Attention: R. Chilton

NASA-Goddard Space Flight Center (1)
Greenbelt, Maryland 20771
Attention: H. Hoffman

NASA-Electronic Research Center (1)
575 Technology Square
Cambridge, Massachusetts 02139
Attention: George Kovatch

NASA-Langley Research Center (1)
Langley Station
Hampton, Virginia 23365
Attention: Harry V. Fuller

NASA-Lewis Research Center (1)
Plum Brook Station
Sandusky, Ohio 44871
Attention: W. E. Kirchmeier

Jet Propulsion Laboratory (1)
4800 Oak Grove Drive
Pasadena, California 91103
Attention: J. Scull

NASA-Lewis Research Center (1)
21000 Brookpark Road
Cleveland, Ohio 44135
Attention: Ruth Weltmann